GEOHYDROLOGY AND POTENTIAL EFFECTS OF DEVELOPMENT OF FRESHWATER RESOURCES IN THE NORTHERN PART OF THE HUECO BOLSON, DOÑA ANA AND OTERO COUNTIES, NEW MEXICO, AND EL PASO COUNTY, TEXAS

By Brennon R. Orr and Dennis W. Risser

U.S. GEOLOGICAL SURVEY
Water-Resources Investigations Report 91-4082

Prepared in cooperation with the
U.S. DEPARTMENT OF THE ARMY (FORT BLISS),
NEW MEXICO STATE ENGINEER OFFICE,
and the
CITY OF EL PASO, TEXAS

Albuquerque, New Mexico

1992

U.S. DEPARTMENT OF THE INTERIOR

MANUEL LUJAN, JR., Secretary

U.S. GEOLOGICAL SURVEY

Dallas L. Peck, Director

For additional information
write to:

District Chief
U.S. Geological Survey
Pinetree Corporate Centre
4501 Indian School Road NE, Suite 200
Albuquerque, New Mexico 87110

Copies of this report can
be purchased from:

U.S. Geological Survey
Books and Open-File Reports
Federal Center
Box 25425
Denver, Colorado 80225

CONTENTS

CONTENTS--Concluded

FIGURES

FIGURES--Continued

FIGURES--Concluded

TABLES

CONVERSION FACTORS AND VERTICAL DATUM

Multiply	By	To obtain
acre	0.4047	hectare
acre-foot	1,233	cubic meter
cubic foot per second	0.02832	cubic meter per second
foot	0.3048	meter
foot per day	0.3048	meter per day
foot squared per day	0.09290	meter squared per day
gallon per minute	0.06309	liter per second
inch	2.540	centimeter
mile	1.609	kilometer
square mile	2.590	square kilometer
foot per mile	0.1894	meter per kilometer

For temperature, degrees Celsius (°C) may be converted to degrees Fahrenheit (°F) by the equation:

$$°F = 9/5\ (°C) + 32$$

Sea level: In this report, "sea level" refers to the National Geodetic Vertical Datum of 1929--a geodetic datum derived from a general adjustment of the first-order level nets of the United States and Canada, formerly called Sea Level Datum of 1929.

GEOHYDROLOGY AND POTENTIAL EFFECTS OF DEVELOPMENT OF FRESHWATER RESOURCES IN THE NORTHERN PART OF THE HUECO BOLSON, DOÑA ANA AND OTERO COUNTIES, NEW MEXICO, AND EL PASO COUNTY, TEXAS

By Brennon R. Orr and Dennis W. Risser

ABSTRACT

Future ground-water development in the New Mexico part of the Hueco Bolson may affect the quantity and quality of water resources. This study was conducted to estimate the effects of possible future development. A flow model was constructed from hydrologic data collected during 1905-83 to estimate these effects. Simulated hydraulic conductivity ranged from 1 to 40 feet per day, simulated specific yield ranged from 0.05 to 0.20, and simulated recharge was 4,500 acre-feet per year.

By 1983, most ground-water flow was toward El Paso and maximum water-level declines were about 200 feet; declines at the New Mexico State line were as much as 25 feet. Water removed from storage during 1905-83 totaled approximately 3.2 million acre-feet, mostly from pumpage.

Two scenarios were used to estimate the effects of ground-water withdrawals in the Hueco Bolson by 2030. In the first scenario, withdrawals remained constant after 1990. In the second scenario, withdrawals were projected using present trends. In both scenarios, 10,000 acre-feet of withdrawals were shifted to New Mexico to simulate development of new well fields. In scenario 1, water-level declines as much as 100 feet were projected at the New Mexico State line by 2030. The rate of withdrawal from storage in 2030 was more than 127,000 acre-feet per year, with a total of 9.6 million acre-feet of water withdrawn from storage. In scenario 2, water-level declines of 125 feet were projected in New Mexico near the State line by 2030. The rate of withdrawal from storage in 2030 was more than 255,000 acre-feet per year, with more than 12.8 million acre-feet of water withdrawn from storage.

In the steady-state simulation, freshwater moved parallel to the freshwater/saline-water boundary as much as 0.20 foot per day. By 1983, withdrawals had altered flow direction and increased velocity near Newman, New Mexico. Maximum encroachment of saline water was approximately 1 mile. In scenario 1, saline-water encroachment near Newman would be about 1.5 miles from 1983 to 2030. In scenario 2, saline-water encroachment would be about 2 miles.

A solute-transport model was used to evaluate the potential for vertical movement of saline water (upconing) in response to withdrawals. At assumed pumping rates, upconing will not seriously affect freshwater zones that are more than 1,000 feet thick. Dispersive processes will result in some mixing and water-quality degradation.

INTRODUCTION

Municipal, military, and other water users near El Paso, Texas, obtain most of their water supplies from basin-fill deposits of the Hueco Bolson (fig. 1). Because of increases in water use in the El Paso area, water users are considering development of additional fresh ground-water supplies. The New Mexico part of the Hueco Bolson contains freshwater-saturated basin-fill deposits that are being considered for development. Large withdrawals of water in the New Mexico part of the bolson could result in declining water levels and mixing of freshwater resources with underlying saline water. Information is needed by water planners to evaluate potential effects on ground-water resources as a result of development of these supplies. The U.S. Geological Survey conducted this study in cooperation with the U.S. Department of the Army at Fort Bliss, Texas and New Mexico; the New Mexico State Engineer Office; and the City of El Paso, Texas.

Purpose and Scope

This report describes the results of a study to: (1) determine ground-water flow in the New Mexico part of the Hueco Bolson; (2) assess the potential effects of increased pumpage on ground water in the New Mexico part of the Hueco Bolson; and (3) assess the distribution and rate of saline-water encroachment that may result from increased pumpage in the New Mexico part of the Hueco Bolson. The report includes descriptions of the occurrence, distribution, and quality of ground water in basin-fill deposits; development of a ground-water flow model to estimate present and potential effects of water withdrawals; and evaluation of the potential for saline-water encroachment.

Location of the Study Area

The Hueco Bolson, a predominantly north- to northwest-trending intermontane basin in south-central New Mexico, west Texas, and northern Mexico, is part of a large intermontane basinal structure. The Tularosa Basin to the north is also part of this structure. The area of study in this report (fig. 1) includes the northern part of the Hueco Bolson and the southern part of the Tularosa Basin bounded by the Hueco Mountains on the east and by the Franklin and southern Organ Mountains on the west. The Rio Grande enters the Hueco Bolson at El Paso del Norte between the Franklin Mountains and Sierra Juarez and flows southeast across the bolson.

El Paso, Texas, and Ciudad Juarez, Mexico, are the major cities in the Hueco Bolson. The southern boundary of the study area was extended to include El Paso and Juarez because ground-water withdrawals near these metropolitan areas add a significant stress to fresh ground-water supplies in the study area. Fort Bliss, in New Mexico and Texas, and suburban communities, including Chaparral, New Mexico, also lie within the area of study.

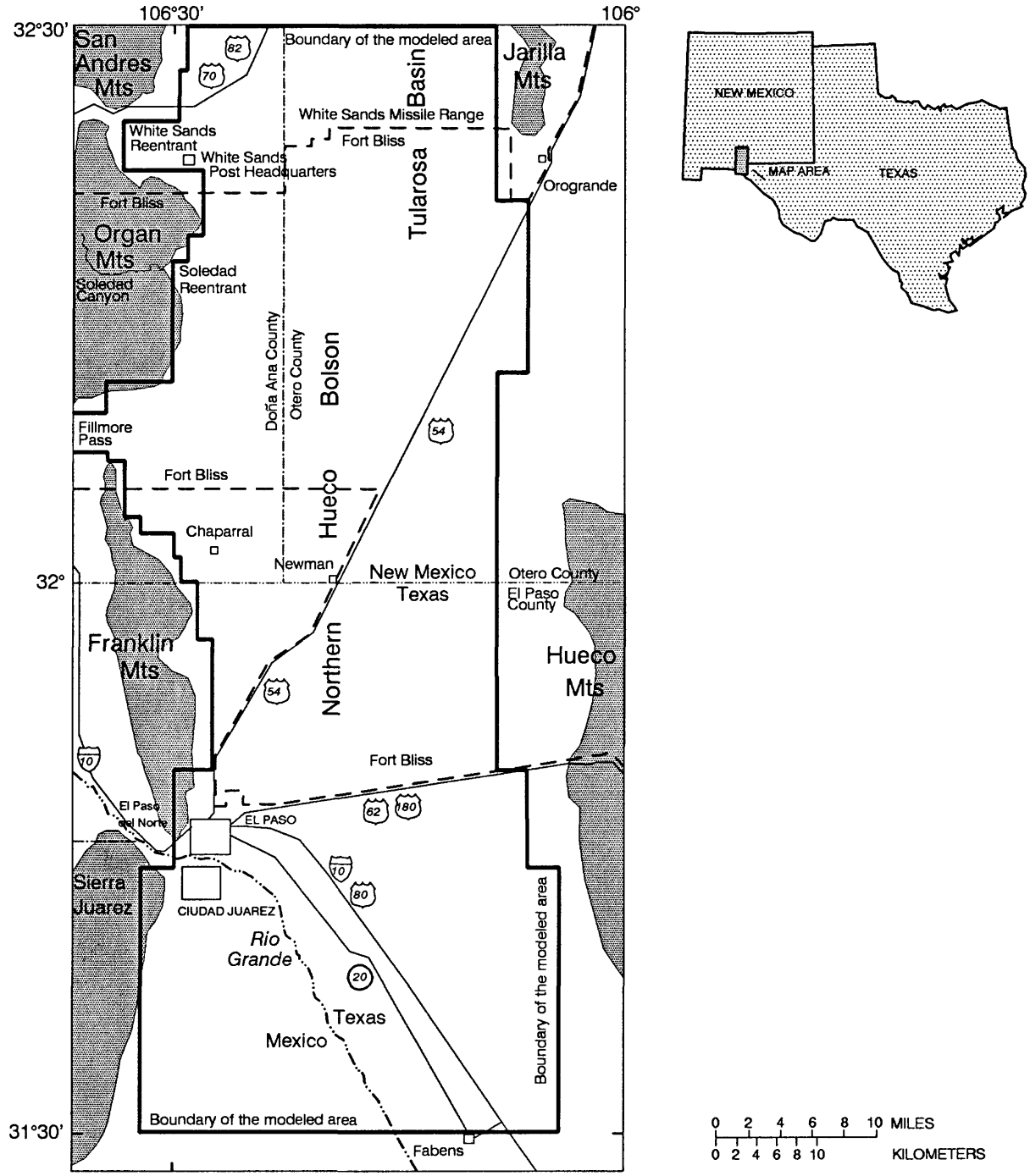

Figure 1.--Location of the study area.

Previous Studies

The Hueco Bolson has been the subject of numerous hydrologic studies throughout this century. For a bibliographic listing of more than 60 publications describing many of these studies, refer to Orr and White (1985). Slichter (1905) and Richardson (1909) described the area when there was very little ground-water development.

Hydrologic data reports of the El Paso area include reports by Scalapino and Irelan (1949), Leggat (1962), Davis (1965), and Meyer and Gordon (1972a). A comprehensive report on ground water in the El Paso area was written by Sayre and Livingston (1945), and a similar report on the Hueco Bolson was prepared by Knowles and Kennedy (1958a). Alvarez and Buckner (1980) compiled an extensive data base of water-level measurements, chemical analyses, and records of salinity of water withdrawn from irrigation wells completed in the Rio Grande alluvium. White (1983) summarized the water situation in the El Paso area from 1903 to 1980 using maps, graphs, and tables. Land and Armstrong (1985) presented an assessment of potential land-surface subsidence in El Paso.

A number of modeling studies of the Hueco Bolson have been conducted that simulated ground-water declines that could be expected under future pumping conditions. Leggat and Davis (1966) developed an analog model of the Hueco Bolson; Meyer (1976) also analyzed the area using a digital model. Knowles and Alvarez (1979) simulated effects of ground-water withdrawals in parts of the Hueco Bolson. G.E. Groschen (U.S. Geological Survey, written commun., 1987) simulated the three-dimensional movement of saline water in the Hueco Bolson.

Systems of Numbering Wells

The system of numbering wells in New Mexico is based on the common subdivision of public lands into sections. The well number, in addition to designating the well, locates its position to the nearest 10-acre tract in the land network. The well number is divided by periods into four segments. The first segment denotes the township north or south of the New Mexico Base Line; the second denotes the range east or west of the New Mexico Principal Meridian; the third denotes the section (fig. 2). All wells in the New Mexico part of the Hueco Bolson are in townships south of the base line and east of the principal meridian. The fourth segment of the number, which consists of three digits, denotes the 160-, 40-, and 10-acre tracts in which the well is located in the section. For this purpose, the section is divided into four quarters, numbered 1, 2, 3, and 4, for the northwest, northeast, southwest, and southeast quarters, respectively. The first digit of the fourth segment gives the quarter section, which is a tract of 160 acres. Similarly, the quarter section is divided into four 40-acre tracts numbered in the same manner, and the second digit denotes the 40-acre tract. Finally, the 40-acre tract is divided into four 10-acre tracts, and the third digit denotes the 10-acre tract. Thus, well 23S.5E.10.413 is in the SW 1/4 of the NW 1/4 of the SE 1/4, section 10, township 23 south, range 5 east (fig. 2). The letters a, b, c, and so on are added to designate the second, third, fourth, and succeeding wells in the same 10-acre tract.

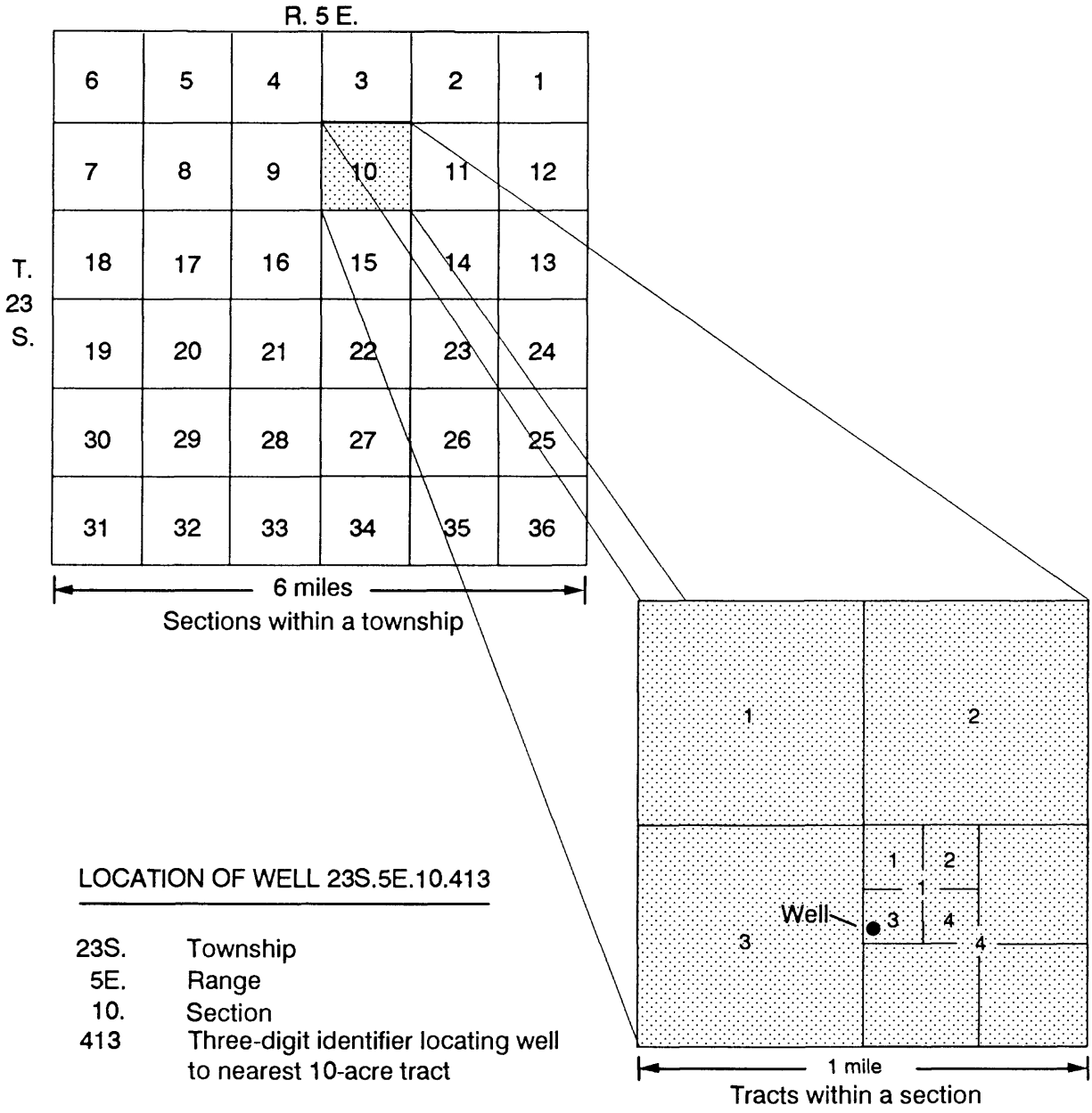

Figure 2.--System of numbering wells in New Mexico.

The well-numbering system used in this report for the Texas part of the Hueco Bolson is that used by the Texas Water Development Board (fig. 3). Under this system, which is based on latitude and longitude, each 1-degree quadrangle in the State is given a two-digit number from 01 through 89. These are the first two digits of the well number. El Paso County is in parts of quadrangles 48 and 49.

Each 1-degree quadrangle is subdivided into 7.5-minute quadrangles that are each given a two-digit number from 01 to 64. These are the third and fourth digits of the well number. Each 7.5-minute quadrangle is further subdivided into 2 1/2-minute quadrangles that are each given a single-digit number ranging from 1 through 9. This is the fifth digit of the well number. Finally, each well within a 2 1/2-minute quadrangle is given a two-digit number in the order in which the well was inventoried, starting with 01. These are the last two digits of the well number.

GEOHYDROLOGY

Evaluation of the occurrence of water in the northern part of the Hueco Bolson is dependent upon an understanding of the ground-water flow system, ground-water quality, and the interaction between ground-water and surface-water flow systems. Storage and movement of water through basin-fill deposits and the distribution of water-quality zones are determined by hydrologic characteristics of these deposits, by structural features that serve as hydrologic boundaries, and by the distribution of recharge from precipitation.

Lithologic and Structural Distribution

The northern part of the Hueco Bolson contains Tertiary and Quaternary basin-fill sedimentary deposits. These basin-fill deposits extend northward into the Tularosa Basin and southward into the southern part of the Hueco Bolson. A series of west-to-east geologic sections constructed by Seager and others (1987) depict the Hueco Bolson as a downfaulted basin characterized by a series of subparallel step faults forming a deep structural bedrock trough on the west side of the basin. Many of these step faults extend to the surface, offsetting basin-fill deposits. Data from geophysical surveys and deep test wells indicate that this structural trough contains the thickest section of basin-fill deposits in the Hueco Bolson (fig. 4).

Seager and others (1987) indicated that the thickness of basin-fill deposits ranges from zero on the east to possibly 8,000 feet along the deepest part of the trough. The approximate areal distribution of thickness of basin-fill deposits is shown in figure 5, constructed from surface-geophysical sounding data and borehole data.

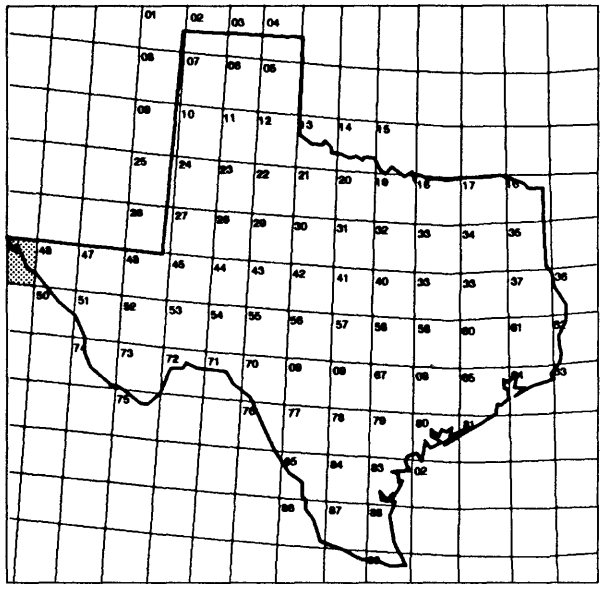

1-degree quadrangles

LOCATION OF WELL 49-06-701

49 1-degree quadrangle

06 $7\frac{1}{2}$-minute quadrangle

7 $2\frac{1}{2}$-minute quadrangle

01 Well number within the $2\frac{1}{2}$-minute quadrangle

01 **49**	02	03	04	05	06	07	08
09	10	11	12	13	14	15	16
17	18	19	20	21	22	23	24
25	26	27	28	29	30	31	32
33	34	35	36	37	38	39	40
41	42	43	44	45	46	47	48
49	50	51	52	53	54	55	56
57	58	59	60	61	62	63	64

$7\frac{1}{2}$-minute quadrangles

1 **06**	2	3
4	5	6
7 ● 01 Well	8	9

$2\frac{1}{2}$-minute quadrangles

Figure 3.--System of numbering wells in Texas.

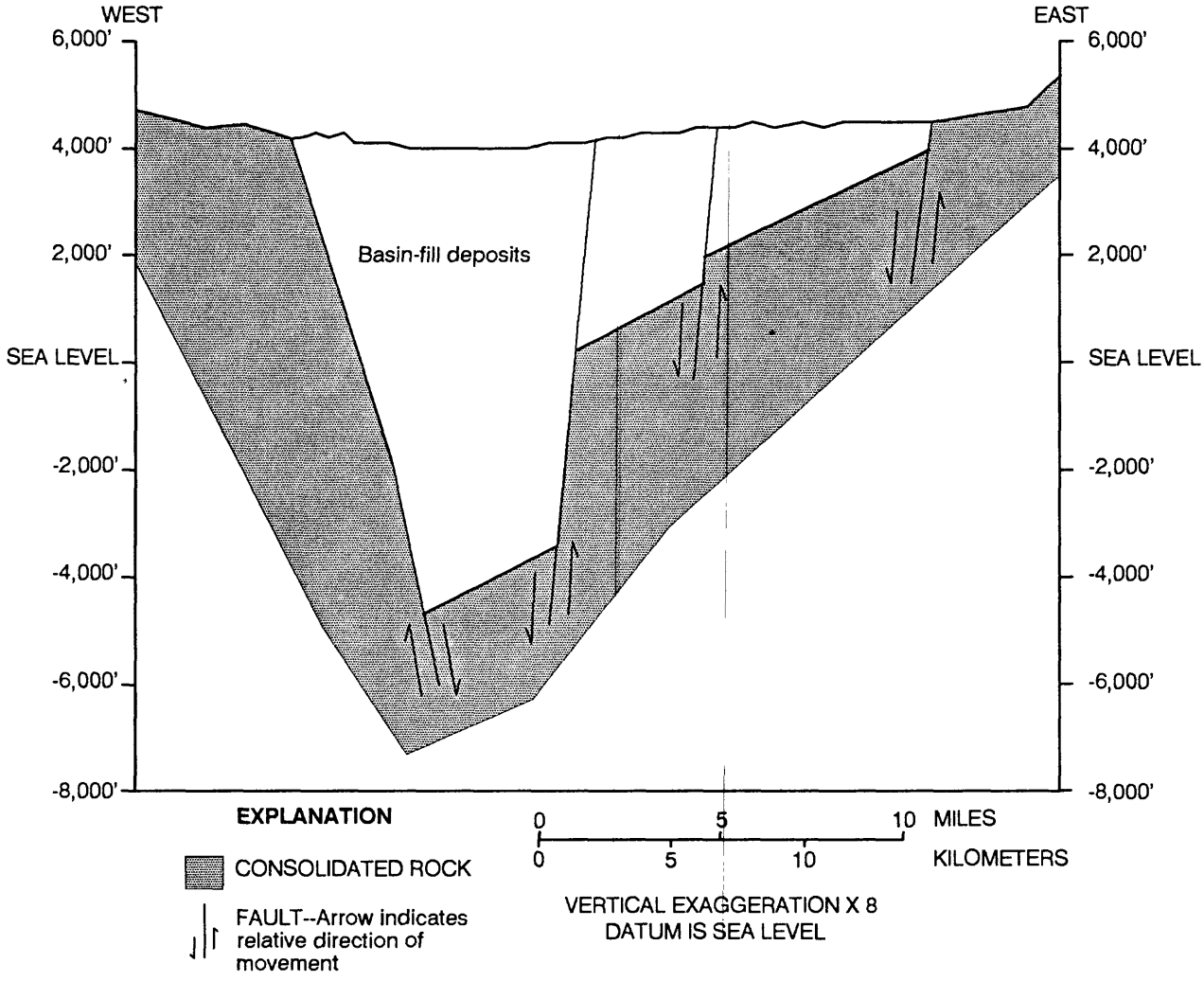

Figure 4.--Generalized west-to-east geologic section of the Hueco Bolson.

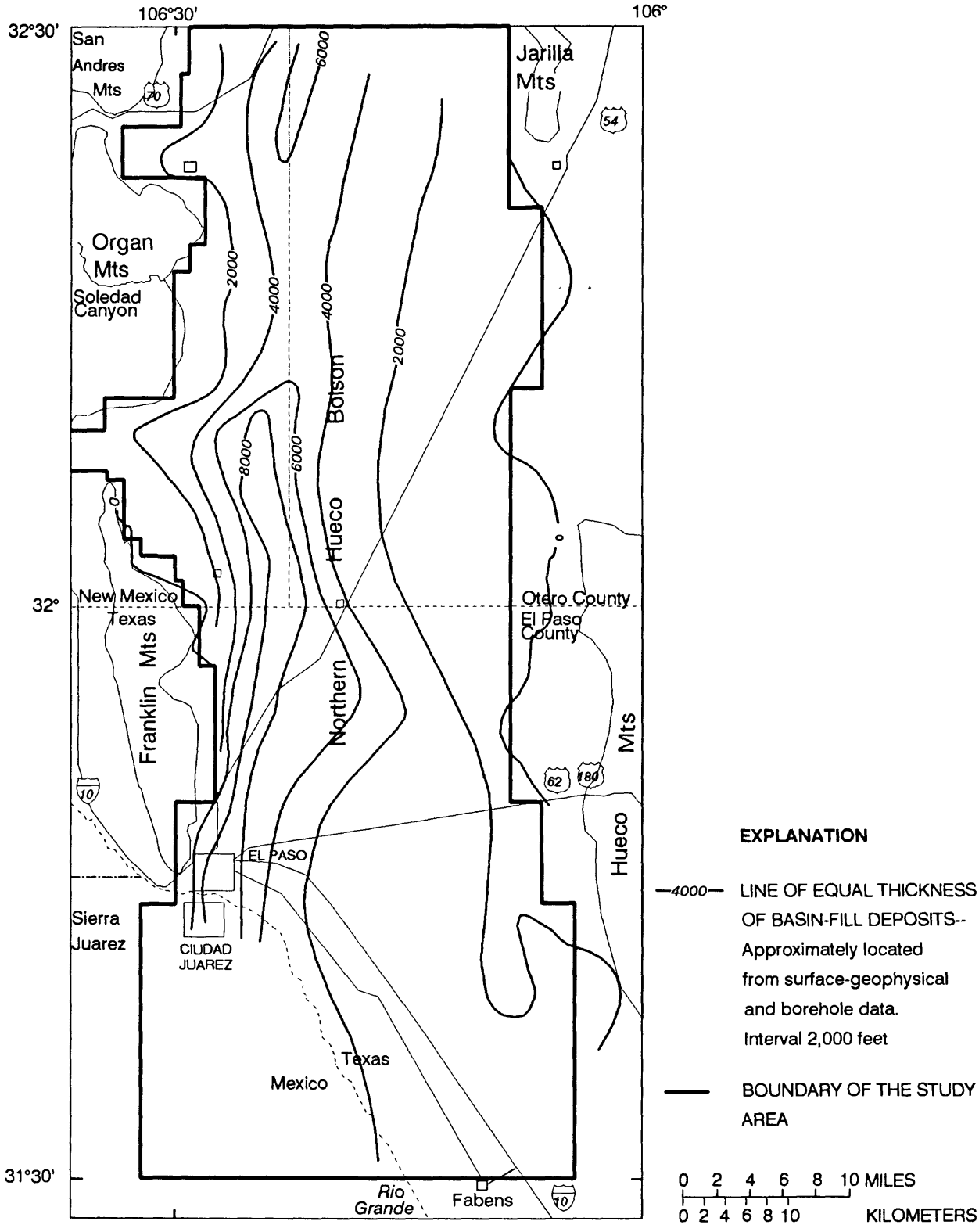

Figure 5.--Thickness of basin-fill deposits.

Basin-fill deposits of the Hueco Bolson include sand, gravel, silt, and clay of fluvial and alluvial-fan deposits; fine-grained, lacustrine deposits of the central basin; and surficial, eolian sand deposits. A composite map showing the approximate percentage of sand in the basin-fill deposits (fig. 6) was constructed using sand-percentage and clay-percentage maps (Kelly, 1973, p. 20; Land and Armstrong, 1985, p. 37) and recent borehole information. The largest percentages of sand occur on the west side of the basin (fig. 6). Generally, grain size decreases eastward and with depth, with an increasing percentage of clay and a corresponding decrease in hydraulic conductivity.

Basin-fill deposits are bounded by less permeable carbonate rocks of the Hueco Mountains to the east; by less permeable igneous, metamorphic, and sedimentary rocks of the Organ and Franklin Mountains to the west; and by similar less permeable consolidated rock below (fig. 4). Basin-fill deposits are in hydraulic continuity with deposits of the Tularosa Basin to the north and with deposits of the southern Hueco Bolson to the southeast.

Fluvial deposits of the Camp Rice Formation of Strain (1966, 1969) of the Santa Fe Group (King and others, 1971, p. 16) occur at or near land surface throughout much of the northern part of the Hueco Bolson (Seager and others, 1987). Geophysical and lithologic logs indicate that the thickness of these Tertiary and Quaternary deposits may be as much as 1,000 feet in places. Underlying the fluvial deposits are closed-basin deposits that include lacustrine clay and evaporites bordered by alluvial-fan sand, gravel, and clay. These typically fine grained deposits may comprise most of the lithologic sequence of the Hueco Bolson.

Distal fan and fluvial deposits in Fillmore Pass (fig. 1) between the Organ and Franklin Mountains may provide some hydraulic connection between the Hueco Bolson and the Mesilla Basin to the west. However, a comparatively steep eastward hydraulic gradient through Fillmore Pass and highly mineralized water west of the pass indicate that these deposits may be characterized by small permeability, precluding movement of large quantities of ground water through the pass. Surface-geophysical soundings (Zohdy and others, 1969; Bisdorf, 1985) and test drilling (Orr and White, 1985) indicate that Fillmore Pass is an upthrown bedrock block overlain by fluvial deposits equivalent to the Camp Rice Formation of the Santa Fe Group. Saturated sediments may be less than 400 feet thick over this horst.

Aquifer Characteristics

Hydrologic properties that determine the movement of water through porous media include horizontal and vertical hydraulic conductivity and storage coefficient. The hydrologic properties of the basin-fill deposits need to be known to define the conceptual model of the hydrologic system. In unconsolidated basin-fill deposits, these properties vary widely, depending upon lithology and sorting.

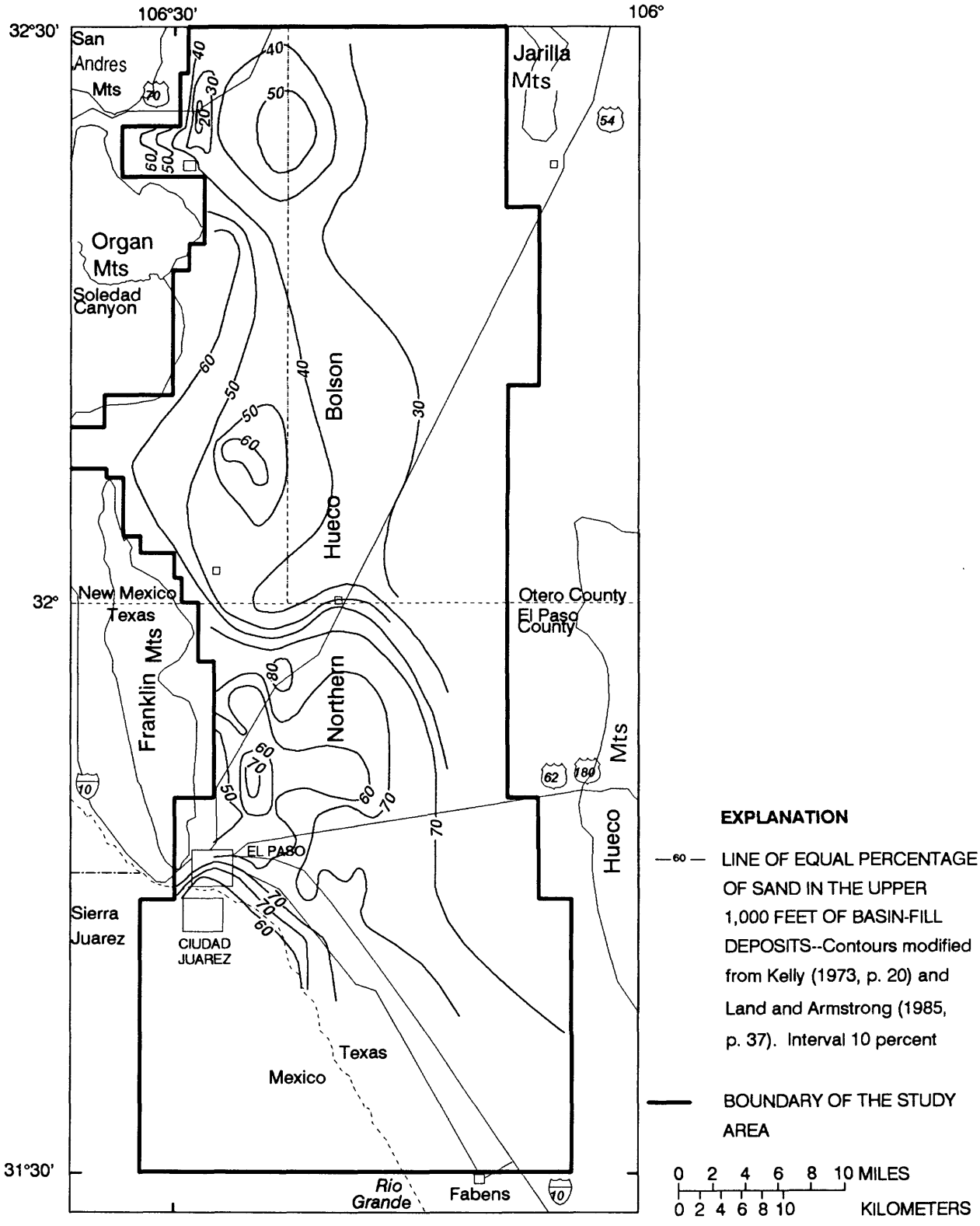

Figure 6.--Approximate percentage of sand in the upper 1,000 feet of basin-fill deposits.

Coarse-grained alluvial-fan deposits near mountain fronts are characterized by relatively large hydraulic conductivity. Fine-grained fan deposits and lacustrine deposits basinward are characterized by relatively small hydraulic conductivity. Large ratios of horizontal to vertical hydraulic conductivity are due to discontinuous, thinly bedded clay units throughout much of the basin-fill deposits. Aquifer-test results in wells in the Hueco Bolson (Knowles and Kennedy, 1958a, p. 33; Herrick, 1960, p. 98) indicate that the small ratio of vertical to horizontal hydraulic conductivity results in delayed drainage of water from overlying deposits and that, in the long term, the storage coefficient should approach the specific yield of an unconfined aquifer.

Hydraulic Conductivity

Hydraulic conductivity, the capability of a unit area of an aquifer to transmit water, can be estimated by dividing transmissivity by the aquifer thickness. Hydraulic-conductivity estimates were derived from aquifer tests in wells in the western half of the Hueco Bolson. Most of these wells penetrate only the upper 1,000 feet or less of basin-fill deposits. Based upon these aquifer-test data, hydraulic-conductivity estimates for basin-fill deposits range from less than 1 to more than 200 feet per day.

Knowles and Kennedy (1958a, p. 33) reported a range in transmissivity of 5,000 to 22,000 feet squared per day from aquifer tests in wells on the west side of the Hueco Bolson in Texas. Hydraulic-conductivity estimates for these wells range from 15 to 43 feet per day. Hydraulic-conductivity estimates from aquifer tests in wells in Texas belonging to Fort Bliss range from 15 to 19 feet per day.

Meyer (1976, p. 15) indicated that the transmissivity of the freshwater-saturated section of the basin-fill deposits in Texas ranges from 1,300 to 37,000 feet squared per day. Meyer's freshwater-thickness map and transmissivity map (1976, figs. 7 and 8) were used to estimate a range of hydraulic conductivity of 5 to 60 feet per day in the El Paso area.

Additional aquifer tests (Lee Wilson and Associates, Inc., 1986, table 3.6-1) in 64 wells owned by the City of El Paso on the west side of the basin were used to estimate hydraulic conductivity. Estimated hydraulic conductivity from these tests ranges from 6 to 130 feet per day and averages 31 feet per day.

Hydraulic-conductivity estimates for two wells completed in alluvial-fan deposits of the Soledad Canyon reentrant are 50 and 60 feet per day (Orr and Myers, 1986, p. 67). In the White Sands Missile Range Post Headquarters area, hydraulic-conductivity estimates range from about 1 to 210 feet per day (Orr and Myers, 1986, p. 68).

Peterson and others (1984, pls. 11 and 12) indicated that basin-fill deposits on the west side of the Hueco Bolson include approximately 1,000 feet of sand with pebble gravel, clay, silt, and sandstone lenses. Kelly (1973, p. 20) constructed a sand-percentage map for the upper 1,000 feet of basin-fill deposits in the White Sands Missile Range Post Headquarters area. Land and Armstrong (1985, p. 37) constructed a clay-percentage map for El Paso and the surrounding area. Aquifer-test data, lithofacies maps, and geophysical and lithologic well logs were used to estimate the areal distribution of the average hydraulic conductivity for the upper 1,000 feet of basin-fill deposits. The estimated average hydraulic conductivity ranged from about 1 to 40 feet per day.

Limited information on the east side of the bolson indicates that basin-fill deposits primarily consist of fine-grained sand, silt, and clay. Throughout much of the west side of the Hueco Bolson, the percentage of clay increases with depth. Basin-fill deposits underlying the sandy deposits predominantly consist of clay and silt, with sand comprising less than 20 percent of the section (Peterson and others, 1984, pls. 11 and 12). Lohman (1972, p. 53) estimated a range of hydraulic conductivity of 1 to 15 feet per day for unconsolidated clay to fine-grained sand in the Arkansas River valley, Colorado. Walton (1970, p. 36) cited representative hydraulic-conductivity values for clay, silt, and sand ranging from 0.0001 to 13 feet per day. The U.S. Bureau of Reclamation (1977, p. 29) listed a range of hydraulic conductivity for mixtures of sand, silt, and clay of 0.001 to 1 foot per day. The average hydraulic conductivity for fine-grained basin-fill deposits in the Hueco Bolson is estimated to be approximately 2 feet per day.

Little information is available concerning the ratio of horizontal to vertical hydraulic conductivity in the Hueco Bolson. Meyer (1976, p. 17) reported that the vertical hydraulic conductivity between the flood-plain alluvium and the bolson deposits ranges from 1×10^{-7} to 1.3 feet per day, values that are significantly smaller than the estimated values of horizontal hydraulic conductivity. In tests in the Mesilla Valley, estimates of the ratio of horizontal to vertical hydraulic conductivity range from 22 to 319 (Wilson and White, 1984, p. 55). Frenzel and Kaehler (1990, p. 54) used a ratio of horizontal to vertical hydraulic conductivity of 200 in the Regional Aquifer-System Analysis model of the Mesilla Basin. A similar ratio probably occurs in the basin-fill deposits of the Hueco Bolson because of similarities in lithology and depositional history.

Storage Coefficient

Storage coefficients derived from short-term aquifer tests in basin-fill deposits of the Hueco Bolson probably are not representative of those to be expected under long-term pumping because of the large ratio of horizontal to vertical hydraulic conductivity (Knowles and Kennedy, 1958a, p. 33). Storage coefficients derived from a comparison of the volume of water pumped from the Hueco Bolson during several years to the volume of dewatered sediments are similar to those often estimated for water-table aquifers and approach the specific yield of the aquifer. Specific-yield estimates for basin-fill deposits in the northern Hueco Bolson probably provide the closest approximation to the storage coefficient.

Leggat and Davis (1966) estimated that the specific yield of basin-fill deposits is 0.15. Meyer (1976, p. 15) reported that the specific yield of the unconsolidated basin-fill deposits in the Hueco Bolson ranges from 0.10 to 0.30. Walton (1970, p. 34) cited representative ranges of specific yield of 0.01 to 0.10 for clay and 0.10 to 0.30 for sand. Johnson (1967, p. D70) reported an average specific yield of 0.02 to 0.08 for clay and silt and 0.21 to 0.27 for fine to coarse sand.

The large percentage of clay in parts of the Hueco Bolson could effectively result in an average specific yield of less than 0.10. Aquifer dewatering increases lithostatic pressure on underlying sediments. When the lithostatic pressure exceeds the preconsolidation pressure, inelastic compaction of clay occurs, additional water is removed from storage, and long-term specific yield increases. Consolidation due to dewatering could increase the long-term specific yield of clay to as much as 0.30. Specific yield for the saturated sand, gravel, silt, and clay could reasonably range from about 0.05 to 0.30.

Lithofacies maps, borehole-geophysical data, and estimates of specific yield for permeable basin-fill deposits were used to estimate the distribution of specific yield for the upper 1,000 feet of basin-fill deposits. This distribution did not take into account the long-term increase in specific yield resulting from the irreversible removal of water from storage in response to inelastic compaction of fine-grained sediments. Long-term increases in specific yield, however, may be less significant in areas of maximum withdrawals because of a smaller percentage of fine-grained deposits in these areas and a corresponding decrease in potential for inelastic compaction.

Recharge, Evapotranspiration, and Discharge

Subsurface recharge to the northern part of the Hueco Bolson is from the Tularosa Basin and, to a much lesser degree, from the Mesilla Basin (west of the study area) through Fillmore Pass. Surface recharge to basin-fill deposits takes place principally in alluvial fans of the Organ and Franklin Mountains in response to storm runoff. Sayre and Livingston (1945, p. 72) assumed that 25 percent of the precipitation falling on mountain drainage areas reaches the saturated zone. They estimated that mountain-front recharge to the Hueco Bolson is approximately 15,000 acre-feet per year. More recent studies indicate that recharge probably is a smaller percentage of precipitation.

Ballance and Basler (1966, p. 11) estimated that surface-water runoff comprises only 3 percent of the precipitation falling on the White Sands reentrant. Scott (1970, p. 10) estimated that the average annual runoff in the White Sands reentrant is 0.1 percent of total precipitation. Both studies indicate that most of the precipitation either infiltrates or evaporates. Kelly and Hearne (1976, p. 39) estimated that the actual amount of water that reaches the saturated zone is only 3 percent of precipitation and that most precipitation probably infiltrates only the first few feet to evaporate or be transpired later. Meyer (1976, p. 18) estimated that the recharge rate to the basin-fill deposits, including underflow from the White Sands reentrant, is 5,640 acre-feet per year.

Surface drainage areas in the Organ and Franklin Mountains that contribute runoff to the Hueco Bolson encompass approximately 225 square miles. If the average annual rainfall over these drainage areas is 12 inches and actual recharge to the basin-fill deposits is only 3 percent of the available precipitation falling on mountain drainage areas, mountain-front recharge to the Hueco Bolson is approximately 4,300 acre-feet per year.

Evapotranspiration is not a significant component of the ground-water flow system throughout most of the northern part of the Hueco Bolson because ground-water levels generally are deeper than 200 feet. In the Rio Grande valley, however, phreatophytes and ground-water levels as shallow as 10 feet discharge water by evapotranspiration.

Natural discharge from the ground-water flow system occurs as seepage to the Rio Grande. Discharge also occurs from withdrawals for municipal, industrial, and military supplies. Combined pumpage withdrawals from 1900 through 1983 and projected withdrawals through 2030 are shown in figure 7. By 1983, combined withdrawals, including municipal, industrial, and military pumpage, were approximately 140,000 acre-feet per year. If the present (1983) withdrawal trend is projected, estimated withdrawals could exceed 300,000 acre-feet per year by 2030. This trend probably represents a scenario for maximum ground-water development.

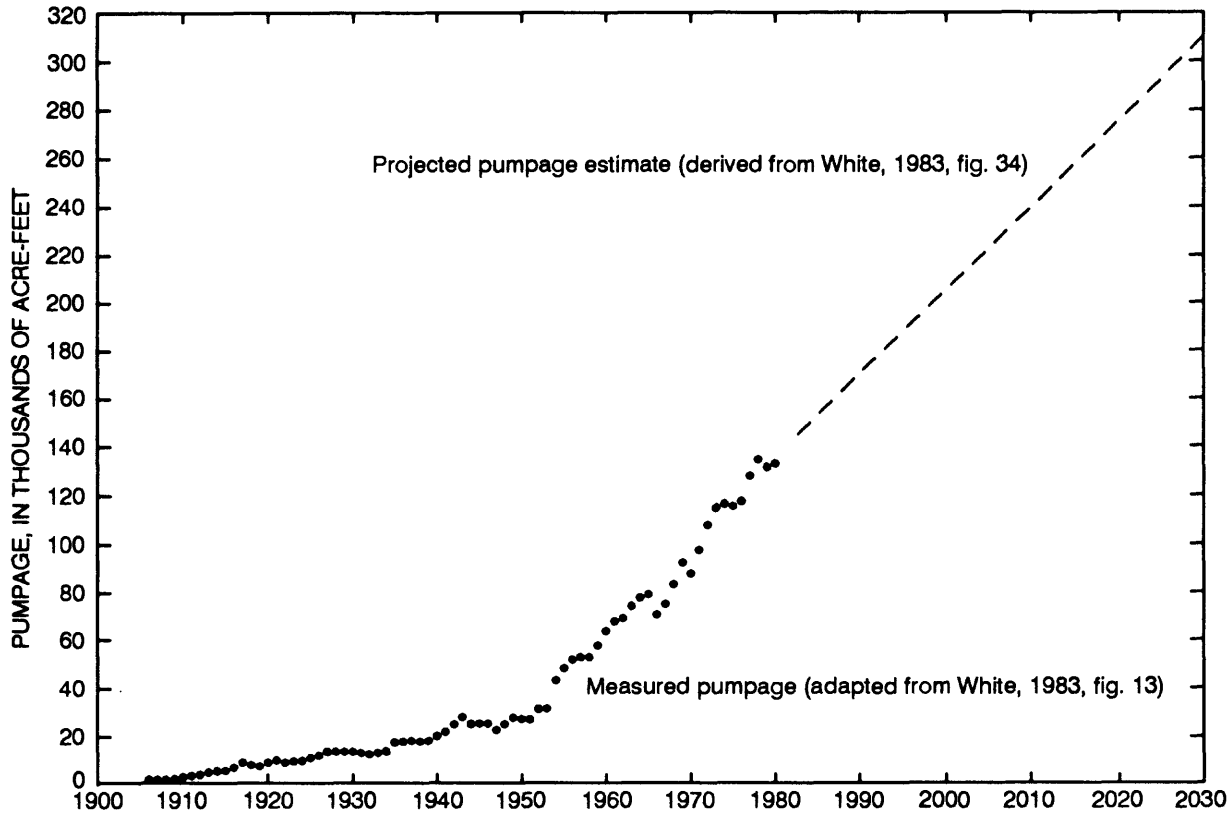

Figure 7.--Measured (1900-83) and projected (through 2030) pumping stresses for the Hueco Bolson.

Ground-Water/Surface-Water Relation

Ground-water recharge and discharge are closely related to the occurrence of surface water in the Hueco Bolson. Throughout most of the northern part of the bolson, the surface-water flow system is ephemeral, predominantly consisting of poorly defined arroyo channels, many of which terminate in depressions and playas at the lower ends of alluvial fans. Overland flow commonly occurs during periods of intense storm activity.

Flow in the Rio Grande and associated irrigation canals is controlled largely by releases from upstream reservoirs, although some peak flows occur in response to storm-water runoff downstream from the reservoirs. Flow fluctuates seasonally, depending upon irrigation requirements downstream.

Long-term records of discharge in the Rio Grande are available for several stations in the Hueco Bolson area (International Boundary and Water Commission, 1984). For the period of record from 1938 to 1984, the average discharge for the Rio Grande at El Paso was 500 cubic feet per second, or about 363,000 acre-feet per year. Largest average discharges occurred during June, July, and August. Smallest average discharges during the period of record occurred during November, December, January, and February.

The Rio Grande and the flood-plain alluvium in the southern part of the northern Hueco Bolson act as hydrologic boundaries to the overall flow system. Seepage from the Rio Grande provides additional recharge to the ground-water flow system near El Paso where the altitude of the potentiometric surface is lower than the altitude of the river because of ground-water pumpage. Conversely, downstream from El Paso, where the potentiometric surface is higher than the river, water discharges to the Rio Grande from the ground-water flow system. River conductance, a function of the vertical hydraulic conductivity of the flood-plain alluvium and the head differential between the river and the aquifer, controls the movement of water between the river and the ground-water flow system. In the Mesilla Valley, vertical hydraulic-conductivity estimates ranged from 0.2 to 3 feet per day (Wilson and White, 1984, p. 28). An approximation of vertical hydraulic conductivity of about 0.3 foot per day, based upon seepage-run and head-differential data in the Mesilla Basin, and an average thickness of 100 feet for the flood-plain alluvium were used to estimate a riverbed conductance per river mile of approximately 2,200 feet squared per day.

Water Budget

The northern part of the Hueco Bolson is part of a complex network of interrelated components (fig. 8). Ground water moves southward into the Hueco Bolson from the Tularosa Basin. Water from precipitation enters the regional flow system primarily as mountain-front recharge from storm runoff to alluvial fans adjacent to the Organ and Franklin Mountains. Recharge to basin-fill deposits on the east side of the basin is minimal because surface drainages from the Hueco Mountains predominantly drain eastward toward the Salt Basin (east of the study area) and because basin-fill sediments near the Hueco Mountains are fine grained.

Shallow ground-water levels in the Rio Grande valley allow evaporation and transpiration from the ground-water flow system. Elsewhere, ground-water levels are too deep to permit evapotranspiration. Evaporation also takes place from the open-water surface of the river.

A network of drains along the Rio Grande has lowered shallow ground-water levels, possibly decreasing evaporation and transpiration losses from the flood plain to the atmosphere and increasing ground-water return flow to the river. Irrigation diversions, canals, and drains may have increased evaporation losses of surface water; infiltration from canals, ditches, and fields recharges the ground-water flow system. Supplemental irrigation pumpage has occurred in years when surface-water supplies have been limited. Some water diverted for irrigation has been used consumptively and some has been returned to the Rio Grande as irrigation-return and drain flow.

Population increases since the early 1900's have required extensive development of available water resources for agricultural, municipal, industrial, and military use. Ground-water pumpage is now a significant component of discharge from the ground-water system. Surface water also is diverted for supplemental municipal and industrial use. Effluent from waste-treatment facilities constitutes an addition to surface water and, on an experimental basis through artificial recharge, to ground water in storage. Some municipal and industrial water is removed from the system by consumptive use.

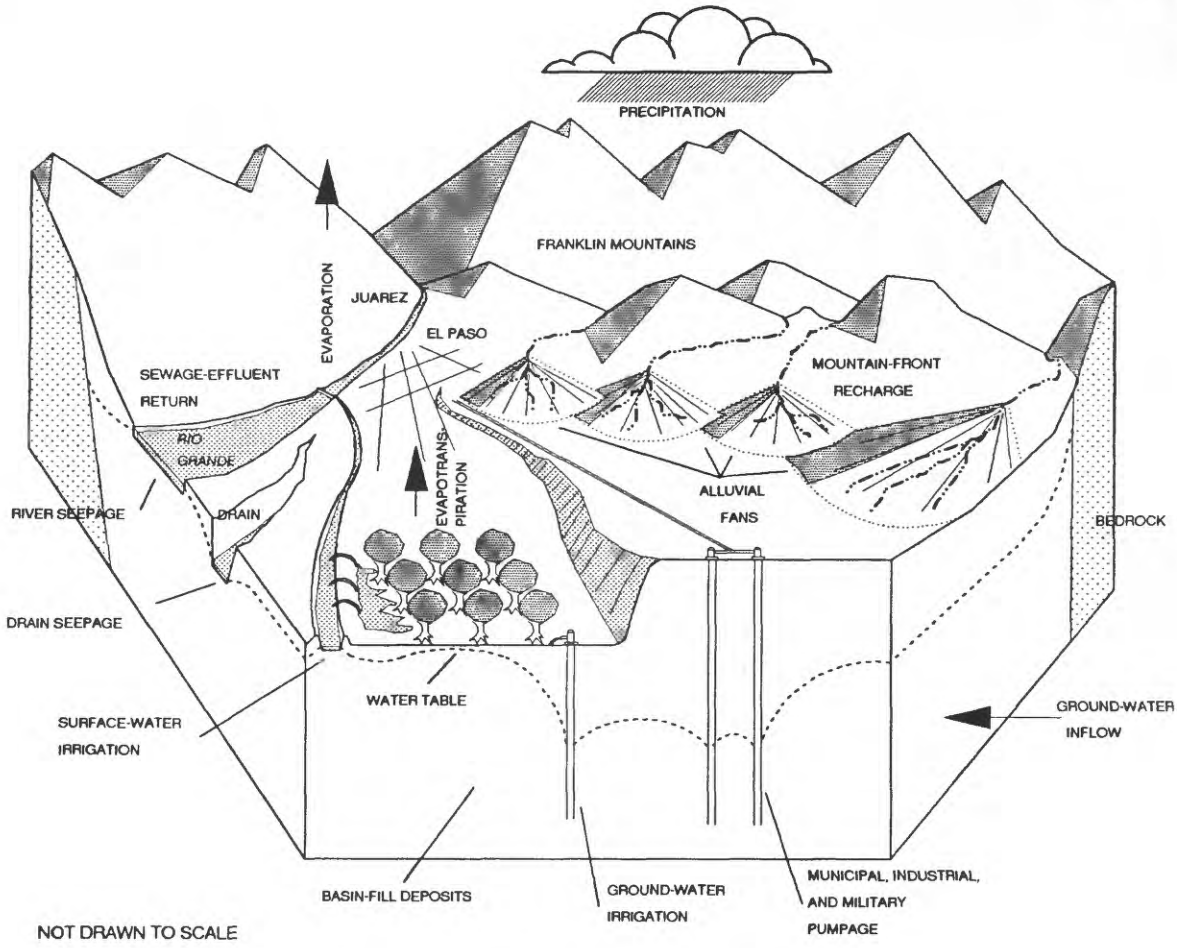

Figure 8.--Water budget for the Hueco Bolson.

DESCRIPTION OF THE GROUND-WATER FLOW MODEL

The model developed to simulate three-dimensional flow in the Hueco Bolson used the Geological Survey modular flow program (McDonald and Harbaugh, 1988). This program employs the finite-difference method to approximate the partial differential equation governing three-dimensional movement of ground water of constant density through porous earth material (McDonald and Harbaugh, 1988, p. 2-1 to 2-2). The model consists of a variable grid spacing of 51 rows and 35 columns (fig. 9). The size of the smallest cell is 0.5 mile on a side and the largest is 3 miles on a side. The grid columns are oriented in a north-to-south direction.

The model consists of three layers. The top layer simulates unconfined conditions and includes the upper 600 to 800 feet of saturated deposits. On the west side of the basin, this layer includes a lithologic sequence that is predominantly sand and gravel and is characterized by relatively large hydraulic conductivity. With several exceptions, the base of layer 1 was set at 3,100 feet above sea level to simulate the transition from upper fluvial deposits to the underlying lacustrine deposits. Layer 1 cells simulating the White Sands reentrant and alluvial fans south along the Organ Mountains were assigned bases ranging from 3,450 to 3,900 feet above sea level to represent displacement along basin-margin fault zones. On the basis of geophysical logs, the bases of cells simulating underflow through Fillmore Pass were assigned an altitude of 3,500 feet to represent uplifted bedrock in the pass. Cells simulating flow in alluvial fans east of the Franklin Mountains were assigned bases ranging from 3,500 to 3,650 feet above sea level, again to represent displacements along the basin-margin fault zone. Layers 2 and 3 each simulate an interval approximately 700 feet thick that consists of thinly interbedded clay and sand lenses. Underlying basin-fill deposits predominantly consist of small-permeability lacustrine clay. The model effectively treats these small-permeability deposits as a no-flow boundary.

Boundary conditions can be represented in the model as constant-flux, constant-head, or head-dependent-flux boundaries. At a constant-flux boundary, water is added or extracted at a constant rate and the hydraulic head is allowed to vary. A no-flow boundary is a specific constant-flux boundary at which no water is added or extracted. At a constant-head boundary, the potentiometric head is held constant and flux through the boundary is allowed to vary dependent upon the hydraulic gradient. At a head-dependent-flux boundary, the amount of water added or extracted across the boundary is allowed to vary in response to head changes.

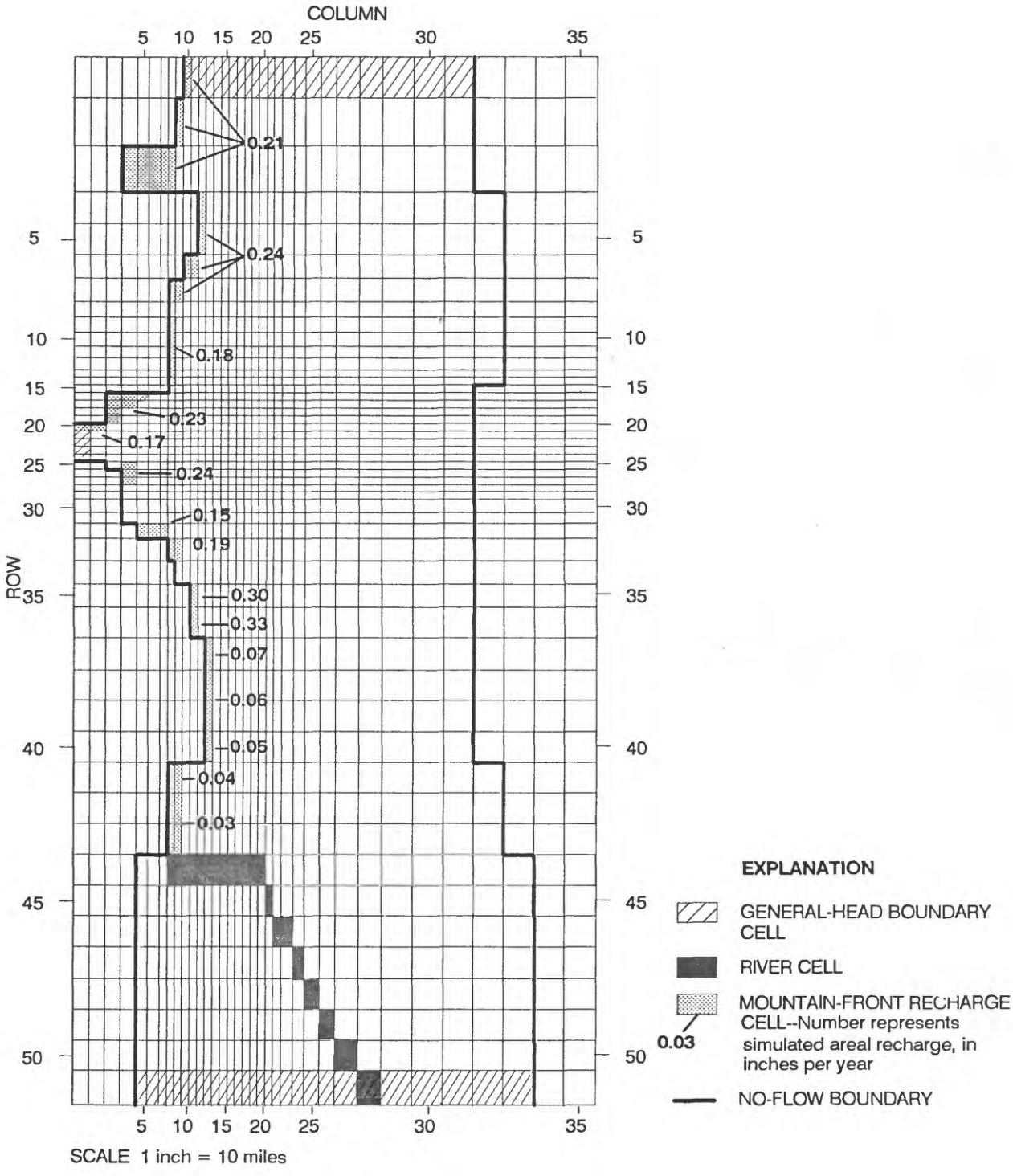

Figure 9.--Model grid and boundaries, adjusted distribution of recharge, and river cells.

Saturated basin-fill deposits in the Hueco Bolson are bounded on the east by a westward-dipping bedrock surface and on the west by uplifted bedrock of the Organ and Franklin Mountains. Bedrock boundaries are represented in the model by no-flow boundaries (fig. 9). The general head boundary package (McDonald and Harbaugh, 1988, p. 11-1) was used to simulate underflow from the Tularosa Basin to the north, underflow to the southern part of the Hueco Bolson, and underflow through Fillmore Pass. The general head boundary helped to decrease the effect of pumpage stresses on these artificial head-dependent boundaries (fig. 9). General head boundaries used in the model employ head-dependent boundary conditions based upon specified heads at some distance outside the model and upon conductance terms derived from the distribution of hydraulic conductivity, the vertical nodal areas at the boundary, and the distances from the boundaries to the specified heads. Measured water levels in three wells outside the model boundaries on White Sands Missile Range, in four wells in Fillmore Pass, and in six wells south of El Paso were used to derive specified heads. The hydraulic-conductivity values of cells at the boundary, the cross-sectional areas of cells parallel to the boundary, and the distances from the boundary to the specified head were used to estimate the conductance terms for the general head boundary. Table 1 shows the location of general-head boundary cells, water-level altitudes, and aquifer-conductance values.

The Rio Grande was simulated across the southwestern corner of the model using the river package (McDonald and Harbaugh, 1988, p. 6-1). Simulated flow of water between the river and the top layer is dependent upon a conductance value derived from the vertical hydraulic conductivity of the streambed material, the thickness of the streambed material, the stream-channel area, and upon the difference in heads between the stream and the aquifer. Flow in irrigation canals, drains, and sewage-effluent returns in the valley was combined with flow in the river because of the coarseness of the model grid in that area. The river was simulated for 21 cells in layer 1 (fig. 10). Table 2 shows the location of river cells, river-stage altitude, and the conductance of the riverbed material assigned to each cell.

Although evapotranspiration from the Rio Grande valley constitutes a major component of ground-water discharge from the valley, no attempt was made to simulate discharge resulting from evapotranspiration because the principal focus of the study was to define flow systems in the New Mexico part of the Hueco Bolson. Hydrologic conditions in the southernmost part of the study area, including the river and the southern model boundary, are not well represented in the model. Refer to the section on model sensitivity for additional discussion about the effect of poorly represented river and model boundaries on simulations.

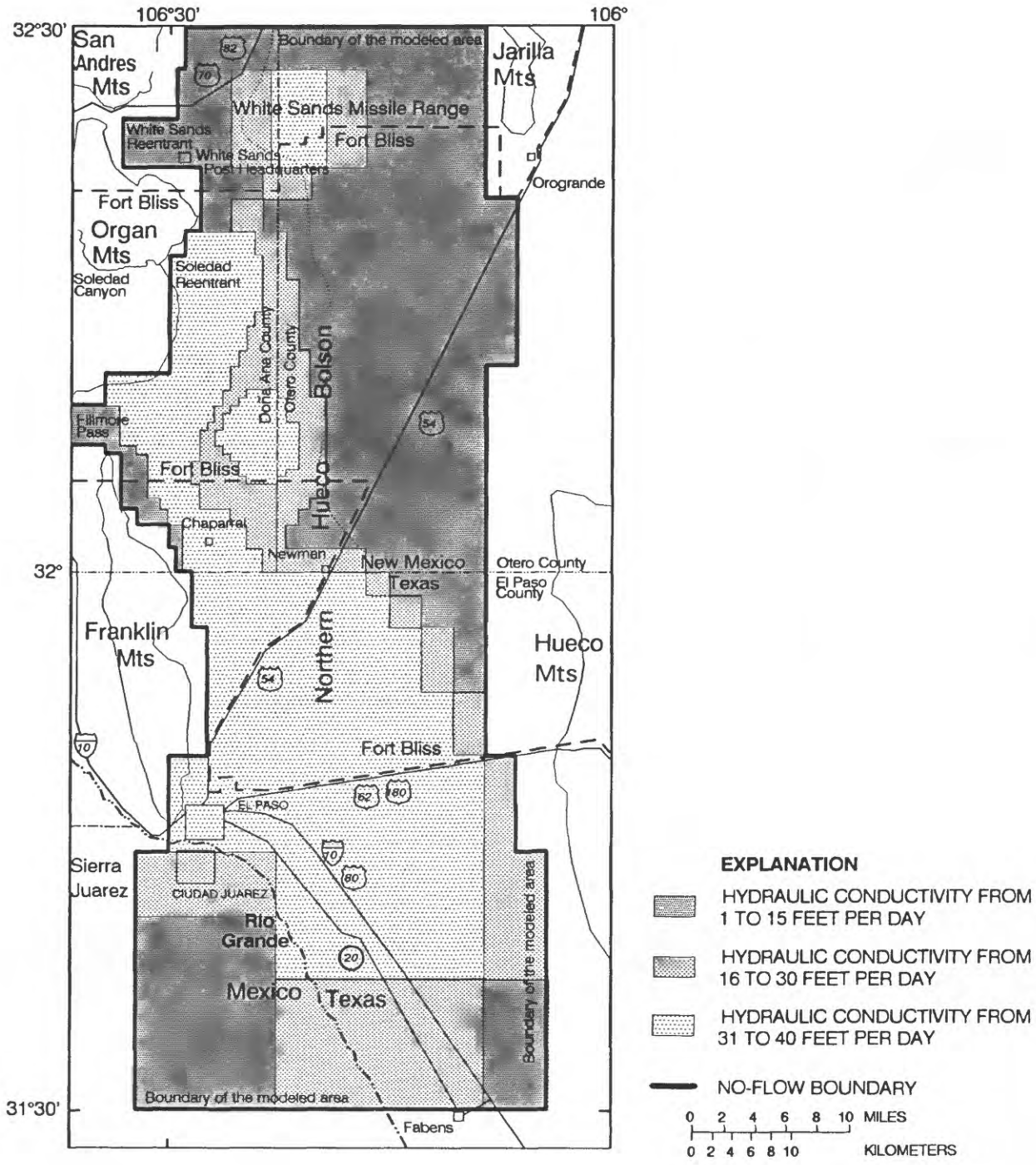

Figure 10.--Adjusted hydraulic conductivity for model layer 1.

Table 1.--Cell locations, altitude of water levels, and aquifer-conductance values used to simulate general head boundaries in the Hueco Bolson model

[Cell location: L, layer; R, row; C, column]

Cell location			Water-level altitude, in feet above sea level	Aquifer conductance, in feet squared per day	Cell location			Water-level altitude, in feet above sea level	Aquifer conductance, in feet squared per day
L	R	C			L	R	C		
1	1	14	3,882	1,250	1	51	17	3,638	1,018
1	1	15	3,876	1,250	1	51	18	3,637	1,018
1	1	16	3,872	1,250	1	51	19	3,636	1,018
1	1	17	3,866	1,250	1	51	20	3,635	1,018
1	1	18	3,860	1,250	1	51	21	3,634	1,018
1	1	19	3,854	1,250	1	51	22	3,632	2,240
1	1	20	3,848	1,250	1	51	23	3,630	3,361
1	1	21	3,842	1,250	1	51	24	3,628	3,361
1	1	22	3,837	1,250	1	51	25	3,624	4,481
1	1	23	3,830	1,875	1	51	26	3,620	4,481
1	1	24	3,827	1,875	1	51	27	3,616	6,722
1	1	25	3,826	2,500	1	51	28	3,612	6,722
1	1	26	3,828	2,500	1	51	29	3,607	8,963
1	1	27	3,832	1,500	1	51	30	3,603	8,963
1	1	28	3,840	1,500	1	51	31	3,595	8,963
1	1	29	3,848	2,000	1	51	32	3,586	4,074
1	1	30	3,859	2,000	1	51	33	3,580	4,074
1	1	31	3,869	2,000	2	1	14	3,882	233
1	20	1	3,816	5,180	2	1	15	3,876	233
1	21	1	3,816	5,180	2	1	16	3,872	233
1	22	1	3,816	5,180	2	1	17	3,866	233
1	23	1	3,816	5,180	2	1	18	3,860	233
1	24	1	3,816	5,180	2	1	19	3,854	233
1	51	5	3,655	1,527	2	1	20	3,848	233
1	51	6	3,654	1,527	2	1	21	3,842	233
1	51	7	3,652	1,018	2	1	22	3,837	233
1	51	8	3,651	1,018	2	1	23	3,830	350
1	51	9	3,650	1,018	2	1	24	3,827	350
1	51	10	3,648	1,018	2	51	5	3,655	389
1	51	11	3,647	1,018	2	51	6	3,654	389

Table 1.--Cell locations, altitude of water levels, and aquifer-conductance values used to simulate general head boundaries in the Hueco Bolson model--Concluded

Cell location			Water-level altitude, in feet above sea level	Aquifer conductance, in feet squared per day	Cell location			Water-level altitude, in feet above sea level	Aquifer conductance, in feet squared per day
L	R	C			L	R	C		
1	51	12	3,646	1,018	2	51	7	3,652	259
1	51	13	3,644	1,018	2	51	8	3,651	259
1	51	14	3,643	1,018	2	51	9	3,650	259
1	51	15	3,642	1,018	2	51	10	3,648	259
1	51	16	3,640	1,018	2	51	11	3,647	259
2	51	12	3,646	259	3	1	23	3,830	350
2	51	13	3,644	259	3	1	24	3,827	350
2	51	14	3,643	259	3	51	5	3,655	389
2	51	15	3,642	259	3	51	6	3,654	389
2	51	16	3,640	259	3	51	7	3,652	259
2	51	17	3,638	259	3	51	8	3,651	259
2	51	18	3,637	259	3	51	9	3,650	259
2	51	19	3,636	259	3	51	10	3,648	259
2	51	20	3,635	259	3	51	11	3,647	259
2	51	21	3,634	259	3	51	12	3,646	259
2	51	22	3,632	259	3	51	13	3,644	259
2	51	23	3,630	389	3	51	14	3,643	259
3	1	14	3,882	233	3	51	15	3,642	259
3	1	15	3,876	233	3	51	16	3,640	259
3	1	16	3,872	233	3	51	17	3,638	259
3	1	17	3,866	233	3	51	18	3,637	259
3	1	18	3,860	233	3	51	19	3,636	259
3	1	19	3,854	233	3	51	20	3,635	259
3	1	20	3,848	233	3	51	21	3,634	259
3	1	21	3,842	233	3	51	22	3,632	259
3	1	22	3,837	233	3	51	23	3,630	389

Table 2.--Cell locations, river-stage altitude, and riverbed-conductance values used to simulate the Rio Grande in the Hueco Bolson model

Cell location			River-stage altitude, in feet above sea level	Riverbed conductance, in feet squared per day	Altitude of riverbed base, in feet above sea level
Layer	Row	Column			
1	44	8	3,711	1,080	3,611
1	44	9	3,708	1,512	3,608
1	44	10	3,706	1,080	3,606
1	44	11	3,703	1,512	3,603
1	44	12	3,701	1,512	3,601
1	44	13	3,698	1,296	3,598
1	44	14	3,696	1,296	3,596
1	44	15	3,693	1,296	3,593
1	44	16	3,691	1,296	3,591
1	44	17	3,688	1,512	3,588
1	44	18	3,686	1,296	3,586
1	44	19	3,683	1,296	3,583
1	44	20	3,679	3,456	3,579
1	45	21	3,674	1,728	3,574
1	46	22	3,671	1,296	3,571
1	46	23	3,667	3,456	3,567
1	47	24	3,661	2,376	3,561
1	48	25	3,655	4,320	3,555
1	49	26	3,645	6,912	3,545
1	50	27	3,631	7,560	3,531
1	51	28	3,620	7,560	3,520

Simulation of Steady-State Conditions

The flow system prior to development (assumed steady state) was simulated by adjusting recharge and hydraulic conductivity within plausible ranges to obtain the best fit between measured and simulated water levels. Because steady-state conditions were assumed, the storage coefficient was not used.

Extensive development of freshwater supplies began in the El Paso area in 1903. In northern areas of the Hueco Bolson, where development of groundwater resources has been minimal, 1903 water-level data are not available. Because steady-state water-level data were not available for the entire basin, earliest available water levels were compared with the results of the steady-state simulation. Simulated water levels were compared with measured water levels from 59 wells (table 3).

Model Adjustments

The approach used to simulate steady-state conditions in the northern part of the Hueco Bolson was to develop an approximate distribution of recharge and hydraulic conductivity. Plausible adjustments were made to recharge and hydraulic conductivity in ensuing simulations until a reasonable match between measured and simulated water levels was obtained.

Most recharge was assigned to cells corresponding to the mouths of canyons draining large areas (fig. 9). Adjustments were made to the rate and distribution of recharge to better match measured and simulated water levels. Adjusted steady-state simulations used an annual recharge rate of 4,500 acre-feet, which is 3.1 percent of the total estimated precipitation over mountain drainages. The adjusted distribution of annual recharge used in the model is shown in figure 9.

Initially, hydraulic-conductivity values derived from aquifer-test data, lithofacies maps (fig. 6), and borehole information were assigned to corresponding model blocks in layer 1. The distribution and magnitude of hydraulic conductivity for layer 1 were adjusted by modifying hydraulic conductivity within reasonable ranges to match measured and simulated steady-state water levels. Hydraulic-conductivity values assigned to model cells generally were largest on the west, gradually becoming smaller eastward, and represent the west-to-east trend of decreasing hydraulic conductivity that occurs as a function of decreasing grain size with distance from source areas.

Adjusted hydraulic-conductivity values for layer 1 ranged from 1 to 40 feet per day (fig. 10). Because aquifer-test data were not available for most of the area being simulated, the hydraulic-conductivity values shown in figure 10 are grouped into three ranges of hydraulic conductivity to preclude a false assumption of precision. A uniform hydraulic conductivity of 2 feet per day, within the plausible range of hydraulic conductivity for clay, silt, and fine-grained sand, was assigned to layers 2 and 3 to simulate the large percentage of fine-grained sediments that generally occurs below a depth of 1,000 feet. The transmissivity of layers 2 and 3 was estimated by multiplying the thickness of each layer by the assumed hydraulic conductivity.

Table 3.--Measured and simulated steady-state water levels for selected wells in the northern Hueco Bolson, in feet above sea level

Well		Cell location		Date (month and year)	Measured water level	Simulated water level	Difference (feet
Name	Location	Row	Column				
T-1	22.4.01.444	2	9	7-53	3,921	3,901	20
T-3	22.4.14.211	3	9	5-53	4,061	4,058	3
T-2	22.4.13.222	3	9	5-53	3,925	3,873	52
SW10	22.4.24.212	3	9	8-53	3,913	3,873	40
SW4	22.5.32.314	4	12	5-53	3,888	3,874	14
SW6	22.5.32.312	4	12	1-53	3,868	3,874	-6
SW5	22.5.32.331	4	12	4-47	3,887	3,874	13
SW8	22.5.32.334	4	12	1-53	3,874	3,874	0
F-1	23.5.35.431	8	17	4-53	3,772	3,785	-13
F-2	23.5.36.332	8	19	4-36	3,793	3,785	8
G-1	23.6.35.124	8	27	3-53	3,793	3,785	8
F-3	24.5.20.341	13	12	6-53	3,755	3,773	-18
F-5	24.5.28.241	14	14	4-43	3,758	3,771	-13
F-4	24.5.33.221	15	14	4-36	3,764	3,770	-6
G-2	24.7.34.233	17	30	7-53	3,758	3,766	-8
L-1	25.6.04.121	18	24	3-53	3,751	3,764	-13
R-15	25.4.11.141	20	6	4-36	3,747	3,765	-18
R-13	25.4.18.234	22	2	5-54	3,819	3,797	22
M-1	25.7.16.122	22	29	3-54	3,746	3,757	-11
L-8	25.6.20.334	25	23	3-54	3,736	3,755	-19
R-16	25.4.35.121	27	6	1-54	3,746	3,759	-13
L-2	25.5.30.344	27	10	5-53	3,738	3,757	-19
L-4	25.5.27.333	27	15	4-53	3,725	3,755	-30
M-2	25.6.28.444	27	25	4-53	3,729	3,751	-22
L-3	25.5.31.343	29	9	4-36	3,739	3,755	-16
L-5	25.5.35.342	29	17	6-37	3,734	3,751	-17
L-9	26.5.07.422	31	10	6-37	3,769	3,750	19
L-10	26.5.19.133	33	9	3-54	3,803	3,749	54
L-11	26.5.21.443	33	14	3-54	3,712	3,740	-28
L-13	26.5.24.144	33	19	6-54	3,716	3,738	-22
M-4	26.7.22.211	33	29	-30	3,722	3,729	-7
L-12	26.5.33.142	35	13	1-54	3,722	3,732	-10
R-2	5-205	35	15	5-40	3,724	3,731	-7
M-6	26.6.34.143	35	25	6-36	3,716	3,723	-7
M-8	26.6.33.244	35	25	2-37	3,723	3,723	0

Table 3.--Measured and simulated steady-state water levels for selected wells in the northern Hueco Bolson, in feet above sea level--Concluded

Well		Cell location		Date (month and year)	Measured water level	Simulated water level	Difference (feet)
Name	Location	Row	Column				
M-5	26.7.31.223	35	28	1-54	3,713	3,720	-7
S-2		35	30	8-35	3,712	3,716	-4
R-9	5-313	36	17	8-35	3,716	3,725	-9
R-10	5-508	37	14	6-40	3,709	3,720	-11
R-11	5-502	37	14	4-40	3,711	3,720	-9
R-14	6-403	37	21	1-42	3,705	3,717	-12
S-6	6-502	37	25	4-36	3,708	3,715	-7
R-22	5-905	38	16	7-36	3,700	3,713	-13
R-20	5-908	38	18	12-40	3,701	3,713	-12
R-18	6-705	38	22	11-40	3,697	3,711	-14
R-17	6-704	38	24	9-40	3,702	3,710	-8
S-7		38	25	10-40	3,700	3,710	-10
S-11		39	30	3-36	3,699	3,699	0
R-42	13-206	40	14	6-39	3,690	3,702	-12
R-39	13-211	40	14	4-39	3,677	3,702	-25
R-47	13-310	40	17	8-35	3,692	3,702	-10
R-50	13-306	40	20	12-40	3,690	3,701	-11
R-53	13-205	41	14	8-37	3,686	3,696	-10
V-2	13-501	41	14	8-35	3,671	3,696	-25
	13-508	42	13	-13	3,686	3,693	-7
	14-502	42	26	6-36	3,688	3,689	-1
	14-613	42	28	7-36	3,684	3,687	-3
	15-901	44	31	4-36	3,674	3,674	0
	22-201	45	25	6-47	3,668	3,675	-7

The simulated steady-state water surface was comparable to earliest measured water levels. However, adjustment of the model to the estimated distribution of recharge and hydraulic conductivity does not constitute a unique solution. Errors introduced into the model resulting from uncertainties in the amount and location of recharge and in the distribution of hydraulic conductivity are discussed in the section on model sensitivity.

Simulation Results

The purpose of the steady-state simulation was to estimate the initial hydraulic-head distribution for the transient model. Figure 11 is a map of the simulated steady-state potentiometric surface in the northern part of the Hueco Bolson. From the contours, the steady-state hydraulic gradient through much of the modeled area ranged from 2.5 to 4 feet per mile with a general flow direction to the south. Contours are only approximate because measured predevelopment water-level data that could be used to adjust the steady-state simulation are lacking for most areas. Simulated hydraulic-head differences between layers 1, 2, and 3 were negligible. The largest differences generally were less than 5 feet, and occurred in areas where recharge flux was applied to layer 1.

Simulated water levels in 51 model cells were compared with early measured water levels in 59 wells (table 3). The arithmetic mean difference between measured and simulated water levels was -5.03 feet. The mean absolute difference was 13.61 feet. The maximum absolute difference was 54 feet.

Although measured steady-state water levels are not available, graphical comparison of early measured and simulated water levels (fig. 12) provides an indication of the extent to which the model represents steady-state conditions. Some variability between measured and simulated water levels may be attributed to the fact that simulated water levels are compared as if they were located at the center of the model cell, whereas wells may be located anywhere within the cell. Assuming a head gradient to the south of 2 to 5 feet per mile, the actual water level within a cell 2 miles in length could vary 4 to 10 feet. Some wells for which historical water-level data are available have been surveyed to known benchmarks. However, the altitudes of many well-measuring points have been interpolated from topographic-contour maps. For these wells, the typical error associated with the determination of the water-level altitude is one-half the contour interval (plus or minus 10 feet, in this case).

Absolute differences greater then 20 feet were observed in several cells near boundaries. In most cases, these differences probably were caused by relatively large cells that preclude an exact simulation of local boundary effects, due, in part, to the block-centered finite-difference method used in the model.

Additional discrepancies between measured and simulated water levels may result because early water levels in some areas were measured in the 1930's, 1940's, and 1950's, after pumping stresses already had caused some decline in water levels. Simulated steady-state water levels in these areas would be somewhat higher than early measured water levels. Figure 13, the frequency distribution of the difference between early and simulated water levels, shows that simulated water levels generally are higher than measured water levels.

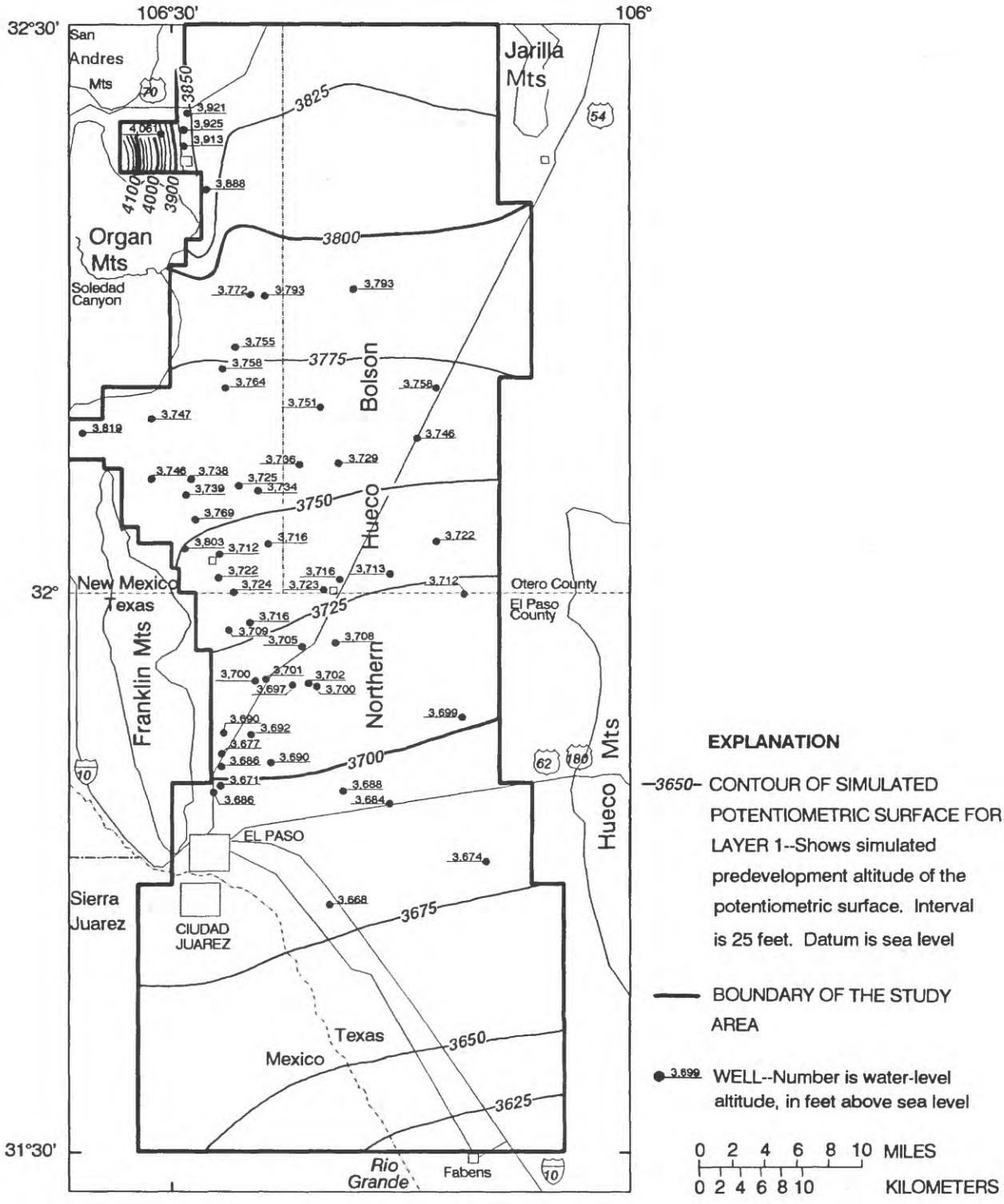

Figure 11.--Simulated steady-state potentiometric surface (1903) and measured predevelopment water levels.

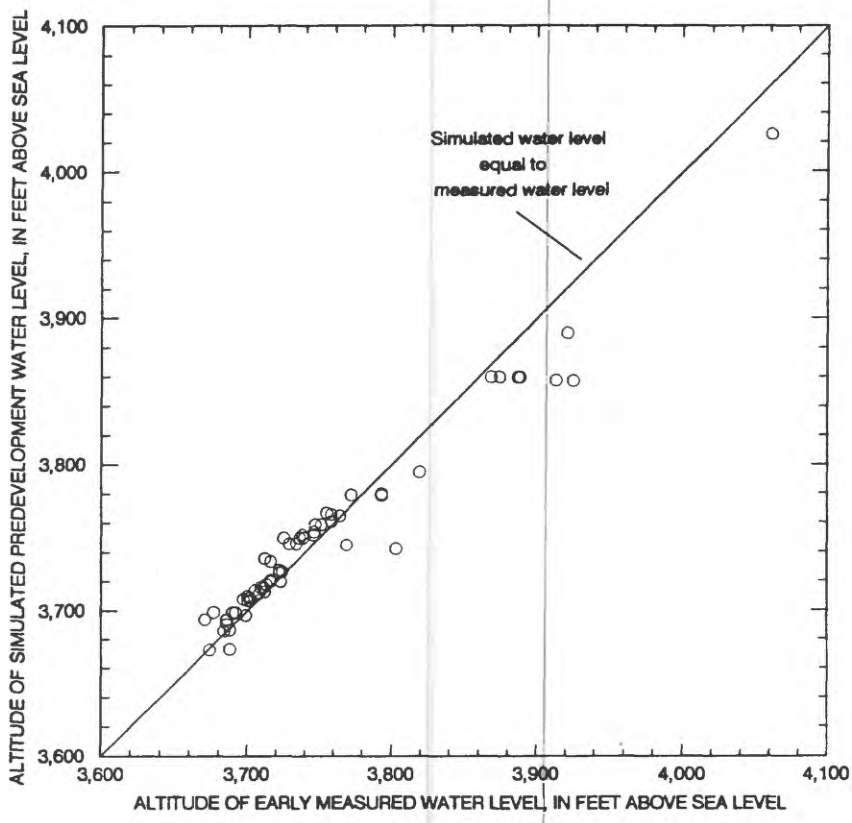

Figure 12.--Relation between simulated predevelopment and early measured water levels.

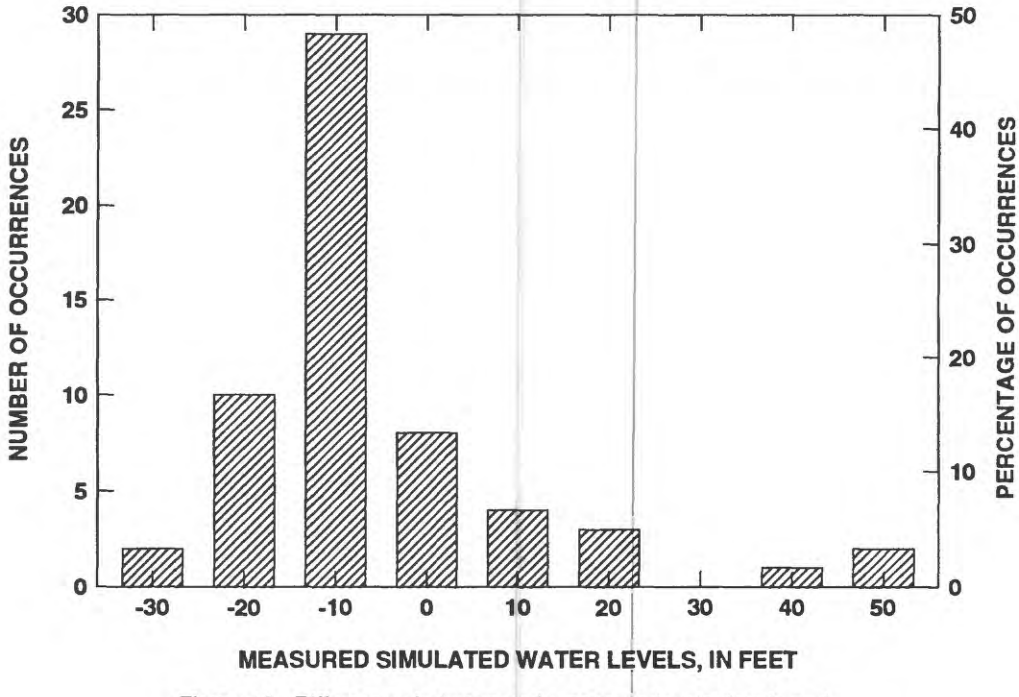

Figure 13.--Differences between early measured water levels and simulated steady-state water levels.

The computed water budget for the steady-state simulation (table 4) shows that simulated mountain-front and river recharge comprised 60 percent of the model inflow (about 5,900 acre-feet per year). The remainder included about 3,700 acre-feet per year as simulated underflow from the Tularosa Basin to the north and about 260 acre-feet per year as underflow through Fillmore Pass. About 82 percent of the underflow into the model across the north boundary took place in layer 1, with the remainder divided evenly between layers 2 and 3. Simulated discharge to the Rio Grande (1,100 acre-feet per year) comprised 11 percent of the total outflow. Most of the flow out of the model area was across head-dependent boundaries as underflow to the south (7,800 acre-feet per year). About 95 percent of this underflow took place in layer 1 with the remainder divided evenly between layers 2 and 3.

Table 4.--Steady-state water budget

[Simulated flow rates are rounded in the text to preclude a false assumption of precision]

Description	Rate of flow, in acre-feet per year
Sources	
Storage	0
Mountain-front recharge	4,499
River leakage	1,396
Head-dependent flux	4,004
Total	9,899
Discharges	
River leakage	1,084
Head-dependent flux	8,981
Total	10,065
Sources minus discharges	-166
Percentage difference	-1.66

Simulation of Transient-Flow Conditions (1905 through 1983)

Simulated steady-state water levels were used as initial water levels for the transient flow model. Known stresses, including withdrawals and changes in recharge, were then superimposed on this steady-state system. Pumpage withdrawals in the El Paso-Ciudad Juarez area, in the study area but south of the New Mexico part of the Hueco Bolson, were added because of the significant influence that they have had on the regional flow system. Major ground-water withdrawals since the early 1900's have consisted of municipal pumpage for El Paso and Ciudad Juarez, industrial and agricultural pumpage, and military pumpage. Pumping stresses in New Mexico have included military pumpage at Fort Bliss training facilities and White Sands Missile Range, and irrigation- and public-supply pumpage in the Chaparral area.

Simulated stress periods and simulated average withdrawal for each stress period (fig. 14) represent the combined ground-water withdrawals through 1983 shown in figure 7. Municipal and industrial pumpage in the El Paso area was simulated by determining the number of wells pumping during a particular stress period, dividing the simulated withdrawal by the number of wells, and assigning the resultant withdrawal to the cell in which each pumping well was located. Detailed pumping stresses for each well in the El Paso area were not precisely defined in this simulation because El Paso, although in the modeled area, is south of the New Mexico part of the Hueco Bolson and because the model grid near El Paso would have to be very finely subdivided.

The period from 1905 through 1983 was divided into 11 stress periods (fig. 14) ranging from 4 to 10 years in length. Combined simulated pumpage stresses increased from approximately 3,600 acre-feet per year in stress period 1 (1905 through 1914) to approximately 144,000 acre-feet per year in stress period 11 (1980 through 1983). Flow to the aquifer from recharge wells was added during stress periods 5, 10, and 11 to simulate artificial recharge by injection wells.

Model Adjustments

Simulated water-level changes with time at specific cells were compared with measured water-level changes in wells located in these cells. Specific yield was estimated by adjusting the specific yield previously estimated from lithofacies maps and well data to obtain a better match between these water levels. No attempt was made to simulate long-term changes in specific yield due to compaction because little is known about the temporal and spatial distribution of these changes. Subsequently, some bias may be introduced into the transient simulation of ground-water flow. The adjusted specific yield for layer 1 (fig. 15) ranged from 0.05 to 0.20, within the plausible range of specific yield for the Hueco Bolson.

A confined storage coefficient of 0.001 was assigned to layers 2 and 3, approximately derived using Lohman's technique for estimating storage by multiplying the aquifer thickness by 0.000001 (Lohman, 1972, p. 8). No adjustment was made to the storage coefficient for layers 2 and 3.

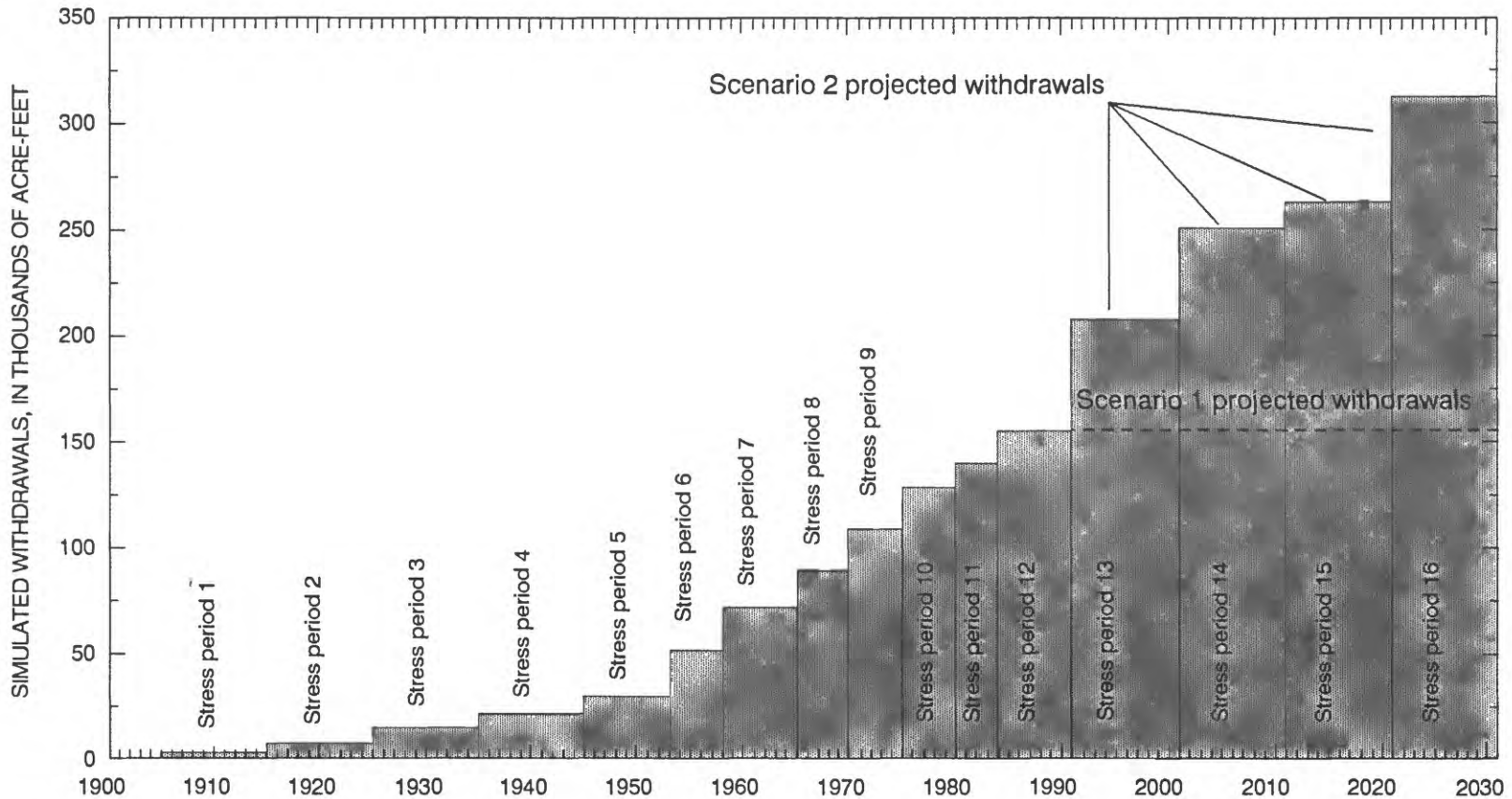

Figure 14.--Simulated stress periods and total simulated ground-water withdrawals from the Hueco Bolson model, including projected withdrawals for scenarios 1 and 2 through 2030.

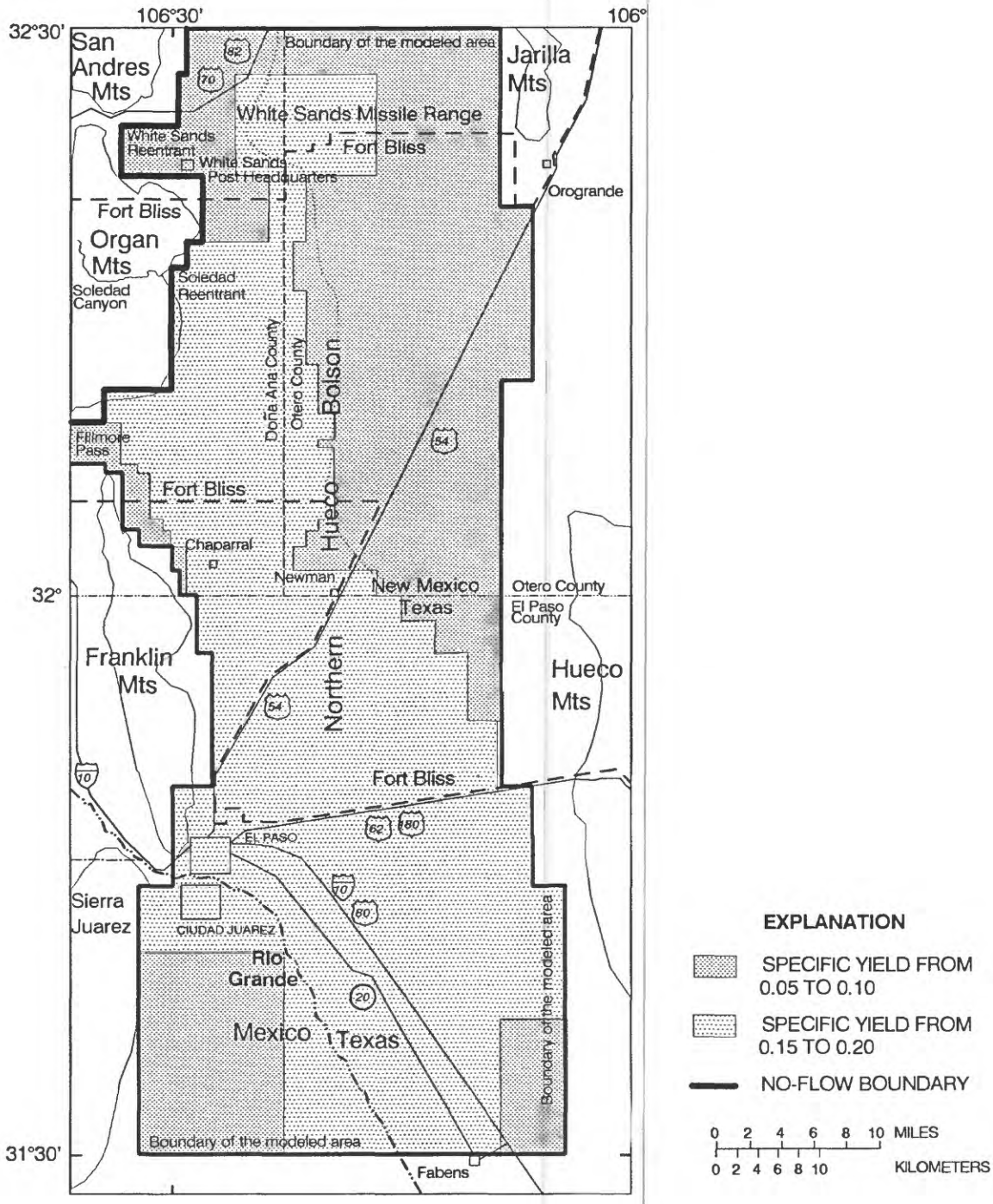

Figure 15.--Adjusted specific yield for model layer 1.

Hydrographs (fig. 16) show measured water levels (through 1985) and simulated water levels for the transient period (through 1983) and for projected simulations (through 2030) for 18 wells and corresponding model cells. Simulated water levels in most of these wells are within approximately 15 feet of measured water levels, and simulated water-level trends reflect measured trends. Exceptions include cells 20-6, 23-2, 26-23, and 33-14. Cell 20-6 is in close proximity to major faults adjacent to Fillmore Pass along which consolidated rock was uplifted to the west, resulting in a flow boundary. Hydrologic conditions resulting from basin-margin fault boundaries that locally were not well simulated could account for the 20 feet of hydraulic-head difference between simulated water levels and measured water levels in wells K-15 and K-29. Cell 23-2 encompasses the horst in Fillmore Pass. The measured water levels in well K-13 represent the potentiometric surface east of the horst, whereas simulated water levels represent the center of the cell. Simulated and measured heads in cells 26-23 and 33-14 have approximately 20 feet of hydraulic-head difference; however, trends in simulated water levels approximate trends in measured water levels. In cells 35-22 and 35-28, divergent trends between simulated water levels and measured water levels may be the result of too large a hydraulic conductivity in the vicinity of these cells.

Simulation Results

The simulated potentiometric surface for layer 1 in 1983 is shown in figure 17. Ground-water flow was to the south, and the hydraulic gradient at the New Mexico-Texas State line ranged from 5 to 9 feet per mile. Examination of figure 17 shows that, by 1983, a significant portion of ground-water flow was toward the El Paso-Ciudad Juarez pumping center. Comparison of the 1983 potentiometric surface to the simulated steady-state surface shows that water levels throughout much of the northern part of the Hueco Bolson had declined. Potentiometric contours drawn from water levels measured in the early 1980's are also shown in figure 17. These contours, although subjective, provide some measure of the hydraulic-head difference between the simulated and measured potentiometric surface.

A map showing simulated water-level declines for layer 1 from 1905 through 1983 was constructed from steady-state and transient water levels (fig. 18). The maximum simulated decline of 200 feet at the end of the transient simulation occurred in the El Paso-Ciudad Juarez area. White (1983, fig. 14) indicated that actual declines in the Ciudad Juarez area exceeded 115 feet by 1980. Land and Armstrong (1985, p. 44) cited water-level declines in the Hueco Bolson aquifer of as much as 150 feet in the same area by 1984. Larger simulated declines may be the result of poorly defined hydrologic boundary conditions in the Ciudad Juarez area. Simulation results indicate that by 1983, water-level declines of about 25 feet had occurred at the New Mexico-Texas State line. White (1983, fig. 30) showed similar declines at the State line. Simulated water-level declines occurred over most of the northern part of the Hueco Bolson in New Mexico. These declines generally were less than 25 feet.

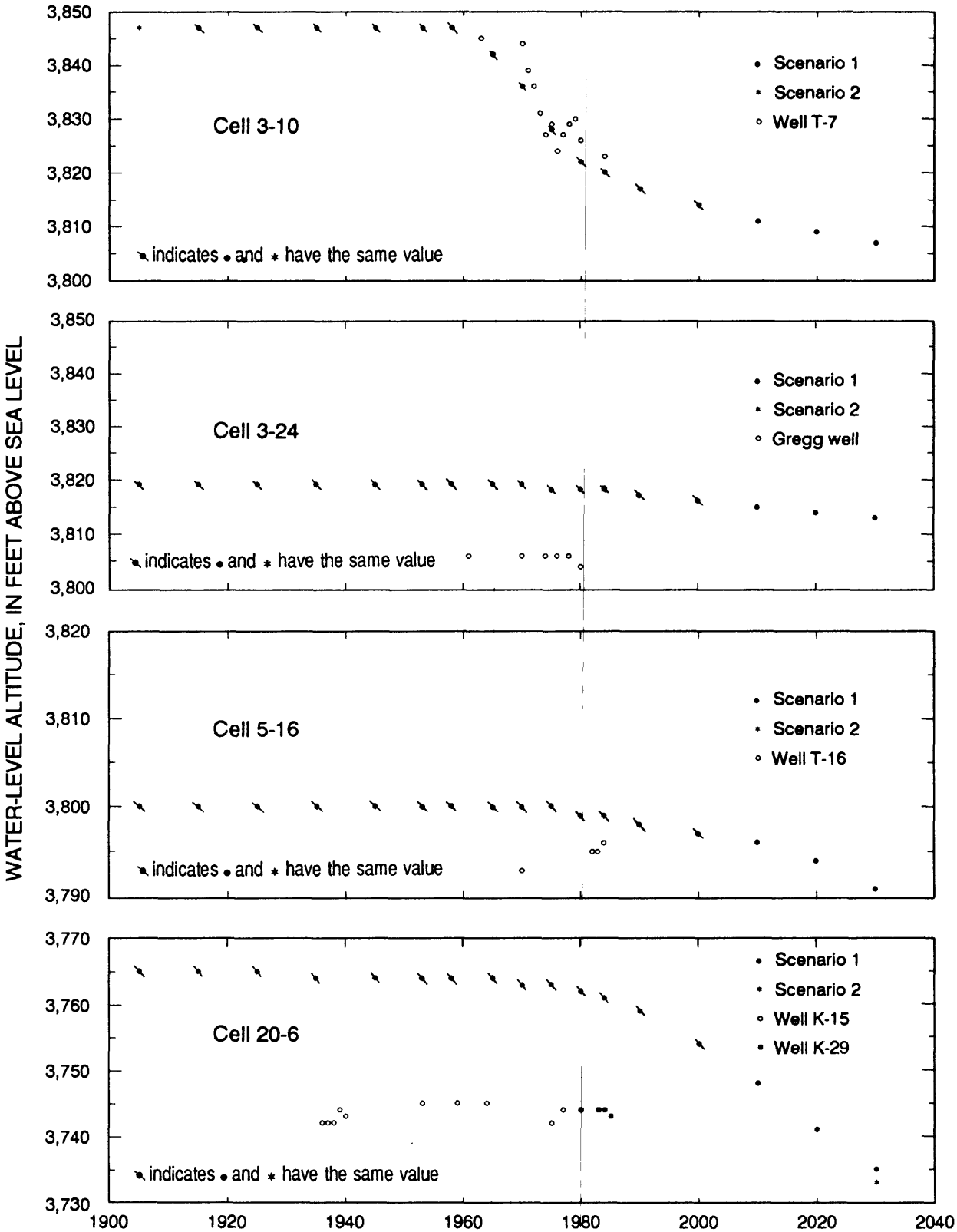

Figure 16.--Measured water levels (through 1985) and simulated water levels (through 2030) for selected wells.

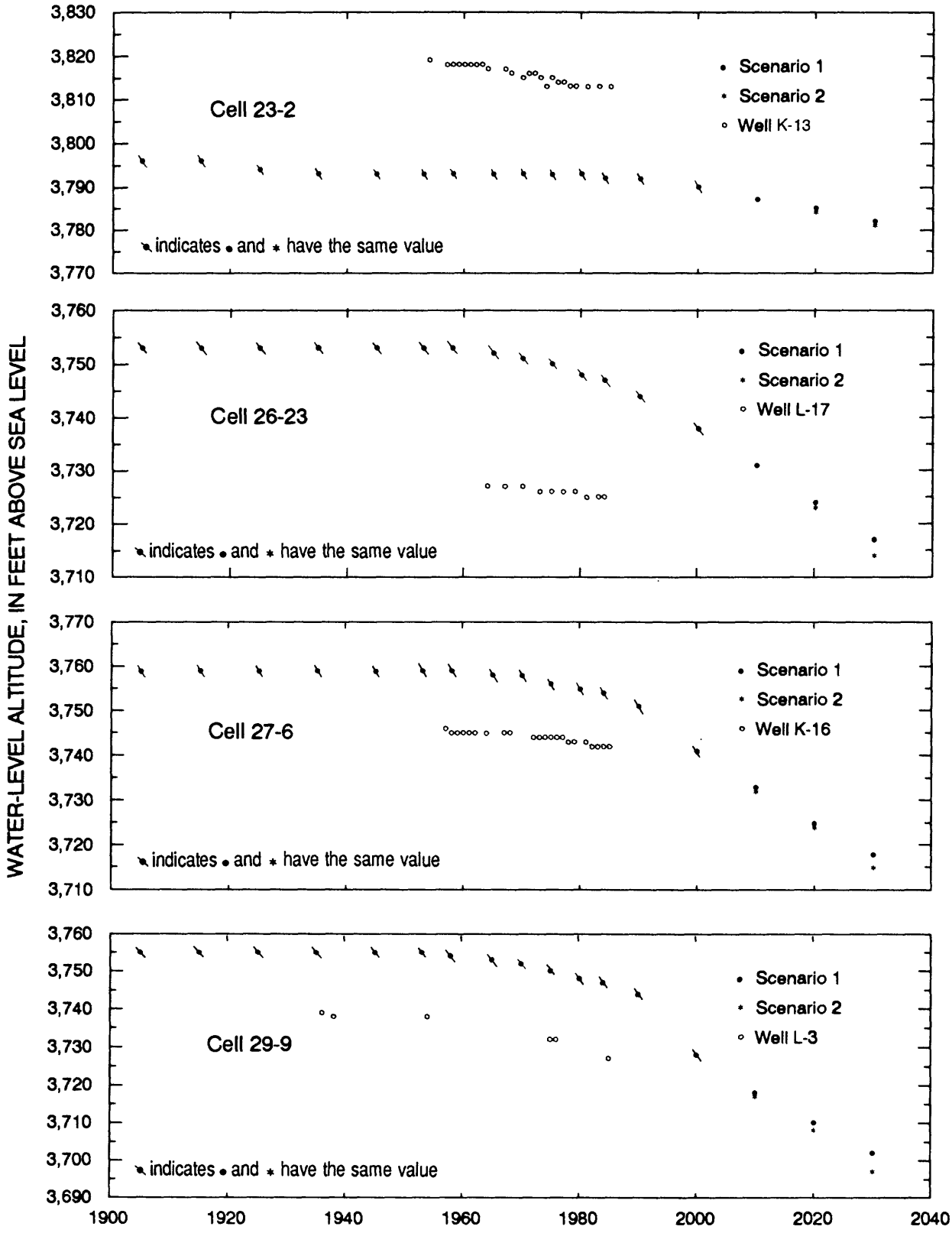

Figure 16.--Measured water levels (through 1985) and simulated water levels (through 2030) for selected wells--Continued.

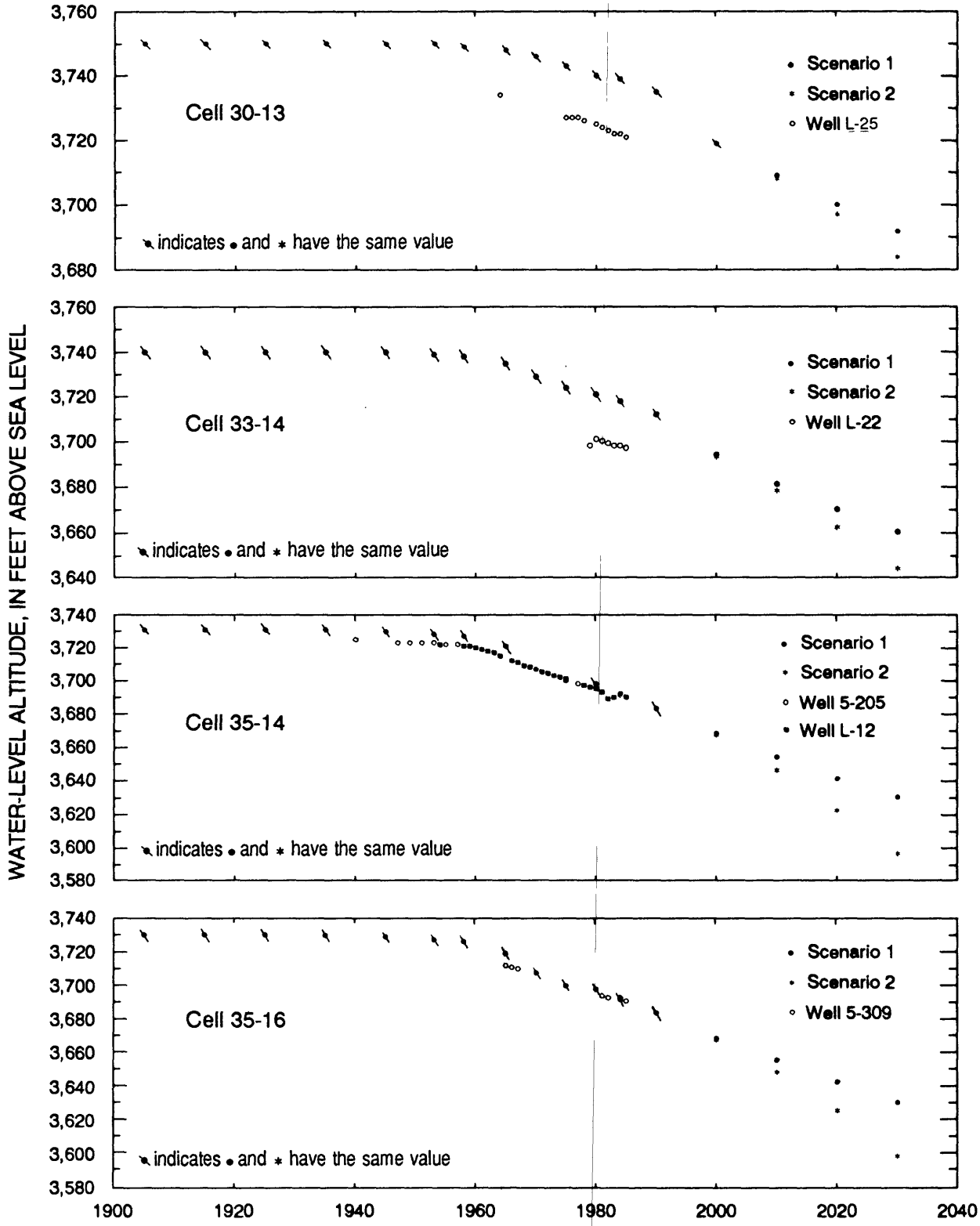

Figure 16.--Measured water levels (through 1985) and simulated water levels (through 2030) for selected wells--Continued.

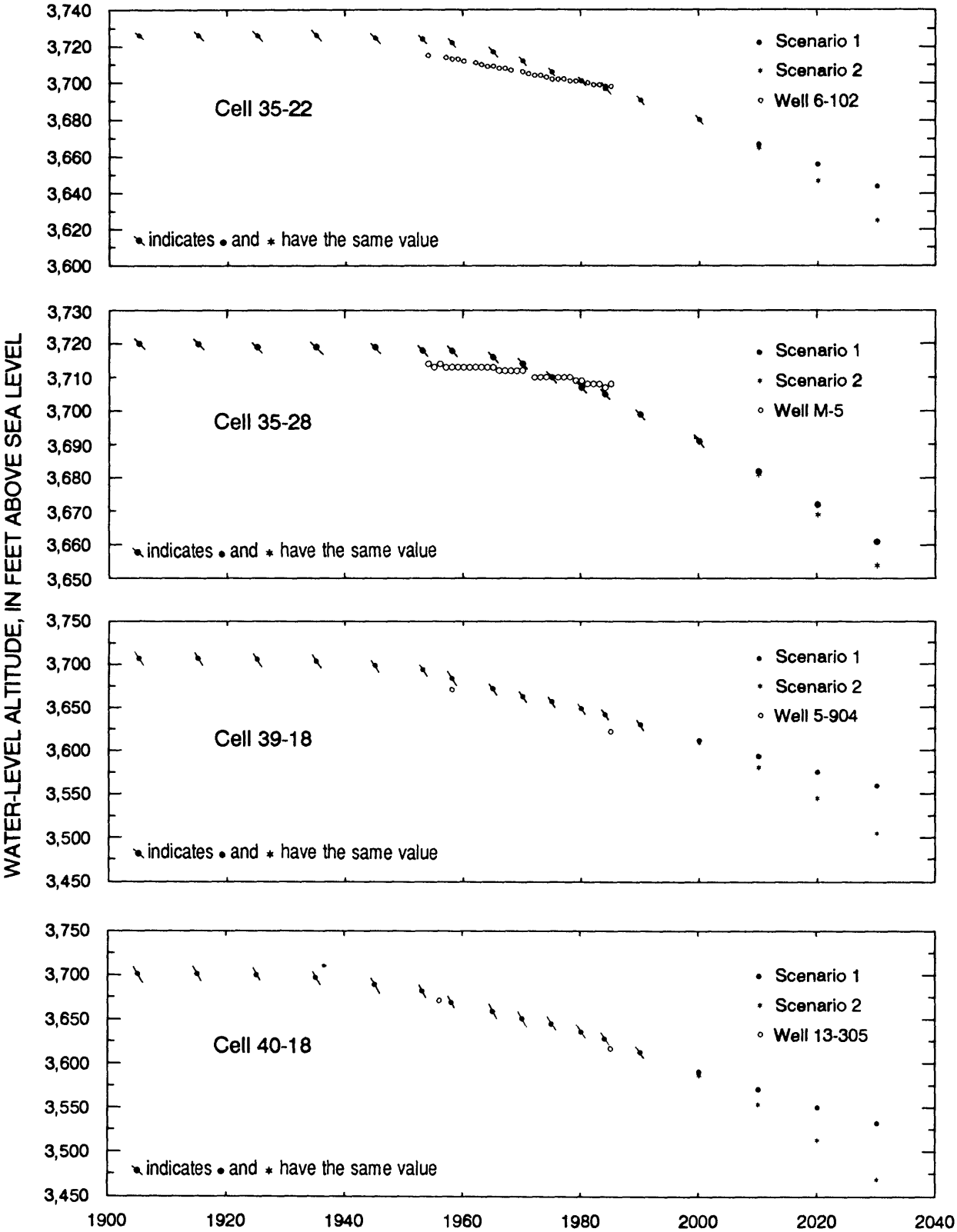

Figure 16.--Measured water levels (through 1985) and simulated water levels (through 2030) for selected wells--Continued.

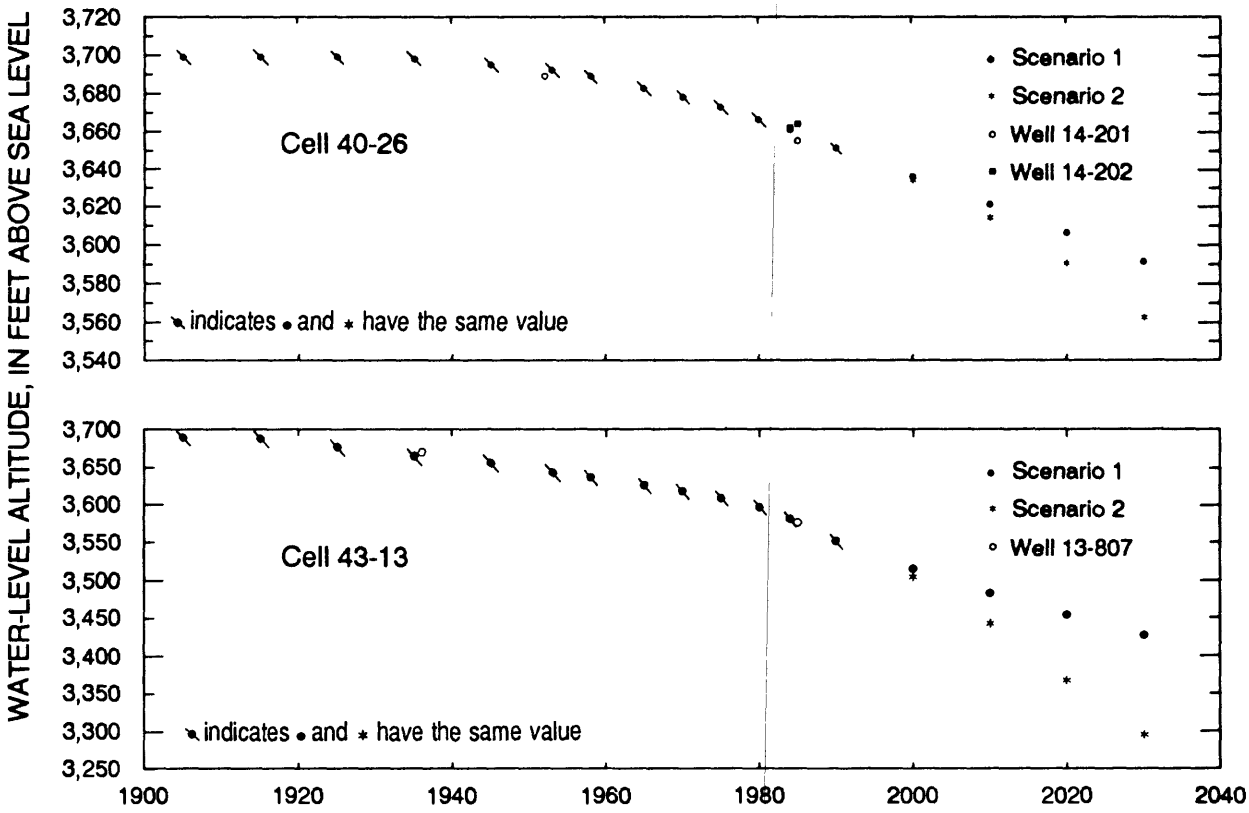

Figure 16.--Measured water levels (through 1985) and simulated water levels (through 2030) for selected wells--Concluded.

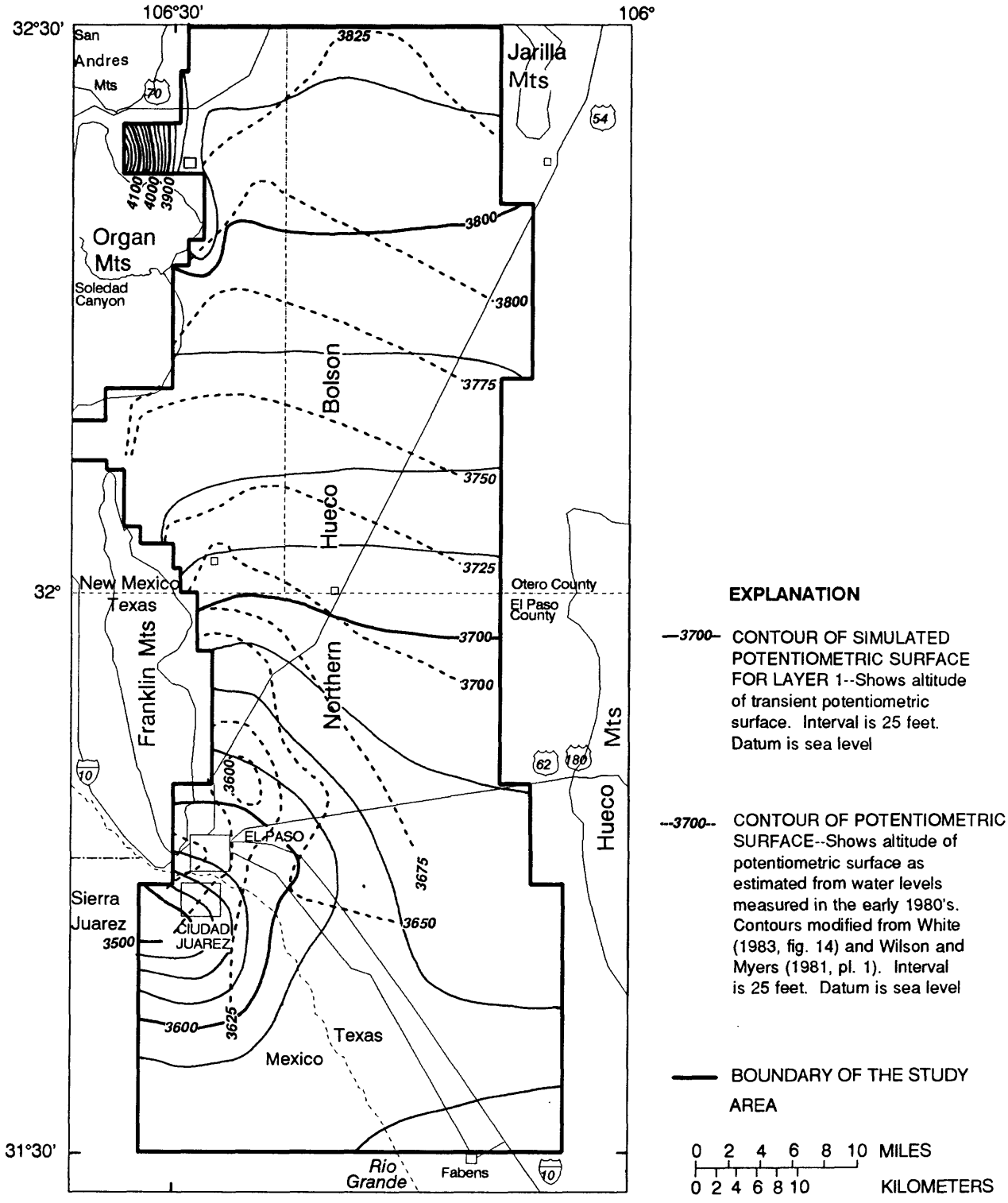

Figure 17.--Simulated potentiometric surface for layer 1 (1983) and potentiometric surface constructed from water levels measured in the early 1980's.

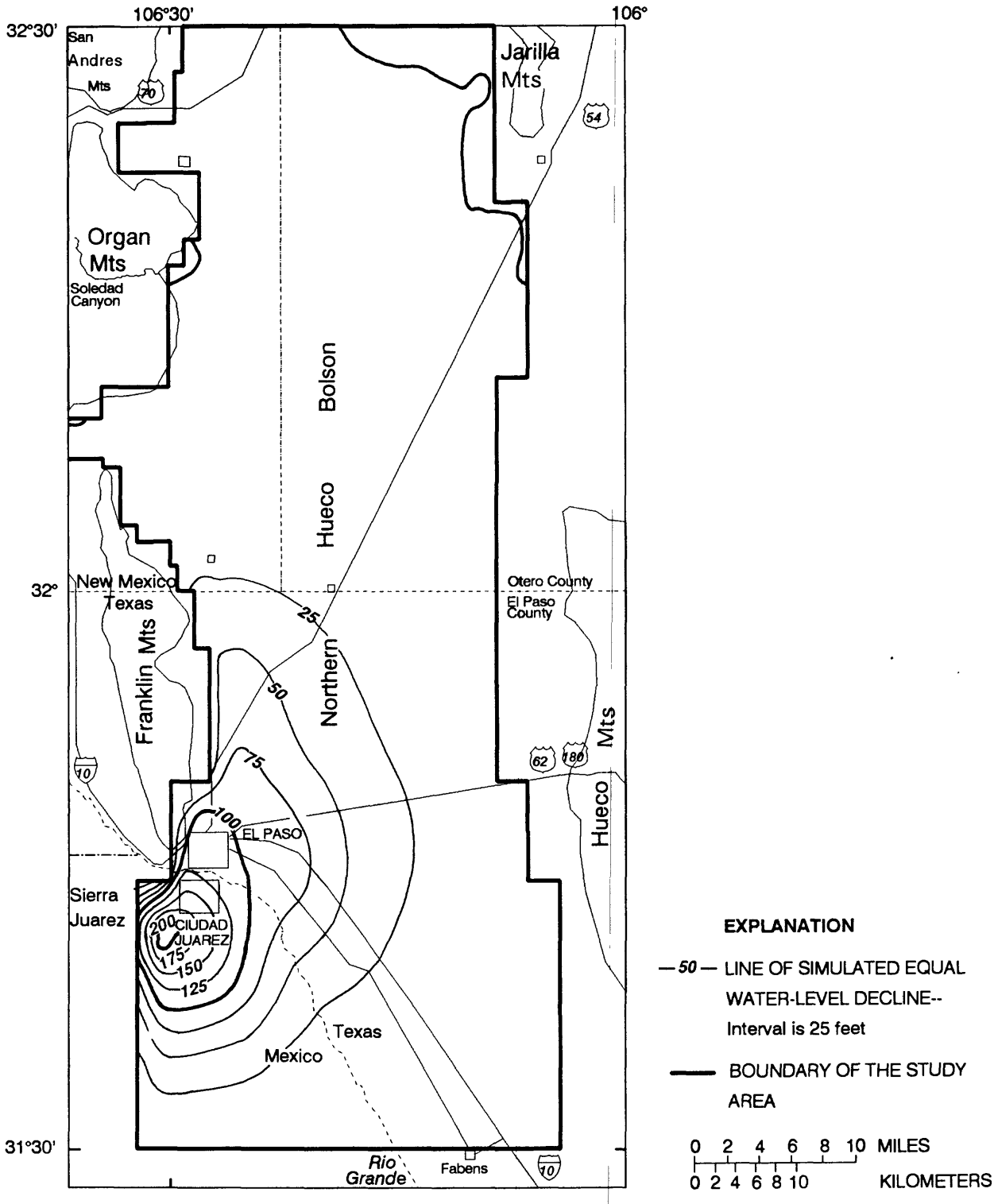

Figure 18.--Simulated water-level declines for layer 1, 1905-83.

Land and Armstrong (1985, p. 38) assumed preconsolidation stresses in the Hueco Bolson to be equivalent to a hydraulic-head change of 85 to 115 feet. The transient simulation indicated that by 1983 these stresses were exceeded only in a small area around El Paso and Ciudad Juarez (fig. 18). No attempt was made to correct the model for water that might be derived from compaction of clays.

The computed water budget for the transient simulation is shown in table 5 and figure 19. At the end of the transient period, pumpage accounted for most of the water moving out of the model area (144,000 acre-feet per year). Most of this water (122,000 acre-feet per year) was removed from storage. Mountain-front recharge to the model totaled 4,500 acre-feet per year. Net leakage from the Rio Grande into the ground-water flow system increased from 800 to 19,000 acre-feet per year from 1905 to 1983 in response to ground-water declines from pumpage.

Table 5.--Water budget for the 1905 through 1983 transient simulation

[Simulated volumes and rates are rounded in the text to preclude a false assumption of precision]

Description	Cumulative water budget, in acre-feet	Rate of flow, in acre-feet per year
Sources		
Storage	3,206,152	122,337
Recharge wells	3,669	133
Mountain-front recharge	355,418	4,499
River leakage	567,608	18,982
Head-dependent flux	326,446	5,228
Total	4,459,293	151,179
Discharges		
Storage	26,070	0
Wells	3,711,203	144,148
River leakage	52,284	205
Head-dependent flux	664,509	6,807
Total	4,454,066	151,160
Sources minus discharges	5,227	19.0
Percentage difference	0.12	0.01

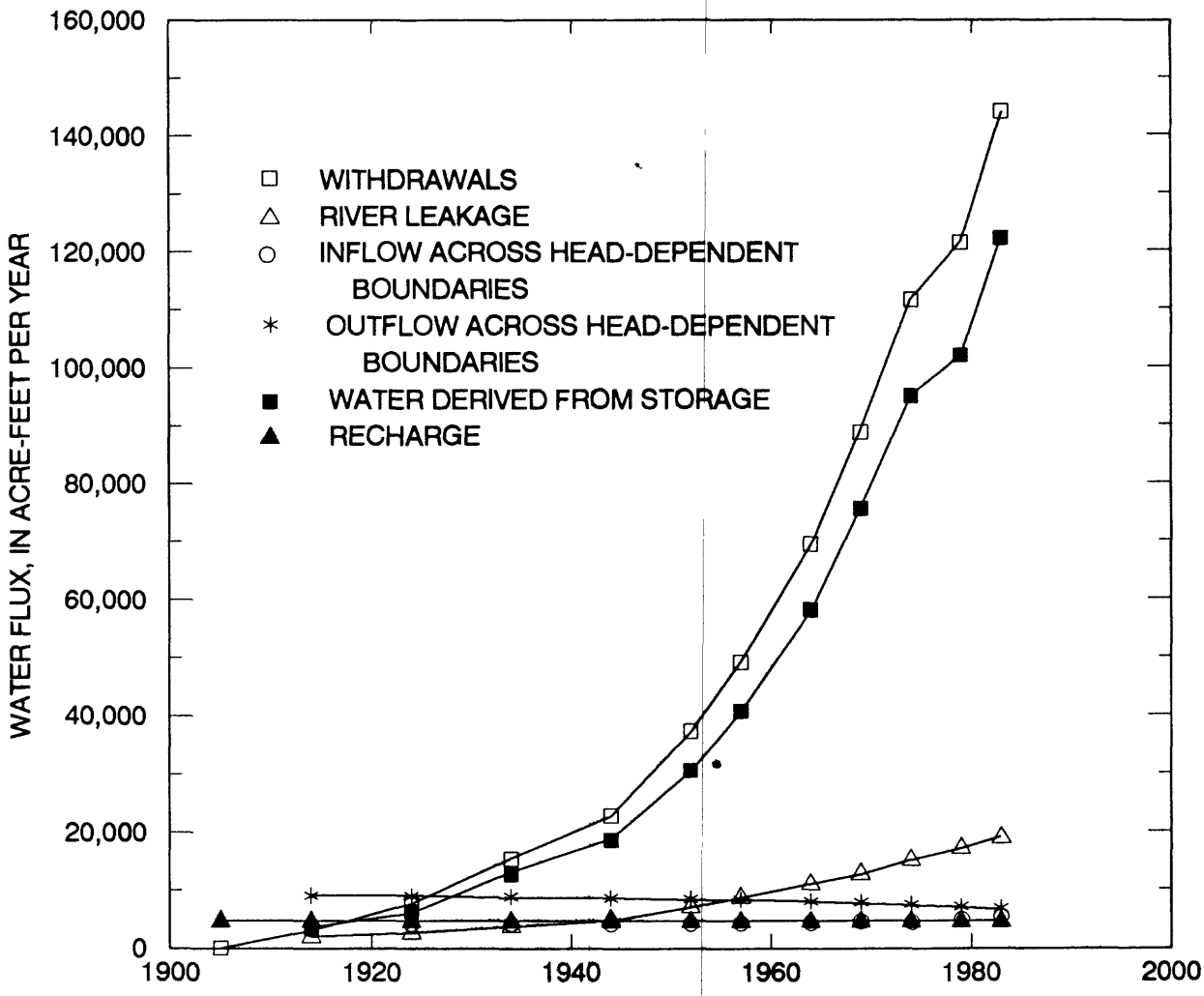

Figure 19.--Simulated water budget, 1905-83.

Underflow across north and south boundaries changed in response to stresses from pumpage during the transient simulation. Underflow from the Tularosa Basin increased slightly to about 3,800 acre-feet per year. Underflow through Fillmore Pass remained at about 260 acre-feet per year. The most apparent changes occurred with underflow to the south. Cumulative outflow across the southern boundary decreased to 5,600 acre-feet per year, about 2,200 acre-feet per year less than that in the steady-state simulation. Underflow in layers 2 and 3 across the southern boundary had reversed, with a combined flow of about 420 acre-feet per year. By 1983, simulated underflow accounted for less than 5 percent of the annual water budget. Water recharged by wells accounted for less than 1 percent of the total water budget. Simulations indicate that approximately 3.2 million acre-feet of water had been removed from storage by 1983, most of that in response to well withdrawals. It needs to be reiterated that this simulated water budget represents only one of many possible solutions, given the degree of uncertainty involved in assigning aquifer properties, distribution of recharge, and distribution of ground-water withdrawals.

Transient-Model Sensitivity

Aquifer characteristics and recharge, which govern flow through basin-fill deposits of the Hueco Bolson, are not known with certainty. It was necessary to test the sensitivity of the model to variations in hydraulic conductivity, recharge, specific yield, and river-boundary conditions to demonstrate how uncertainties in these variables can affect projected simulations.

The sensitivity of the transient (standard) simulation (1905 to 1983) was tested by running perturbed simulations in which specific characteristics were varied within a reasonable range while other characteristics were held constant. The hydraulic-head distribution and water budget for the perturbed simulation were then compared to those for the standard simulation. This procedure permitted a subjective analysis of the simulated response to reasonable variations in characteristics. A discussion of steady-state sensitivity is not presented because of a lack of predevelopment data and because the steady-state model provides only an approximation of initial hydraulic heads for the transient model.

Hydraulic Conductivity

The hydraulic conductivity used in simulations ranged from 1 to about 40 feet per day (fig. 10). The sensitivity of the model to variations in hydraulic conductivity was tested in two simulations by uniformly doubling and halving the hydraulic conductivity in all three layers. The maximum and minimum values used in the sensitivity tests are within the plausible range of hydraulic conductivity.

Cells in the transient model that are distant from simulated withdrawals or mountain-front recharge were moderately insensitive to plausible changes in hydraulic conductivity. In these cells, maximum hydraulic-head differences between the standard simulation and the perturbed simulations do not exceed the measurement errors found in water-level and altitude data. Hydrographs for representative cells (fig. 20) show that, in the perturbed simulations, 1983 water levels in cells distant from withdrawals or recharge generally differed by less than 10 feet from those in the standard simulation (within the typical measurement error).

Cells close to simulated withdrawals or recharge were moderately sensitive to changes in hydraulic conductivity. Increased hydraulic conductivity permitted increased transmission of water, resulting in smaller declines in response to nearby stress but larger declines in response to distant stress (cells 3-24, 27-6, and 20-6, fig. 20). Conversely, larger declines resulted from decreased hydraulic conductivity. With doubled hydraulic conductivity, the simulated water level in cell 44-6 was 62 feet higher than that in the standard simulation (greatly exceeding the typical measurement error). With halved hydraulic conductivity, the simulated water level in the same cell was 79 feet lower than that in the standard simulation.

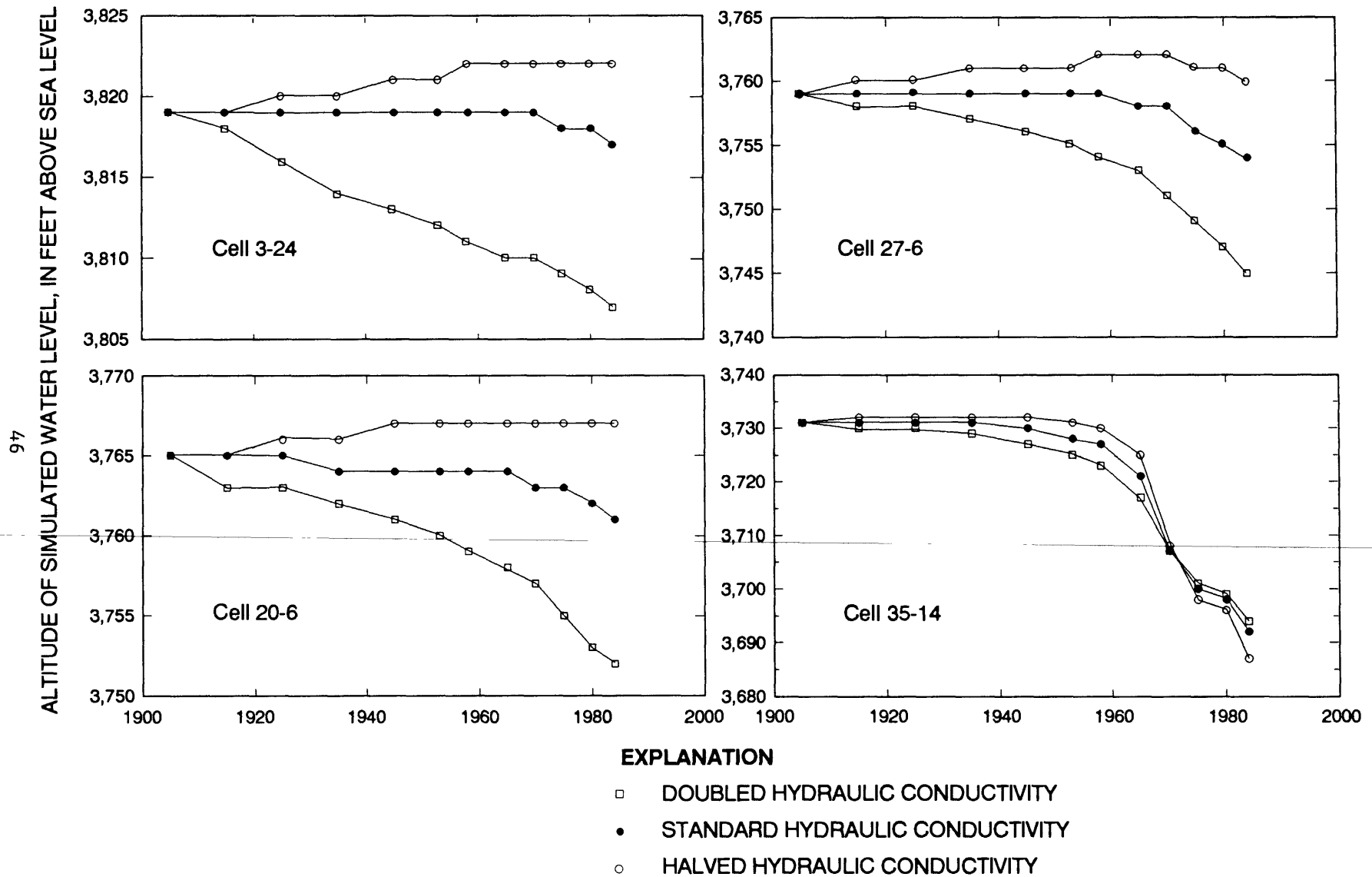

Figure 20.--Sensitivity of computed water level at cells 3-24, 27-6, 20-6, and 35-14 to variations in hydraulic conductivity, 1905-83.

Increased hydraulic conductivity permitted more rapid drainage from cells near mountain-front recharge, resulting in water levels much lower than those in the standard simulation. Reduced hydraulic conductivity resulted in higher water levels near recharge areas. With doubled hydraulic conductivity, the water level in cell 3-4 was 82 feet lower than that in the standard simulation. With halved hydraulic conductivity, the water level in the same cell was 68 feet higher than that in the standard simulation.

Changes occurred in the cumulative water budget as a result of doubling and halving the hydraulic conductivity. For doubled hydraulic conductivity, the flux of water moving into the model from storage, which accounted for about 71 percent of the total flux into the model, increased by 10 percent. Flux of water out of the model across head-dependent boundaries increased by 56 percent and river leakage into the model decreased by 9 percent. Leakage to the river, which accounted for about 1 percent of the flux out of the model, increased by 218 percent. Flux of water out to storage, less than 1 percent of the total flux out of the model, increased by 384 percent. For halved hydraulic conductivity, the flux of water moving into the model from storage increased by less than 1 percent, flux of water out of the model across head-dependent boundaries decreased by about 34 percent, and river leakage into the model decreased by 1 percent. Leakage to the river decreased by 55 percent and flux of water out to storage increased by 718 percent.

Rates of flow into and out of the modeled area by the end of the perturbed simulations (1983) differed from those of the standard simulation by less than 2 percent. Generally, the model was not very sensitive to doubling or halving hydraulic conductivity.

Recharge

The amount of mountain-front recharge applied to the transient model (1905 to 1983) was doubled and halved to test the sensitivity of water levels to changes in recharge. This large range in recharge, from 2,250 to 9,000 acre-feet per year, was used because of the uncertainty of present recharge estimates.

Water-level declines from 1905 to 1983 for representative cells are shown in figure 21. Water levels rose slightly in response to doubled recharge and dropped slightly in response to halved recharge. By 1983, water-level changes of 5 feet or less occurred in most cells in response to doubling or halving the recharge. Water levels in cells at or adjacent to recharge areas were more sensitive to changes in recharge. With doubled recharge, the water level in cell 3-4 was 107 feet higher than that in the standard simulation (again greatly exceeding the typical measurement error). With halved recharge, the water level in the same cell was 57 feet lower than that in the standard simulation.

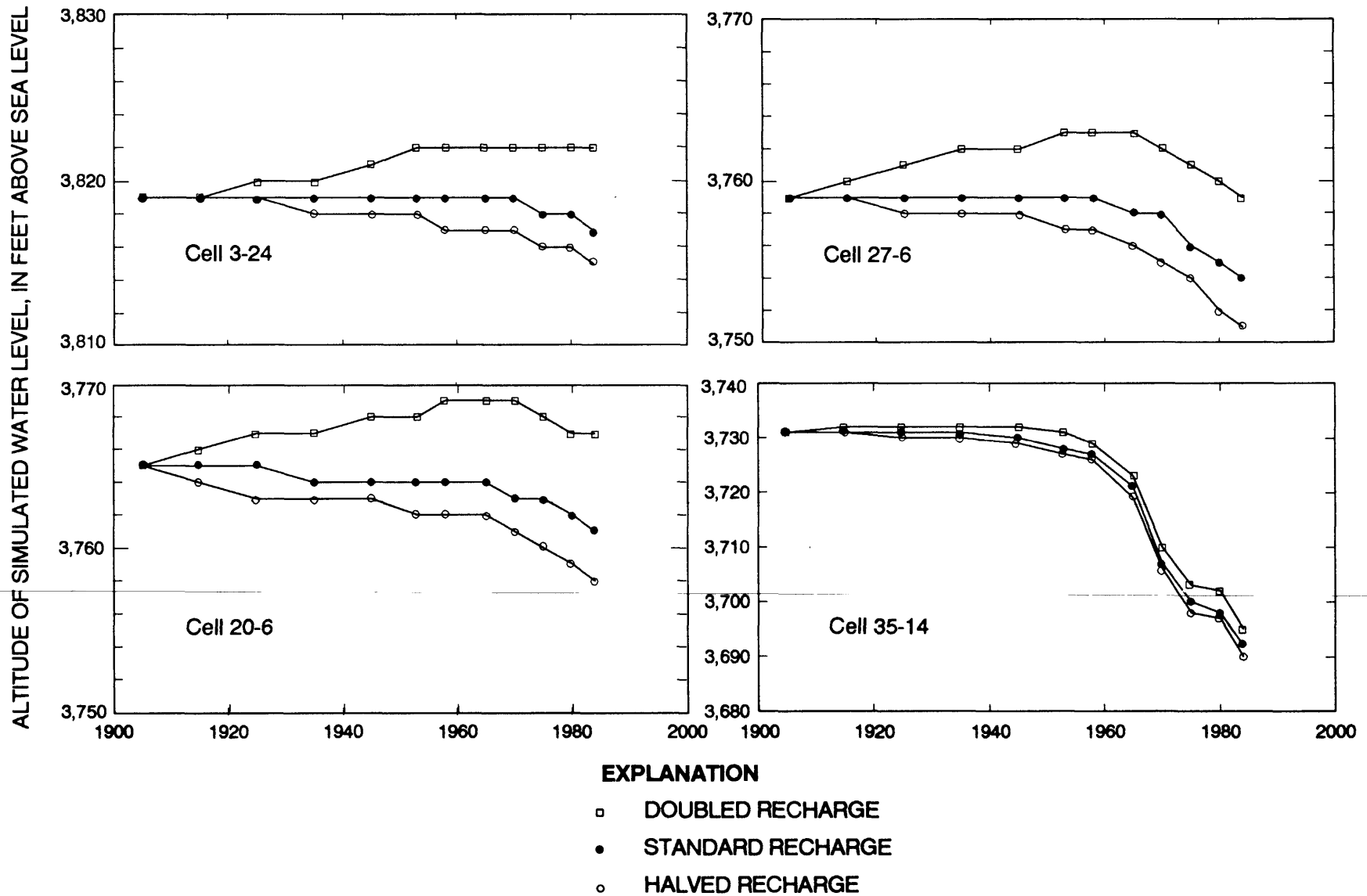

Figure 21.--Sensitivity of computed water level at cells 3-24, 27-6, 20-6, and 35-14 to variations in recharge in model layer 1, 1905-83.

Slight percentage changes in the cumulative water budget took place in response to changes in recharge. Doubled recharge resulted in a 4-percent decrease of water moving into the model from storage, no change in flux out of the model across head-dependent boundaries, a 1-percent decrease in leakage from the river, and no change in leakage to the river. Flux into the model across head-dependent boundaries, 7.5 percent of the total flux in, was decreased by 43 percent. Water simulated as moving into storage, 0.6 percent of the flux out of the model, was increased by 860 percent to accommodate the increased recharge. Halved recharge increased movement of water into the model from storage by 5 percent. No budget change occurred across head-dependent boundaries or as a result of leakage to or from the river.

The rate of flow into and out of the model by 1983 was the same for the perturbed simulations as that for the standard simulation. The model generally was not sensitive to doubling or halving recharge.

Specific Yield

The adjusted specific yield of the top layer for the transient simulation (1905-83) ranged from 0.05 to 0.20 (fig. 15). Because the maximum plausible limit of specific yield of basin-fill deposits probably does not exceed 0.25, modelwide increases and decreases of 20 percent of the specific yield were applied to the transient model to test the sensitivity of water levels. Small changes in water-level declines occurred in response to a 20-percent increase and a 20-percent decrease in specific yield for layer 1. Changes in water-level declines for selected cells are shown in figure 22.

Increased specific yield caused water levels simulated for 1983 to be negligibly higher than those of the standard simulation in areas with little pumping stress. In the White Sands Missile Range well fields (cell 3-8), declines were 6 feet less than those in the standard simulation; in the El Paso-Ciudad Juarez area, declines were as much as 19 feet less (cell 44-6). Reduced declines from pumpage stresses in the El Paso-Ciudad Juarez area were observed as far north as row 22. A decrease in specific yield resulted in 2 feet or less of increased water-level declines compared to those of the standard simulation in areas of little pumpage. Declines were as much as 8 feet larger in the White Sands Missile Range well field (cell 3-8) and as much as 24 feet larger in the El Paso-Ciudad Juarez pumping area (cells 44-5 and 44-6).

Slight changes in the cumulative water budget occurred in response to modifications in the specific yield. In both simulations, cumulative flow into the model from storage and flow into or out of the model across general head boundaries differed by 3 percent or less from those of the standard simulation. Leakage of water to or from the river varied from that of the standard simulation by 9 percent or less. The volume of water going into storage, less than 1 percent of the cumulative water moving out of the model, differed by 16 percent.

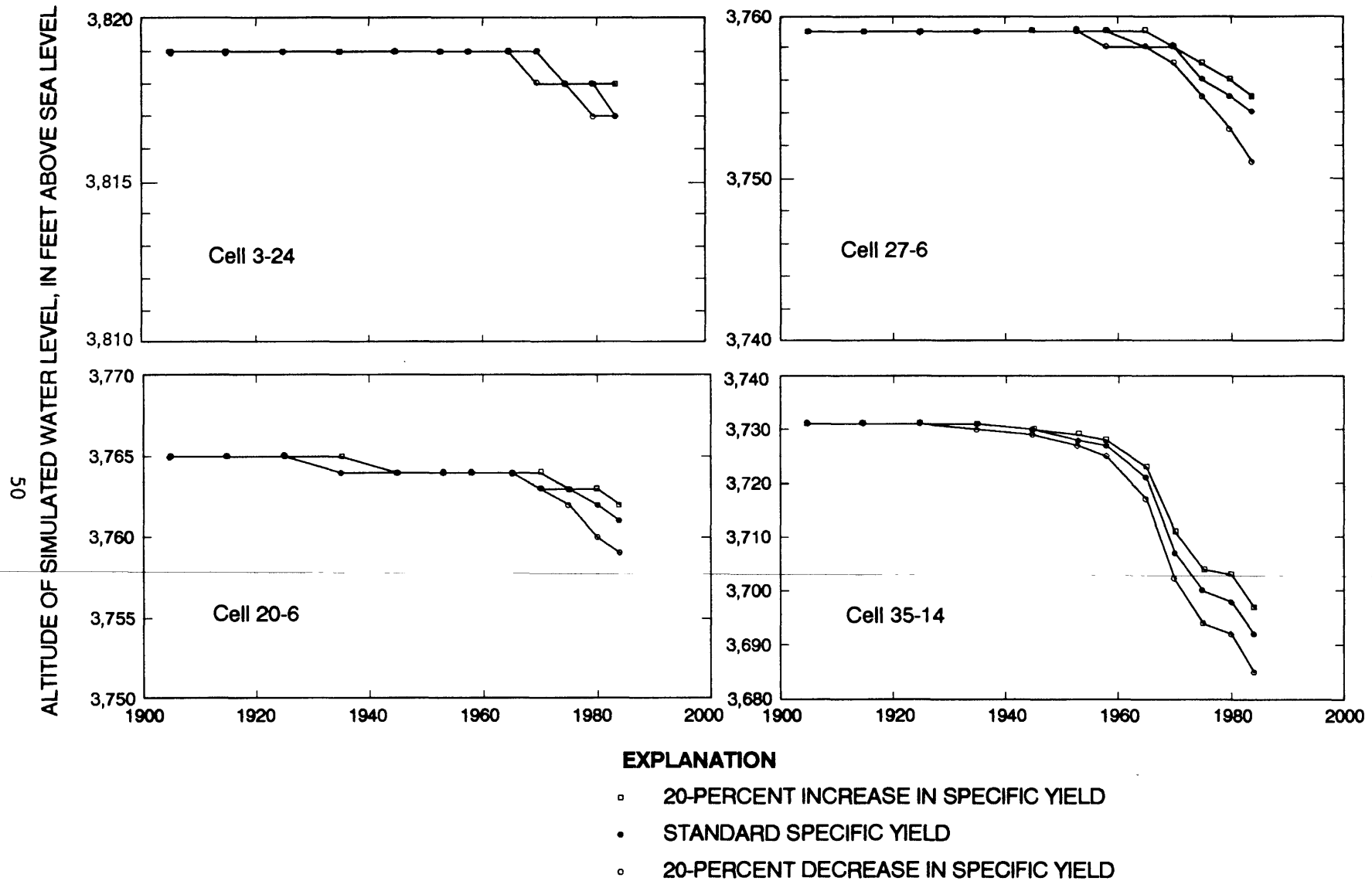

Figure 22.--Sensitivity of computed water level at cells 3-24, 27-6, 20-6, and 35-14 to variations in specific yield, 1905-83.

By 1983, the rates of movement of water into and out of the model were essentially the same for the perturbed simulations as for the standard simulation. The model generally was not very sensitive to 20-percent variations in specific yield.

River-Boundary Conditions

Large cells in the southern third of the model precluded an accurate representation of river-boundary conditions used to simulate the Rio Grande as it flows across the modeled area southeast from El Paso. The sensitivity of simulated hydraulic-head changes in response to variations in river-boundary conditions was tested by doubling and halving the simulated vertical conductance of the riverbed.

In the standard simulation, the river supplied 13 percent of the cumulative inflow to the model during 1905-83. Outflow to the river for the same period was approximately 2 percent of the cumulative outflow. In the simulation in which the riverbed conductance was doubled, the total inflow from the river increased by 63 percent from the standard simulation; by the end of the last stress period the rate of inflow from the river had increased by 72 percent. Similar magnitudes in change were observed in the amount and rate of flow out of the model to the river, although this flow was a much smaller percentage of the total water budget. In the simulation in which the riverbed conductance was halved, the total inflow from the river decreased by 44 percent; by the end of the last stress period the rate of inflow had decreased by 54 percent. In both simulations, most of the changes in the water budget were absorbed by changes in water released from or taken into storage.

No observed change in simulated hydraulic head occurred north of the New Mexico-Texas State line in response to doubling or halving the riverbed conductance. Hydraulic-head changes were principally restricted to cells near the river. Therefore, although the overall water budget was modified by variations in riverbed conductance, the hydraulic-head distribution in the New Mexico part of the Hueco Bolson was not affected by these variations.

Simulated Response to Projected Withdrawals

The response of the Hueco Bolson aquifer was simulated to 2030 using the simulated steady-state water levels as the initial condition. Known pumping stresses through 1983 and projected pumping stresses to 2030 were added. Projected stresses were based upon extrapolations of trends through 1983. Two scenarios were simulated.

For scenario 1, water-development trends were projected from 1983 to 1990 using pre-1983 pumpage trends (fig. 7). After 1990, all new water development would take place outside of the Hueco Bolson and pumping stresses from the freshwater reserves in the Hueco Bolson would remain constant, with the exception of 10,000 acre-feet of ground-water withdrawals to be shifted from the existing well fields to new well fields in New Mexico. Locations of new simulated well withdrawals were based on applications for withdrawal requested by El Paso. These requested withdrawals total approximately 10,000 acre-feet per year.

For scenario 2, present (1983) trends in ground-water withdrawals were projected to 2030 (fig. 7). In this scenario, after 1990, 10,000 acre-feet of pumped water would again be shifted from existing well fields in El Paso to new well fields in New Mexico.

The actual distribution and rate of ground-water withdrawals probably will not match either of these scenarios. However, present trends indicate that actual withdrawals will be within the range of those used in these simulations. If this is the case, simulations may provide some understanding of anticipated declines in water levels in the Hueco Bolson.

Simulated Response With No Additional Development in the Hueco Bolson

The projected potentiometric surface for the northern Hueco Bolson, using pumping stresses assumed in scenario 1, is shown in figure 23. In this simulation, pumping stresses would completely dewater two cells in layer 1 during the later stress periods. To maintain the projected stresses, pumpage from these dewatered cells was moved to layer 2 in subsequent stress periods. In reality, wells probably would be deepened, replaced, or abandoned prior to complete dewatering because of decreasing yield or increasing salinity.

By 2030, the cone of depression would have deepened considerably around the El Paso-Ciudad Juarez area (fig. 24) and simulated ground-water flow in layer 1 would be completely diverted toward the pumping center. Comparison with the 1983 surface (fig. 17) shows that a deepening trough in the potentiometric surface would extend to the north, partially in response to the shifting of pumpage into New Mexico. The hydraulic gradient at the New Mexico-Texas State line would range from about 6 to 12 feet per mile, and flow would be to the south and southwest.

Water-level declines for scenario 1 throughout the northern part of the Hueco Bolson in 2030 are shown in figure 24. Simulations indicate that water levels would decline by more than 475 feet near El Paso. Water-level declines in New Mexico near the State line would be as much as 100 feet. By 2030, simulated water-level declines would exceed the preconsolidation stress threshold (equivalent to a change in hydraulic head of 85 to 115 feet) over much of the southwest quarter of the modeled area. As declines exceed this threshold, more water is available from storage in response to the release of water from inelastic compaction of clay in the aquifer. Because of a limited understanding of factors controlling clay compaction in the Hueco Bolson, no attempt was made to account for this effect. Increased long-term storage coefficient could result in smaller water-level declines and some land-surface subsidence, but the magnitudes of these changes are unknown.

Projected hydrographs (fig. 16) show that scenario 1 water-level declines would continue through 2030. Projected declines in most cells show a near-constant rate of change, perhaps reflecting the constant rate of total pumpage assumed after 1990.

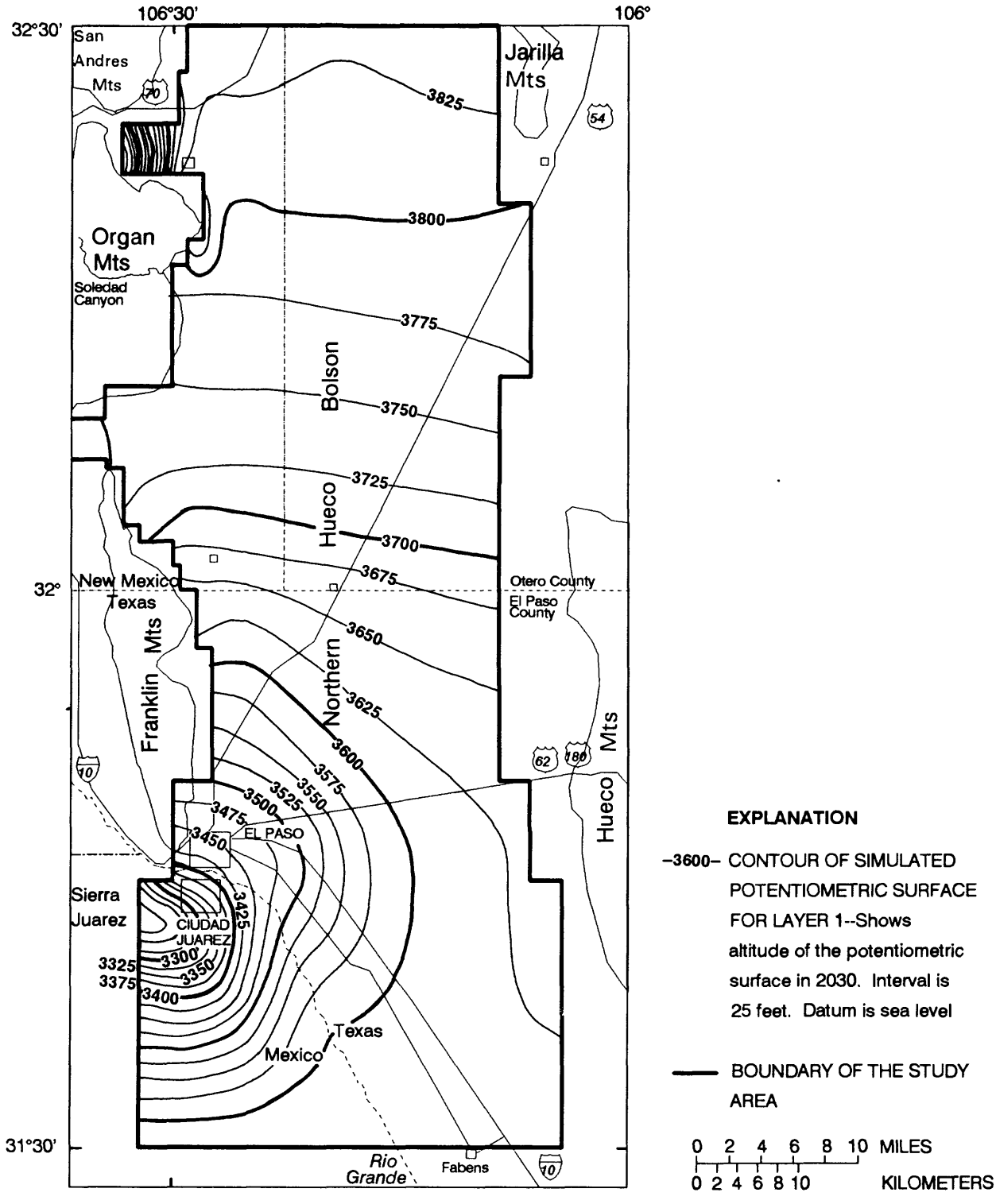

Figure 23.--Simulated potentiometric surface for scenario 1, 2030.

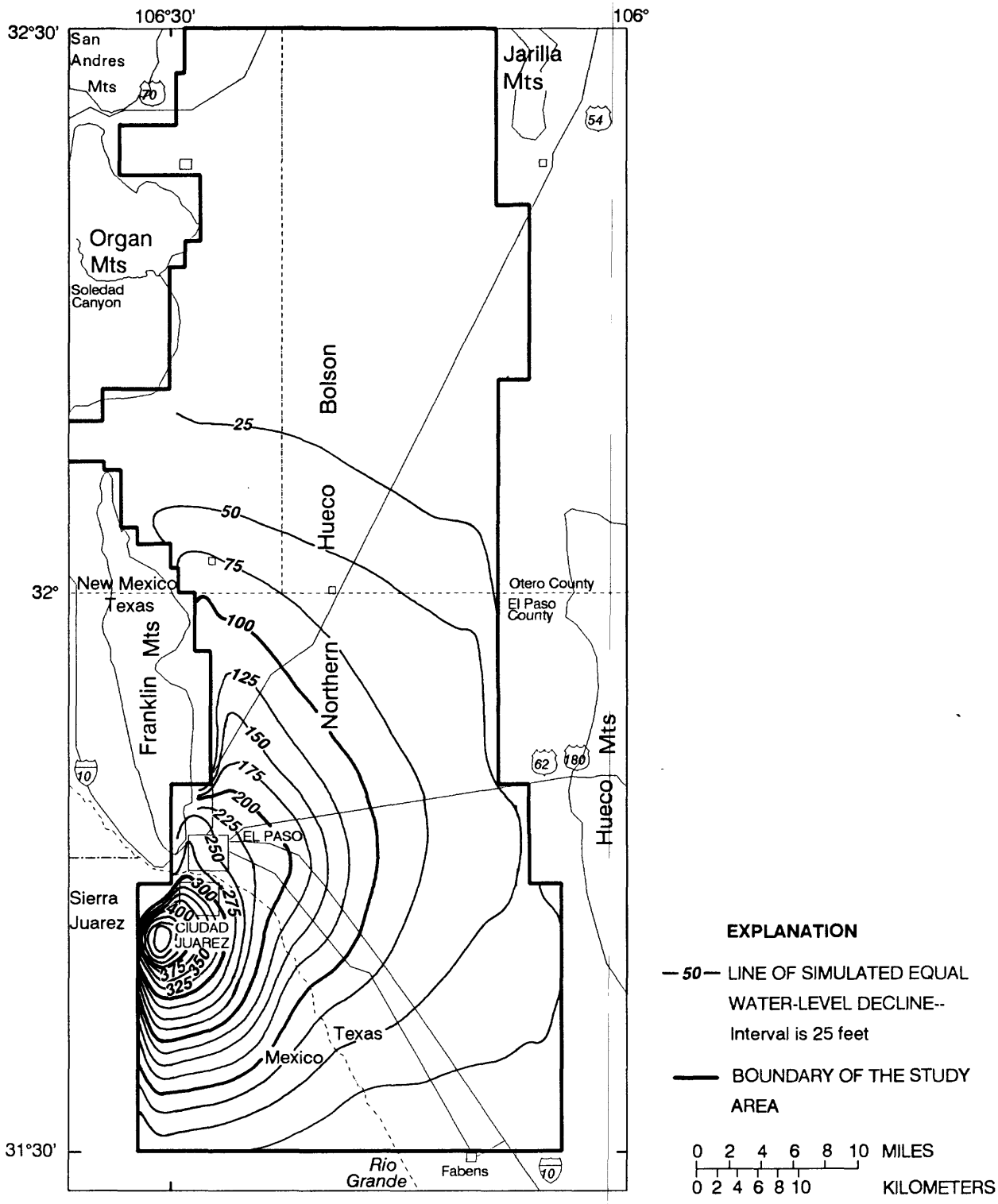

Figure 24.--Simulated water-level declines for scenario 1, 1905-2030.

The rate of removal of water from storage from 1984 to 2030 increases slightly to 127,000 acre-feet per year in the scenario 1 simulation. In this simulation, approximately 6.4 million acre-feet of water would be removed from storage from saturated basin-fill deposits in the northern Hueco Bolson from 1983 to 2030, with a total of about 9.8 million acre-feet of water removed from storage from 1905 to 2030. Underflow across northern boundaries would increase to 4,400 acre-feet per year and underflow through Fillmore Pass would increase to 350 acre-feet per year. By 2030, underflow into the simulated area across southern boundaries would be about 6,000 acre-feet per year, still a small part of the total water budget.

Simulated Response With Projected Increasing Development in the Hueco Bolson

The simulated potentiometric surface, using pumping stresses assumed in scenario 2, is shown in figure 25. In this simulation, simulated pumping stresses completely dewatered 11 cells in layer 1 during stress periods 15 and 16. Again, to maintain the assumed stresses, pumpage from dewatered cells was moved to layer 2 in subsequent stress periods.

By 2030, the simulated cone of depression around the El Paso-Ciudad Juarez area (fig. 25) will be significantly deeper than the cone of depression for scenario 1 (fig. 23). Water-level contours for scenario 2 again show that ground-water flow from the north is completely diverted toward the pumping center. The hydraulic gradient at the New Mexico-Texas State line ranges from 6 to 18 feet per mile, and the flow direction is to the south and southwest.

Scenario 2 water-level declines throughout the northern part of the Hueco Bolson in 2030 are shown in figure 26. The simulated water-level declines of as much as 875 feet near El Paso certainly would result in extensive dewatering of freshwater zones and probably are very unlikely. Drastically reduced well yields, increases in dissolved-solids concentrations in ground water, and well abandonment probably would occur before water-level declines exceeded those simulated using scenario 2 withdrawals. Again, the long-term storage coefficient in areas of large-scale withdrawal may increase due to the one-time release of water from storage in response to inelastic compaction of clay.

Water-level declines in New Mexico near the State line range from 25 to 125 feet. Projected hydrographs (fig. 16) show that by 2030, scenario 2 water-level declines are very similar to scenario 1 declines in the northern part of the study area. In the southern part of the study area scenario 2 water levels are as much as 100 feet deeper then those for scenario 1.

Scenario 2 is intended to represent a maximum potential pumping stress. Actual pumping rates and distributions probably will not match those in scenario 2, but simulations may provide an indication of the magnitude of water-level changes that could occur.

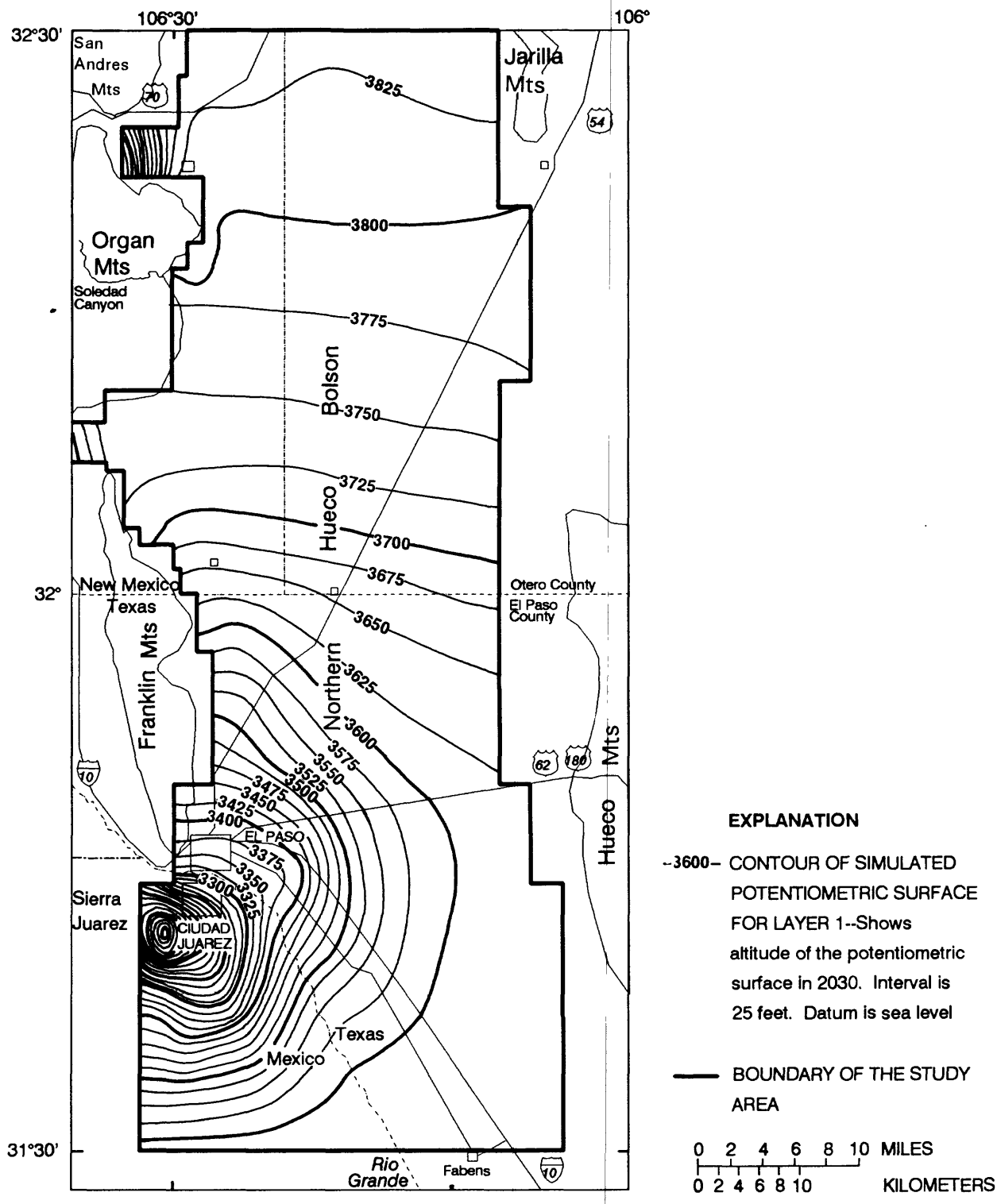

Figure 25.--Simulated potentiometric surface for scenario 2, 2030.

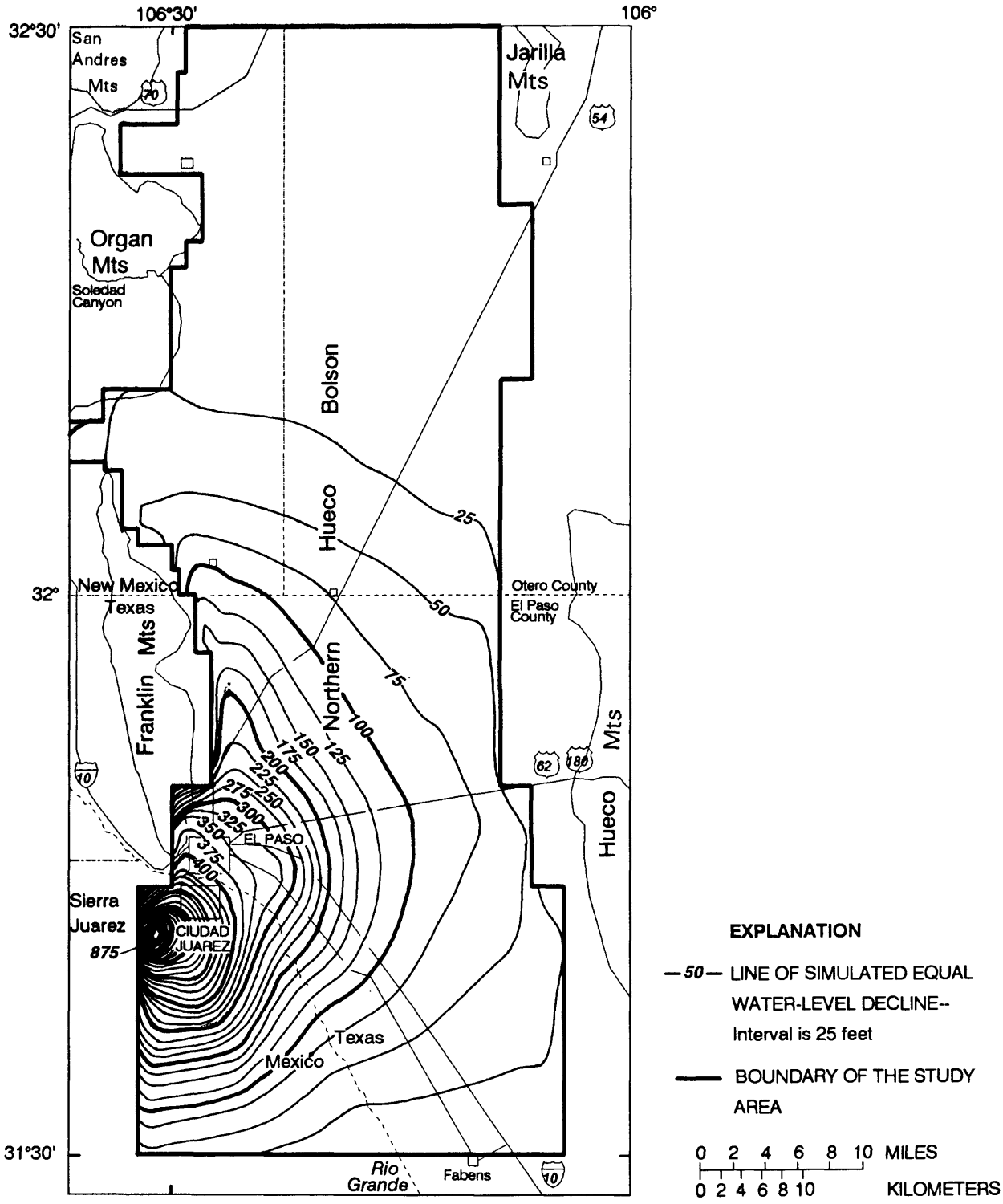

Figure 26.--Simulated water-level declines for scenario 2, 1905-2030.

The simulated rate of removal of water from storage in response to increased pumping withdrawals assumed in scenario 2 increases to approximately 255,000 acre-feet per year by 2030. On the basis of the scenario 2 simulation, about 9.6 million acre-feet would be withdrawn from storage from 1983 to 2030, with a total of about 12.8 million acre-feet of water removed from storage from 1905 to 2030. Underflow across northern boundaries would be about 350 acre-feet per year. Underflow through Fillmore Pass would be about 350 acre-feet per year. Inflow across southern boundaries would be about 9,500 acre-feet per year, with marked increases in inflow in layers 2 and 3 when compared with inflow in scenario 1.

Ground-water withdrawals as projected in scenario 2 probably would exceed the freshwater reserves in the northern part of the Hueco Bolson and would result in decreased well yields, water-quality deterioration, and eventual well abandonment prior to complete withdrawal of these reserves. Although the likelihood of this scenario probably is minimal, it does demonstrate an upper limit to the development of freshwater in the bolson.

Simulations of projected response to pumpage tested the sensitivity of the model to general head boundaries to the north and south. No simulation showed that stresses were affecting the northern boundary. Projected water-level declines at the south boundary (fig. 26) were as large as 25 feet by 2030. However, the pumping center directly to the north had declines as large as 800 feet, indicating that boundary effects were proportionally small compared with actual pumpage effects. It should be reiterated that hydrologic conditions are not well represented in the El Paso area.

EVALUATION OF POTENTIAL FOR SALTWATER ENCROACHMENT

Freshwater (containing less than 1,000 milligrams per liter dissolved solids) in the Hueco Bolson occurs primarily along the western edge of the basin (fig. 27) where it is recharged by runoff from the Franklin and Organ Mountains. Freshwater in the northern part of the Hueco Bolson constitutes only a small percentage of ground water in the basin-fill deposits. Because of their lower density, lenticular bodies of less dense freshwater lie on top of denser saline water and are thickest where major ephemeral streams debouch onto the bolson-fill sediments. The interface between the freshwater and saline-water zones generally consists of a thin transition zone. Large-scale withdrawals of ground water will cause some degree of encroachment of saline water toward wells completed in the freshwater part of the aquifer. Encroachment may occur laterally and vertically (upconing).

The degree to which saline-water encroachment will occur depends upon several factors, including thickness of freshwater-saturated sediments, well location, pumping rate, depth of well completion, hydrologic properties of the basin-fill deposits, and density of the saline water. These factors were incorporated into models that were used to evaluate the possibility of saline-water encroachment into the New Mexico part of the Hueco Bolson caused by ground-water withdrawals in Texas and New Mexico. The actual movement of saline water will be controlled by the pumping schedules of individual wells and well fields. Simulations provide only an indication of the potential for encroachment of saline water.

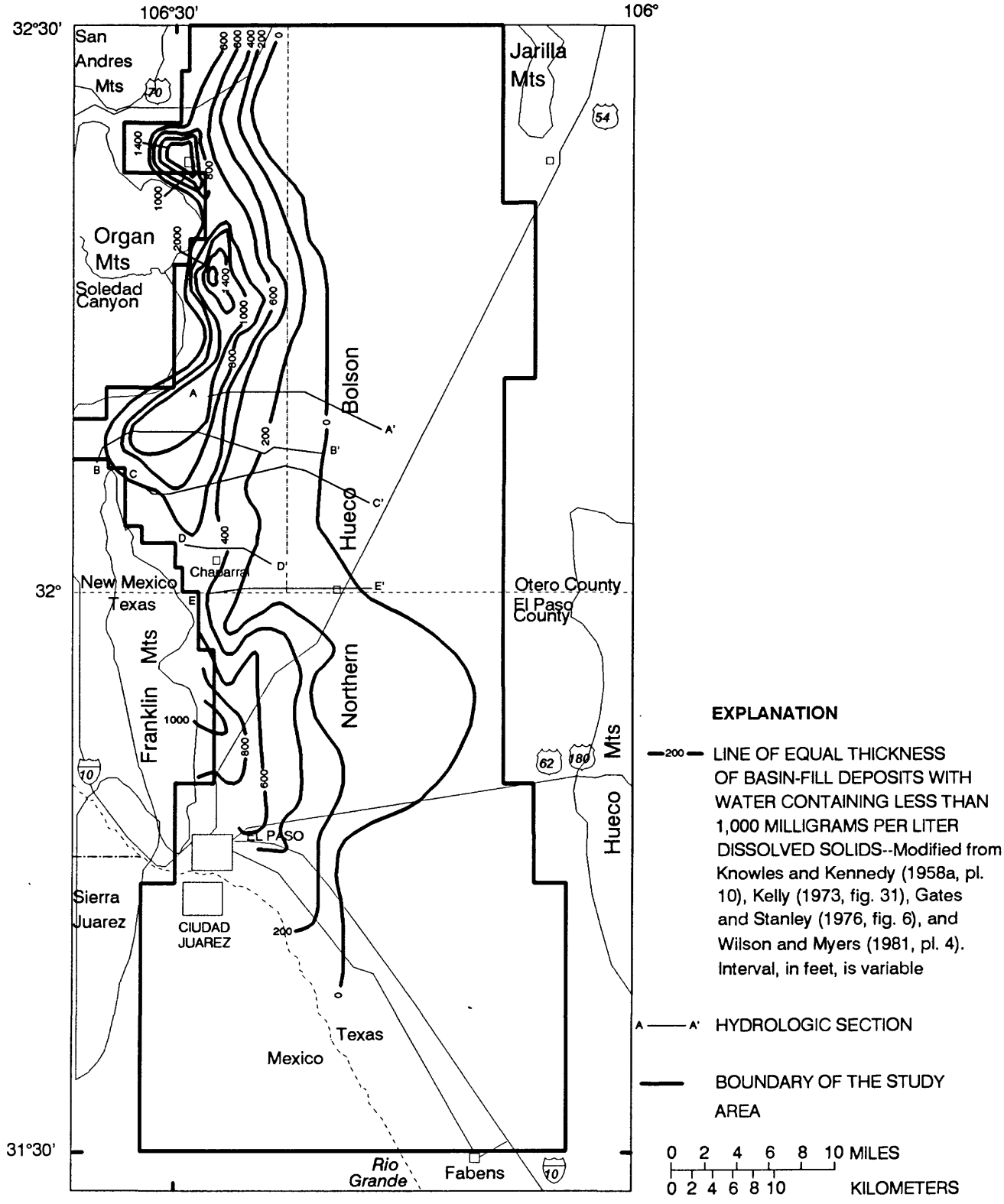

Figure 27.--Approximate thickness of basin-fill deposits that contain water having dissolved-solids concentrations less than 1,000 milligrams per liter.

Distribution of Freshwater-Saturated Deposits

Knowles and Kennedy (1958a, pl. 10) mapped the aggregate thickness of basin-fill deposits that contain water having less than 250 milligrams per liter of dissolved chloride from El Paso to the southern end of the Organ Mountains. Kelly (1973, fig. 31) mapped the thickness of deposits that contain water having less than 1,000 milligrams per liter dissolved solids in the White Sands Missile Range Post Headquarters area. Wilson and Myers (1981, pl. 4) mapped the freshwater thickness of alluvial-fan deposits in the Soledad Canyon reentrant. The approximate thickness and distribution of freshwater in the northern part of the Hueco Bolson are shown in figure 27, which was compiled from these maps and from recent chemical analyses. Freshwater-saturated deposits may be as thick as 2,000 feet in the Soledad Canyon reentrant. Elsewhere, thicknesses range from about 1,000 feet on the west to zero on the east. The thick section of freshwater-saturated deposits on the west reflects the general occurrence of coarser grained fluvial and alluvial-fan deposits east of the Franklin and Organ Mountains. Comparison of figures 27 and 6 indicates that the occurrence of freshwater may be due, at least in part, to flushing of saline water in areas characterized by coarser grained deposits. Conversely, finer grained deposits typically may contain more saline water because the flushing process is slower.

The thick section of freshwater on the west is also due, in part, to recharge from the mountainous drainage areas on the eastern slopes of the Franklin and Organ Mountains. The thickest sections of freshwater-saturated deposits occur where large surface drainages discharge to the basin. Alluvial-fan deposits at the mouth of Soledad Canyon are saturated with as much as 2,000 feet of freshwater. Soledad Canyon drains about 20 square miles in the Organ Mountains. Similarly, the White Sands reentrant to the north drains about 50 square miles; deposits within the reentrant contain as much as 1,400 feet of freshwater.

Surface-electrical-resistivity sounding data (Bisdorf, 1985) and test-well data were used to construct five east-to-west hydrologic sections (fig. 28) in the vicinity of Chaparral, New Mexico. Section traces are shown in figure 27. Freshwater lenses along these sections range in thickness from zero to about 1,000 feet. Concentrations of dissolved solids in water samples collected from wells along these sections ranged from 210 to 9,700 milligrams per liter.

A zone of small resistivity (less than 10 ohm-meters) consistently occurs at depth along all sections (fig. 28). The approximate depth to this zone ranges from about 1,000 to 2,500 feet. This zone probably represents fine-grained lacustrine deposits that are saturated with saline water. Resistivity curves typical of consolidated rock were obtained at depth at several soundings in the vicinity of U.S. Highway 54.

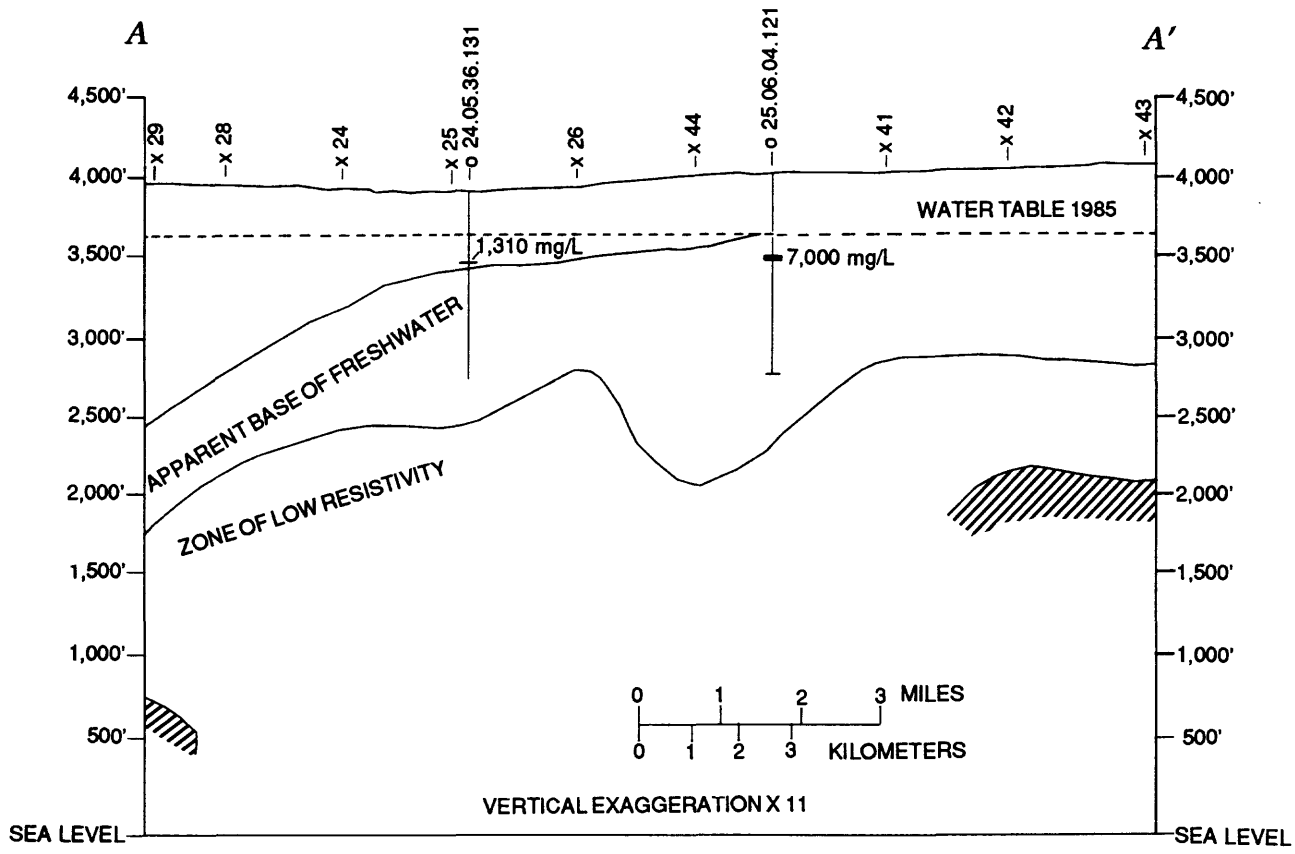

EXPLANATION

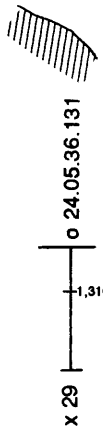

CONSOLIDATED ROCK--Estimated from borehole data or from vertical-electrical-sounding data

WELL

DISSOLVED-SOLIDS CONCENTRATION, IN MILLIGRAMS PER LITER--Values are based on chemical analyses or specific-conductance values of water samples from the depths indicated

VERTICAL-ELECTRICAL SOUNDING--Sounding locations and resistivity data are from Bisdorf (1985)

Figure 28--Distribution of water quality with depth - Continued.
(Location of sections is shown in figure 27.)

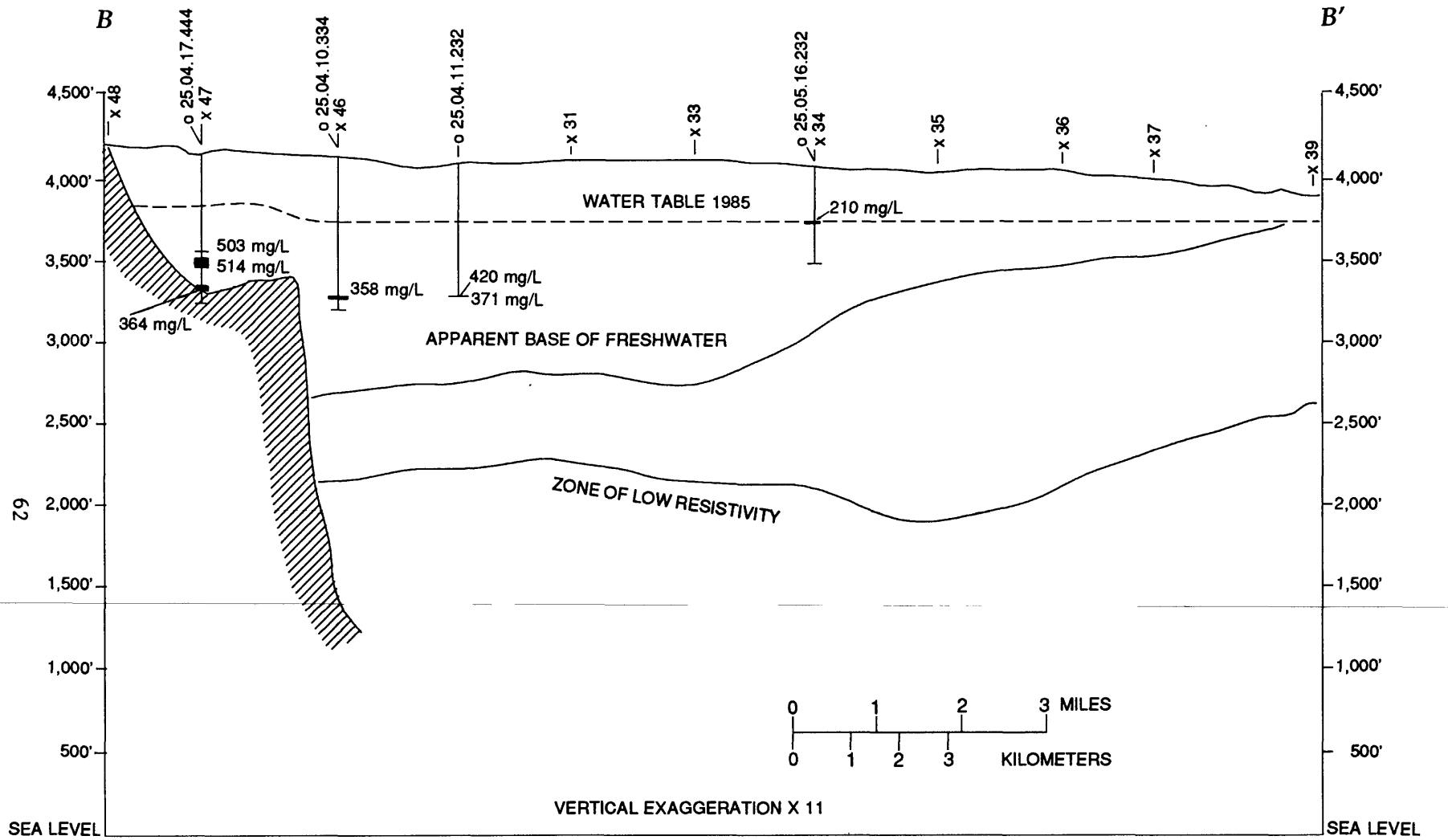

Figure 28.--Distribution of water quality with depth - Continued.

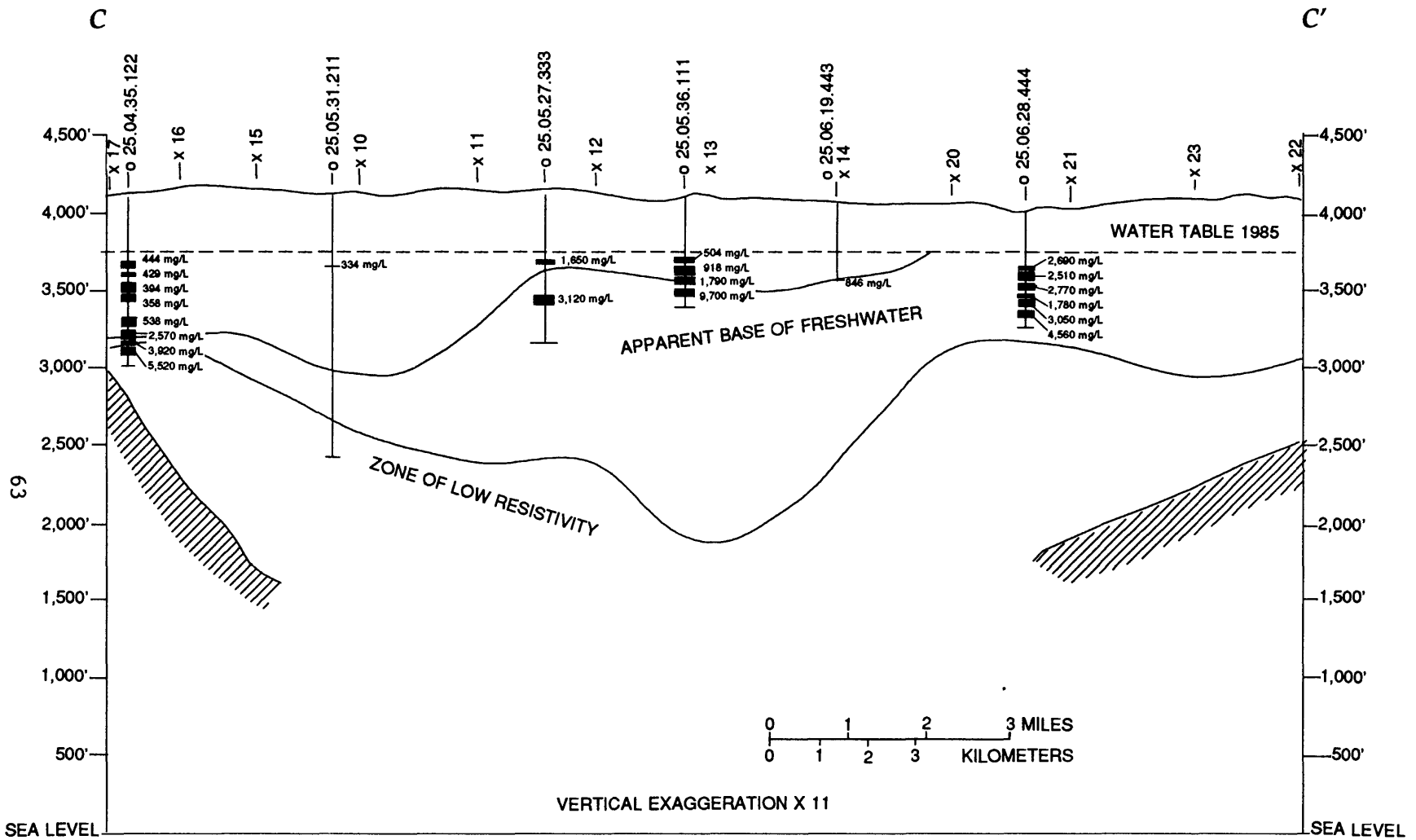

Figure 28.--Distribution of water quality with depth - Continued.

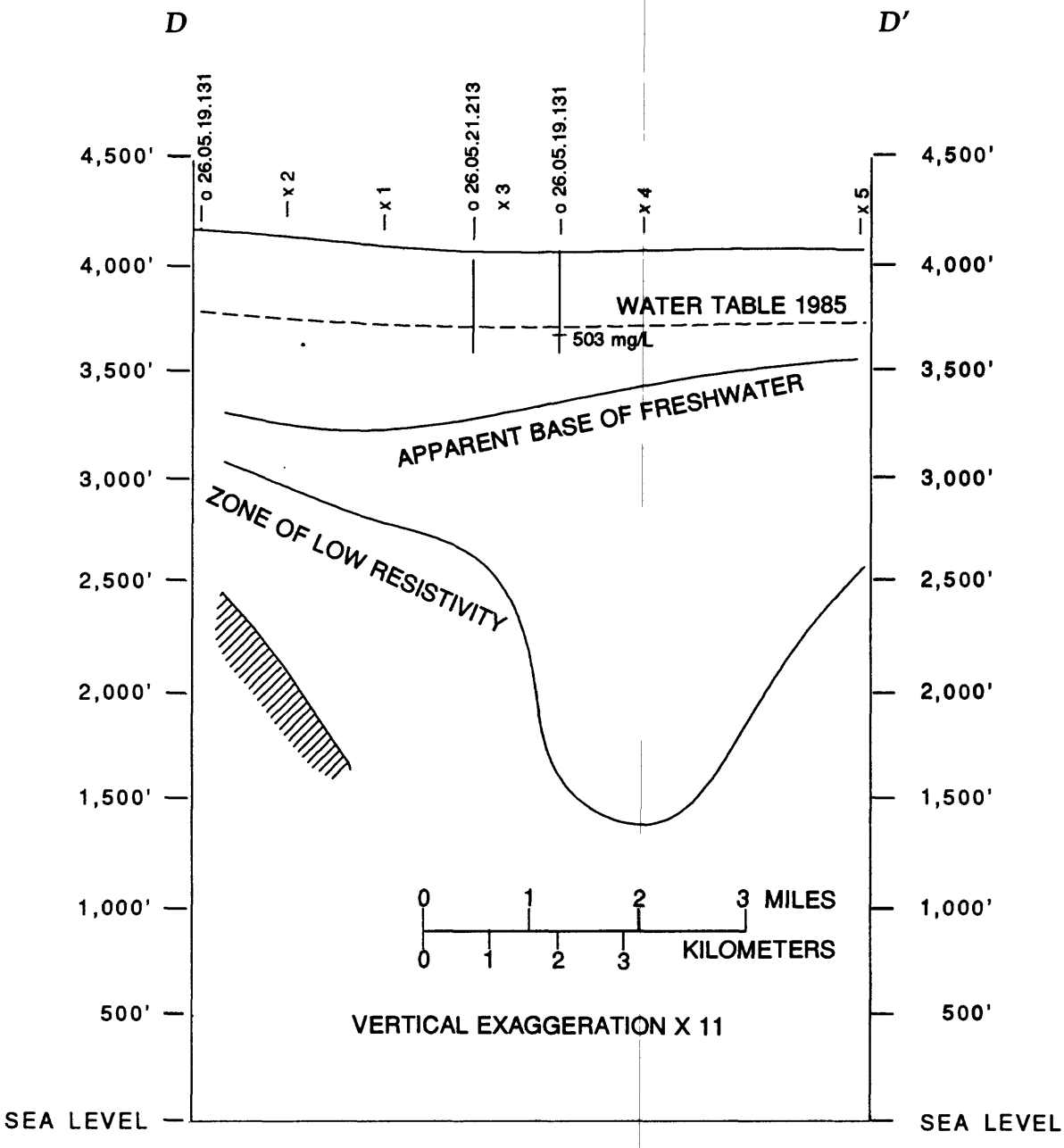

Figure 28.--Distribution of water quality with depth - Continued.

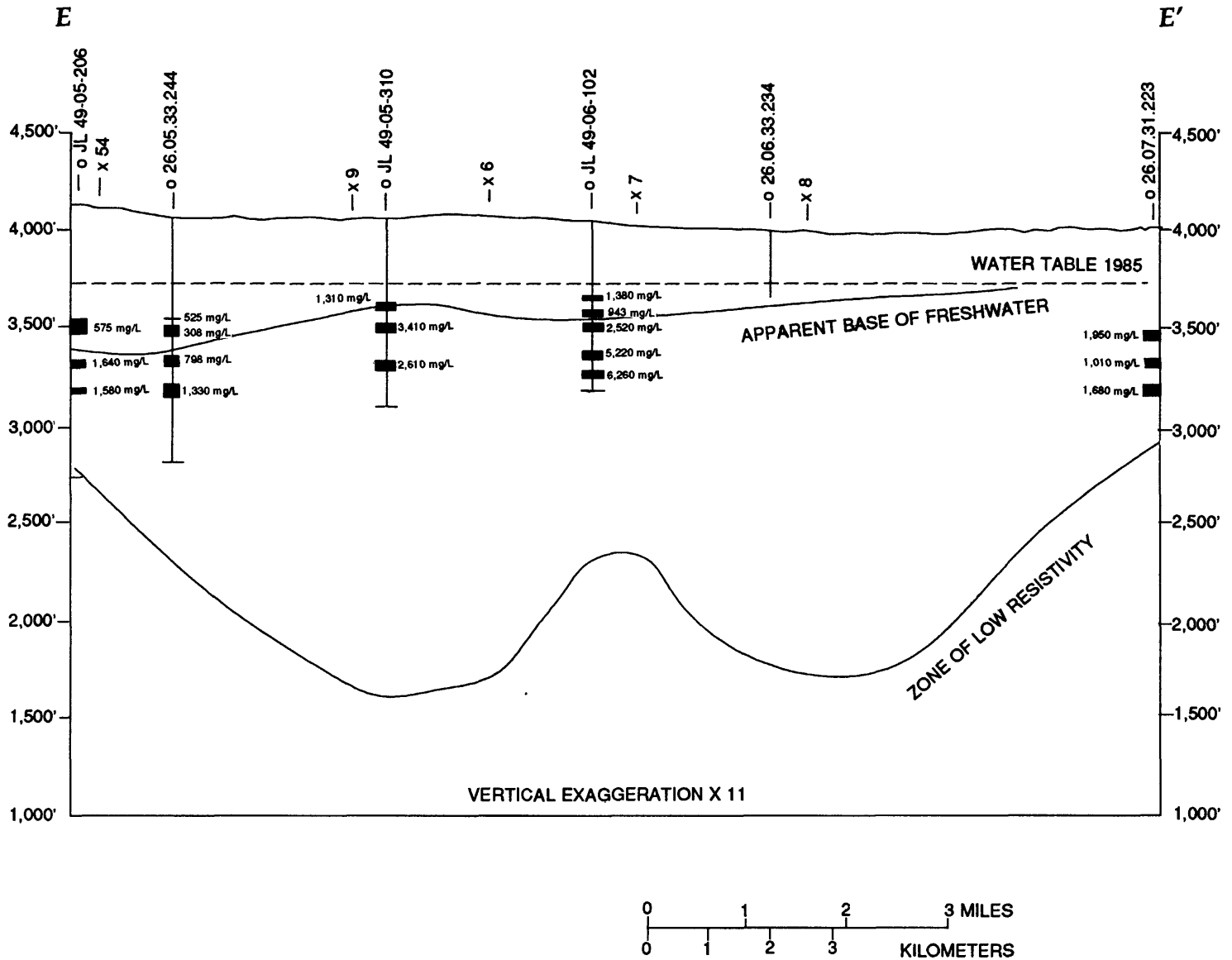

Figure 28.--Distribution of water quality with depth - Concluded.

Lateral Movement of Saline Water

Prior to ground-water development in the Hueco Bolson, movement of ground water was north to south along the mountain front. The velocity and direction of ground water in the New Mexico part of the basin as simulated in layer 1 of the steady-state ground-water flow model are shown in figure 29. The velocities were computed from cell-by-cell flux values assuming that the porosity of the aquifer was 0.15. This small porosity value was used so that computed velocities would represent the upper limit of average ground-water flow rates. The velocity vectors are close together where model cells are small. The vectors show that freshwater moves almost parallel to the approximate boundary between fresh and saline water at rates between 0.10 and 0.20 foot per day. On the basis of these rates, water moved 40 to 70 feet per year prior to ground-water development in the basin. Simulated average velocity of saline water in the eastern part of the basin was about 0.02 to 0.05 foot per day (7 to 20 feet per year).

Ground-water development in Texas and New Mexico from 1905 through 1983 caused water levels to decline as simulated in the transient flow model (fig. 18). Ground-water flow in 1983 simulated for the New Mexico part of the basin (fig. 30) is similar to steady-state flow (fig. 29), with a few exceptions. One difference is in the velocity of ground-water flow. By 1983, simulated ground-water withdrawals in Texas had caused an increase in simulated freshwater velocity at the New Mexico-Texas State line to about 0.6 foot per day (200 feet per year). Although ground-water velocity increased from 1905 through 1983, most freshwater flow continued to move along the mountain front. As long as water moved along the mountain front, freshwater of similar quality replaced that pumped by wells.

The potential for encroachment of saline water was most probable where the direction of velocity vectors changed near the saline-water boundary. The major change in direction of flow occurred along a 3-mile section of the eastern boundary of freshwater near Newman, New Mexico (figs. 29 and 30). In this area, ground-water flow turned slightly westward, probably causing lateral movement of saline water. At the freshwater boundary near Newman, ground-water velocity increased from 0.10 foot per day in 1905 to about 0.20 foot per day in 1983. Therefore, from 1905 through 1983, saline water could have encroached laterally a maximum of 1 mile due to the advection of ground water in the southeast quarter of Township 26 S., Range 6 E., near Newman. This estimate is based on the movement of a sharp interface between freshwater and saline water and does not incorporate any effects of hydrodynamic dispersion or differences in density.

To estimate the possible extent of future lateral encroachment of saline water, velocity vectors were plotted on the basis of results simulated for 2030 from the three-dimensional flow model (figs. 31 and 32). Using ground-water withdrawal rates from model scenario 1, the simulated ground-water velocity vectors are shown in figure 31. The simulated velocity of ground-water movement increased to nearly 0.4 foot per day at the boundary between freshwater and saline water near Newman. Therefore, the maximum predicted encroachment of saline water caused by advective transport from 1983 through 2030 would be about 1.5 miles.

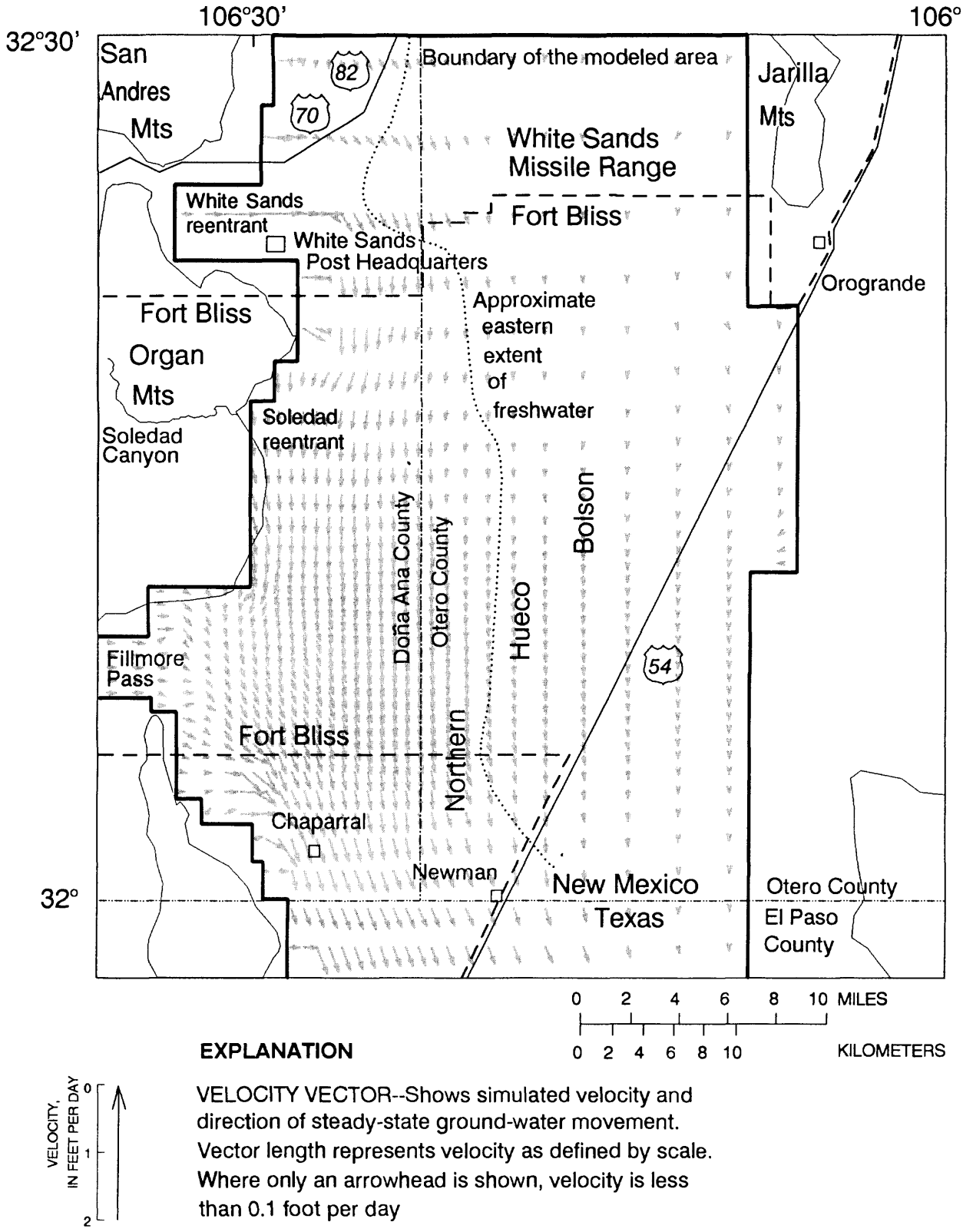

Figure 29.--Velocity and direction of simulated steady-state ground-water movement in model layer 1 in the New Mexico part of the Hueco Bolson.

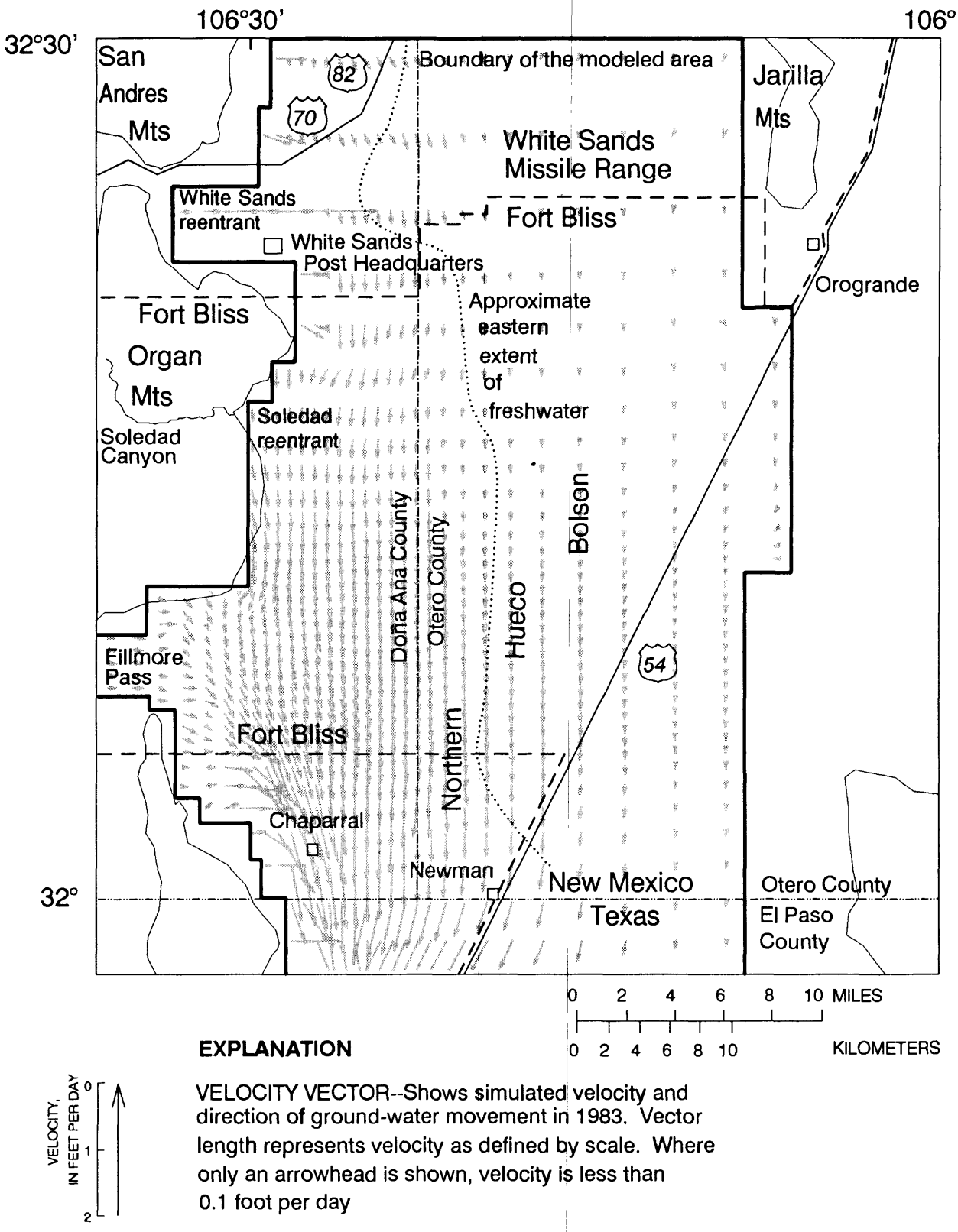

Figure 30.--Velocity and direction of simulated transient ground-water movement in 1983 in model layer 1 in the New Mexico part of the Hueco Bolson.

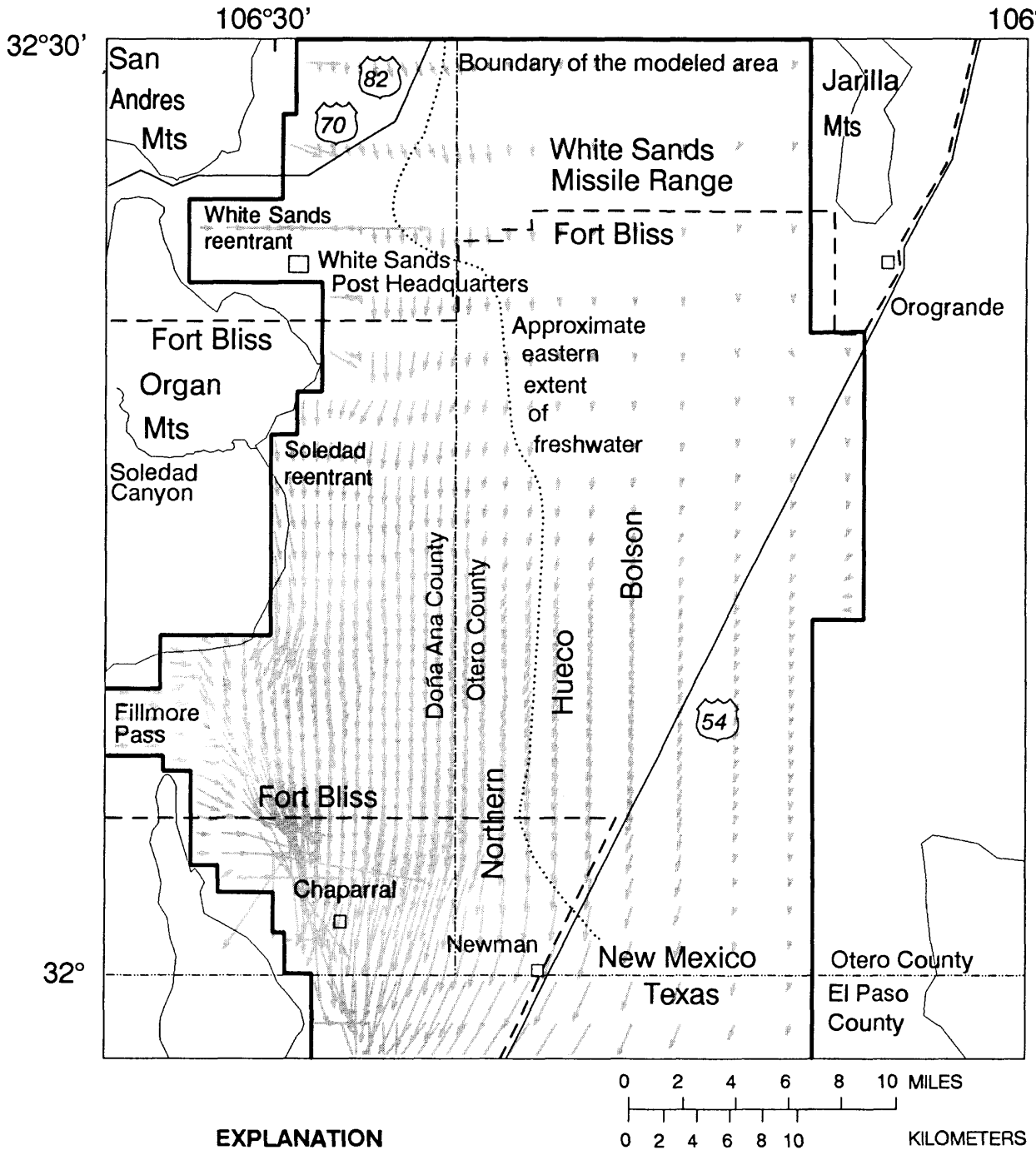

Figure 31.--Velocity and direction of simulated transient ground-water movement in 2030 in model layer 1 in the New Mexico part of the Hueco Bolson assuming no new ground-water withdrawals after 1990.

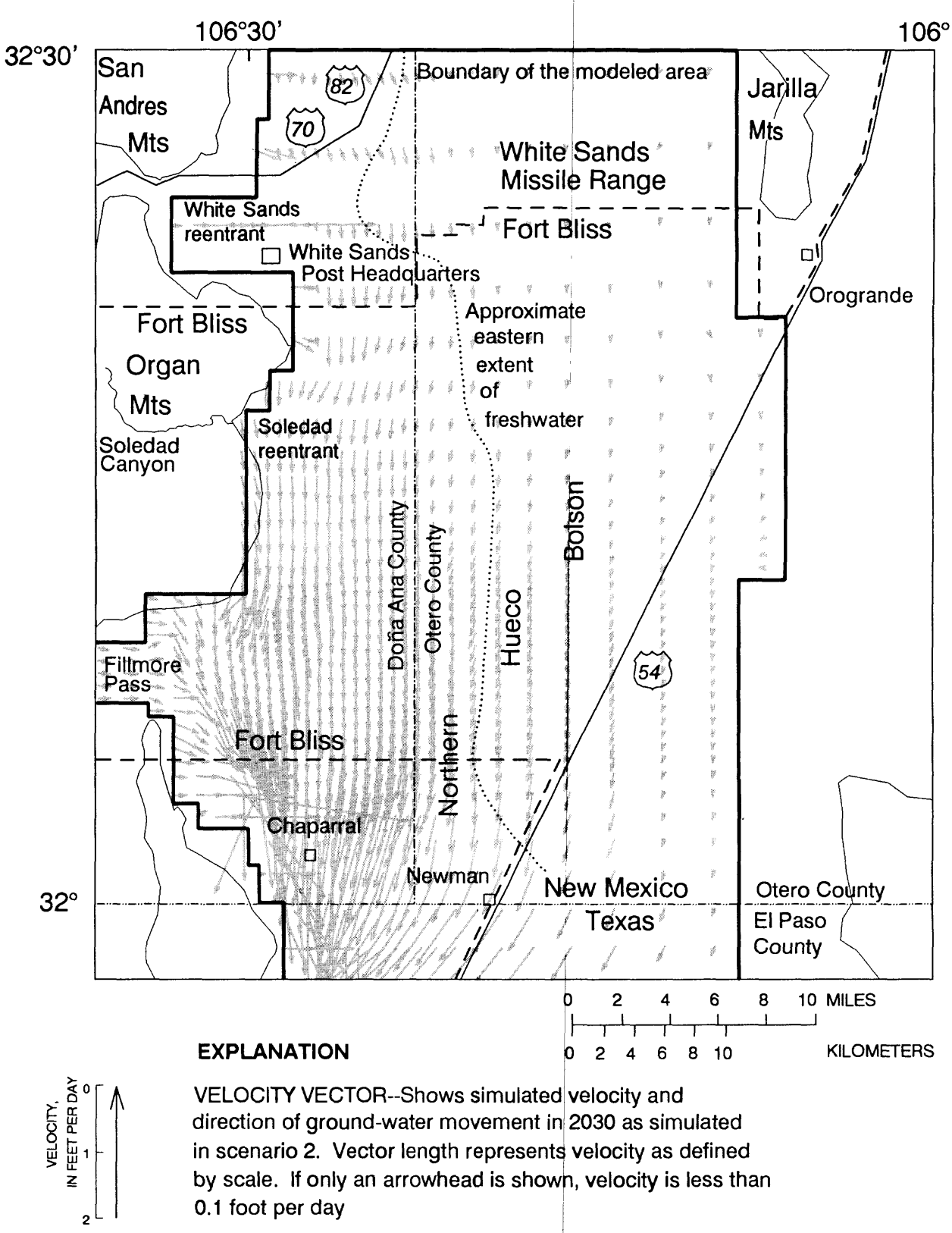

Figure 32.--Velocity and direction of simulated transient ground-water movement in 2030 in model layer 1 in the New Mexico part of the Hueco Bolson assuming continued development of ground-water withdrawals.

If greater amounts of ground water are withdrawn from the Hueco Bolson in Texas and New Mexico, as described in model scenario 2, the velocity and direction of movement of ground-water flow will be slightly different. The simulated velocity and direction of ground-water movement in model layer 1 for pumping scenario 2 are shown in figure 32. Again the area of concern, where saline water is moving into an area previously occupied by freshwater, is in Township 26 S., Range 6 E., near Newman. Given the larger pumping amount, the rate of saline-water movement, based on advective flow, could be as large as 0.5 foot per day, which could cause saline-water encroachment of about 2 miles from 1983 through 2030.

Because the effects of hydrodynamic dispersion and density differences were not included, the estimation of saline-water encroachment using velocity vectors from the three-dimensional flow model needs to be viewed as a general guide to areas where encroachment will be most likely. The western half of Township 26 S., Range 6 E. near Newman appears to be the area where encroachment of saline water is most probable. Observation wells drilled in this area would be helpful in monitoring the timing and extent of water-quality changes. Other parts of the aquifer that contain freshwater in New Mexico should not be affected as much by lateral movement of saline water. However, vertical movement of saline water from beneath well fields in New Mexico could cause significant degradation in the quality of water produced by those wells. Analysis of saline-water upconing is addressed in the following section.

Vertical Movement (Upconing) of Saline Water

Withdrawal of freshwater from the Hueco Bolson may cause saline water to move vertically upward beneath pumping wells, a phenomenon called upconing. The degree to which upconing will occur is dependent upon aquifer properties, contrast in density between freshwater and saline water, and pumping rate.

Sharp-Interface Analysis

If a sharp interface between freshwater and saline water is assumed, the position of the upconed saline water will stabilize beneath the well at pumping rates less than a critical value based upon the range of aquifer properties and conditions. In this stable position, only water in the freshwater part of the aquifer will reach the well. As pumping rates increase, the interface rises (fig. 33). When the pumping rate reaches the critical value, the interface reaches the well and saline water will be pumped by the well.

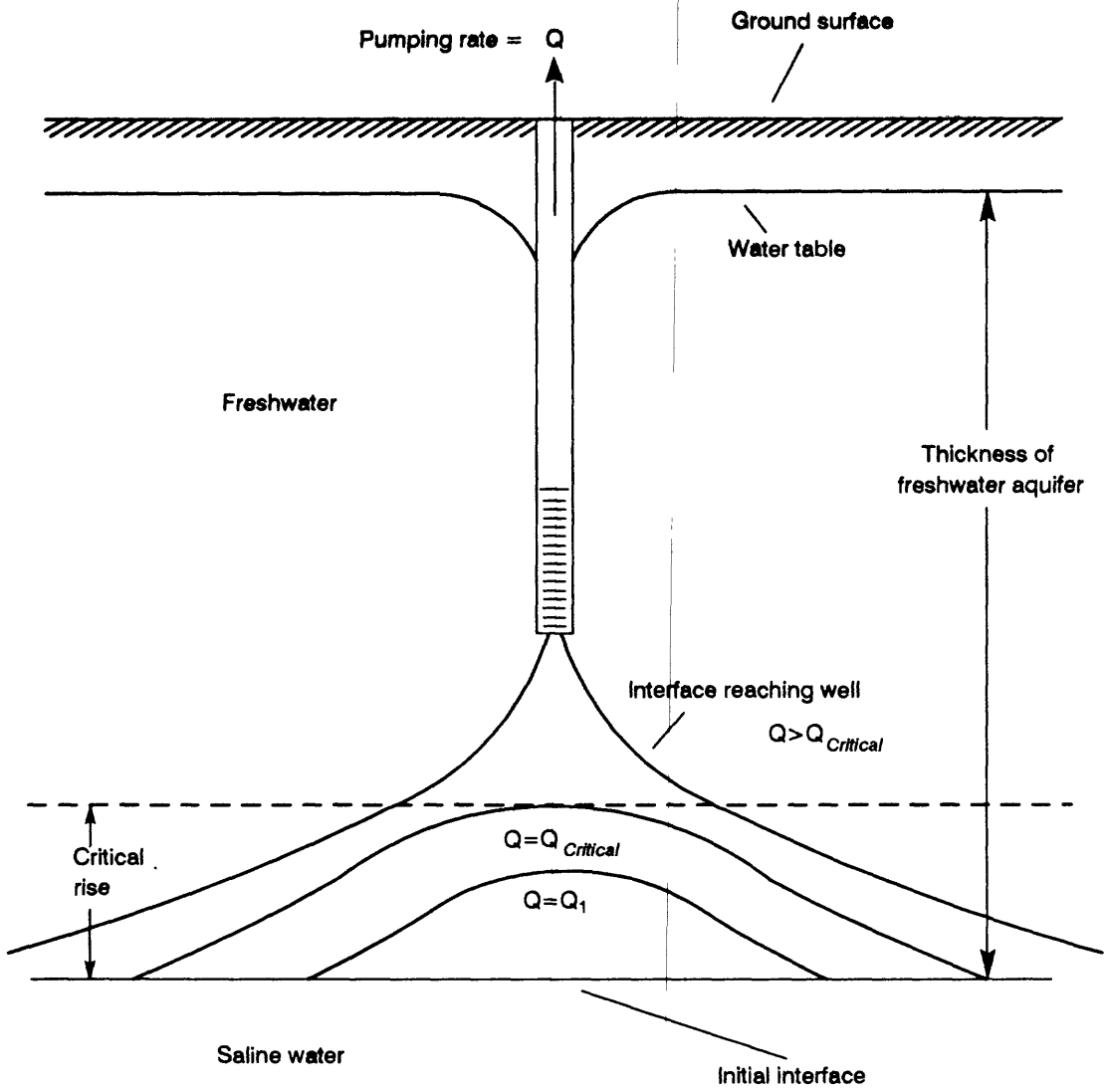

$Q_{Critical}$ -Pumping rate at which the stabilized interface between freshwater and saline water reaches the well

Q_1 -Pumping rate at which the stabilized interface between freshwater and saline water remains below the well

Critical rise -The position of the interface between freshwater and saline water at which saline water will be pumped by the well

Figure 33.--Saline-water upconing beneath a pumped well (modified from Reilly and others, 1987).

An analytical method to predict critical pumping rates was developed by Bennett and others (1968) and reevaluated by Reilly and others (1987). The method assumes cylindrical symmetry around the well and a sharp interface between freshwater and saline water. This method assumes a semi-infinite aquifer (infinite supply of salt water). In the Tularosa Basin, the base of freshwater often coincides with the decrease in hydraulic conductivity; this solution therefore provides a worst-case analysis. Critical pumping rates were estimated using this method for wells in the freshwater part of the Hueco Bolson in New Mexico. For the analysis, recharge to the bolson fill was assumed to be areally distributed at a rate of 0.2 inch per year. Other factors that affect the critical pumping rate were varied as shown below:

Parameter	Range tested
Hydraulic conductivity	10 to 35 feet per day
Horizontal to vertical anisotropy ratio	10 to 1,000
Saline-water density	1.0076 to 1.0250 grams per cubic centimeter
Freshwater thickness	100 to 2,000 feet
Location of well screen	Upper 15 to upper 65 percent of thickness of freshwater aquifer

The critical pumping rates calculated using these properties are listed in tables 6-8. These tables can be used as a guide in selecting maximum pumping rates for wells in the Hueco Bolson. For example, if a well were screened in the upper 15 percent of a freshwater-saturated zone 1,000 feet thick with a hydraulic conductivity of 20 feet per day, a horizontal to vertical anisotropy ratio of 200, and a density of 1.0076 grams per cubic centimeter for the underlying saline water, the critical pumping rate would be 1,072 gallons per minute (table 6). If this well were screened in the upper 45 percent of the same freshwater-saturated thickness, the critical pumping rate would be 818 gallons per minute (table 7). It is apparent from the tables that the critical pumping rate is very sensitive to the aquifer characteristics, position of well screen, and saline-water density.

Table 6.--Critical pumping rates, in gallons per minute, for wells screened in the upper 15 percent of the freshwater part of the aquifer

Hydraulic conductivity, in feet per day	Horizontal to vertical anisotropy ratio	Saline-water density, in grams per cubic centimeter	Freshwater thickness, in feet								
			100	250	500	750	1,000	1,250	1,500	1,750	2,000
35	1,000	1.0250	59	372	1,486	3,344	5,945	9,290	13,377	18,208	23,781
35	1,000	1.0152	42	260	1,040	2,340	4,159	6,499	9,359	12,738	16,637
35	1,000	1.0076	26	163	654	1,471	2,615	4,086	5,884	8,009	10,460
35	200	1.0250	44	276	1,105	2,486	4,420	6,907	9,946	13,537	17,681
35	200	1.0152	29	179	718	1,615	2,872	4,487	6,461	8,794	11,486
35	200	1.0076	16	102	409	919	1,635	2,554	3,678	5,006	6,538
35	100	1.0250	42	260	1,039	2,339	4,157	6,496	9,354	12,732	16,630
35	100	1.0152	26	165	658	1,481	2,633	4,114	5,924	8,063	10,531
35	100	1.0076	14	90	359	808	1,436	2,243	3,231	4,397	5,743
35	10	1.0250	39	243	973	2,189	3,891	6,080	8,755	11,916	15,564
35	10	1.0152	24	149	595	1,338	2,378	3,716	5,351	7,283	9,512
35	10	1.0076	12	75	301	678	1,204	1,882	2,710	3,689	4,818
20	1,000	1.0250	40	249	996	2,241	3,984	6,225	8,964	12,201	15,937
20	1,000	1.0152	29	178	713	1,604	2,852	4,456	6,417	8,734	11,407
20	1,000	1.0076	18	115	460	1,035	1,841	2,876	4,142	5,638	7,363
20	200	1.0250	27	170	681	1,533	2,725	4,258	6,132	8,346	10,901
20	200	1.0152	18	113	454	1,021	1,815	2,837	4,085	5,560	7,262
20	200	1.0076	11	67	268	603	1,072	1,675	2,413	3,284	4,289
20	100	1.0250	25	156	622	1,401	2,490	3,890	5,602	7,625	9,959
20	100	1.0152	16	101	402	905	1,609	2,513	3,619	4,926	6,435

Table 6.--Critical pumping rates, in gallons per minute, for wells screened in the upper 15 percent of the freshwater part of the aquifer--Concluded

Hydraulic conductivity, in feet per day	Horizontal to vertical anisotropy ratio	Saline-water density, in grams per cubic centimeter	Freshwater thickness, in feet								
			100	250	500	750	1,000	1,250	1,500	1,750	2,000
20	100	1.0076	9	57	227	511	908	1,418	2,042	2,780	3,631
20	10	1.0250	22	140	559	1,258	2,237	3,495	5,033	6,850	8,947
20	10	1.0152	14	86	343	772	1,372	2,144	3,087	4,202	5,489
20	10	1.0076	7	44	175	394	701	1,095	1,578	2,147	2,804
10	1,000	1.0250	25	157	628	1,413	2,513	3,926	5,654	7,696	10,052
10	1,000	1.0152	18	115	460	1,035	1,841	2,876	4,142	5,638	7,363
10	1,000	1.0076	12	76	305	686	1,219	1,905	2,743	3,733	4,876
10	200	1.0250	16	97	389	876	1,558	2,434	3,505	4,770	6,231
10	200	1.0152	11	67	268	603	1,072	1,675	2,413	3,284	4,289
10	200	1.0076	7	41	165	372	661	1,033	1,487	2,025	2,644
10	100	1.0250	14	85	341	766	1,363	2,129	3,066	4,173	5,451
10	100	1.0152	9	57	227	511	908	1,418	2,042	2,780	3,631
10	100	1.0076	5	34	134	302	536	838	1,206	1,642	2,145
10	10	1.0250	11	71	283	638	1,134	1,772	2,551	3,472	4,535
10	10	1.0152	7	44	175	394	701	1,095	1,577	2,147	2,804
10	10	1.0076	4	23	91	205	365	570	821	1,117	1,459

Table 7.--Critical pumping rates, in gallons per minute, for wells screened in the upper 45 percent of the freshwater part of the aquifer

Hydraulic conductivity, in feet per day	Horizontal to vertical anisotropy ratio	Saline-water density, in grams per cubic centimeter	Freshwater thickness, in feet								
			100	250	500	750	1,000	1,250	1,500	1,750	2,000
35	1,000	1.0250	46	284	1,138	2,560	4,551	7,110	10,239	13,936	18,203
35	1,000	1.0152	31	196	785	1,767	3,141	4,908	7,068	9,620	12,565
35	1,000	1.0076	19	121	486	1,093	1,943	3,036	4,372	5,951	7,773
35	200	1.0250	35	221	883	1,987	3,532	5,518	7,947	10,816	14,127
35	200	1.0152	23	142	567	1,275	2,267	3,543	5,101	6,943	9,069
35	200	1.0076	13	79	317	712	1,266	1,978	2,849	3,877	5,064
35	100	1.0250	34	210	841	1,892	3,364	5,256	7,568	10,301	13,455
35	100	1.0152	21	132	528	1,188	2,112	3,300	4,752	6,468	8,448
35	100	1.0076	11	71	283	638	1,134	1,771	2,551	3,472	4,535
35	10	1.0250	32	200	799	1,799	3,198	4,996	7,195	9,793	12,790
35	10	1.0152	20	122	488	1,098	1,952	3,050	4,391	5,977	7,807
35	10	1.0076	10	62	246	554	985	1,540	2,217	3,018	3,942
20	1,000	1.0250	30	188	751	1,690	3,004	4,694	6,759	9,200	12,017
20	1,000	1.0152	21	133	531	1,195	2,125	3,321	4,782	6,509	8,501
20	1,000	1.0076	14	85	338	761	1,354	2,115	3,046	4,146	5,415
20	200	1.0250	21	134	537	1,208	2,148	3,357	4,834	6,579	8,593
20	200	1.0152	14	88	353	794	1,412	2,206	3,176	4,323	5,646
20	200	1.0076	8	51	204	460	818	1,277	1,839	2,504	3,270
20	100	1.0250	20	125	499	1,122	1,995	3,117	4,489	6,110	7,980
20	100	1.0152	13	80	319	717	1,274	1,991	2,867	3,903	5,098

Table 7.--Critical pumping rates, in gallons per minute, for wells screened in the upper 45 percent of the freshwater part of the aquifer--Concluded

Hydraulic conductivity, in feet per day	Horizontal to vertical anisotropy ratio	Saline-water density, in grams per cubic centimeter	Freshwater thickness, in feet								
			100	250	500	750	1,000	1,250	1,500	1,750	2,000
20	100	1.0076	7	44	176	397	706	1,103	1,588	2,162	2,823
20	10	1.0250	18	115	459	1,032	1,835	2,868	4,130	5,621	7,342
20	10	1.0152	11	70	281	632	1,123	1,755	2,528	3,441	4,494
20	10	1.0076	6	36	143	321	571	892	1,285	1,749	2,284
10	1,000	1.0250	19	117	466	1,049	1,865	2,914	4,196	5,711	7,460
10	1,000	1.0152	14	85	338	761	1,354	2,115	3,046	4,146	5,415
10	1,000	1.0076	9	55	222	499	887	1,387	1,997	2,718	3,550
10	200	1.0250	12	75	301	677	1,204	1,882	2,710	3,688	4,817
10	200	1.0152	8	51	204	460	818	1,277	1,839	2,504	3,270
10	200	1.0076	5	31	124	279	495	774	1,114	1,516	1,981
10	100	1.0250	11	67	269	604	1,074	1,678	2,417	3,290	4,297
10	100	1.0152	7	44	176	397	706	1,103	1,588	2,162	2,823
10	100	1.0076	4	26	102	230	409	639	920	1,252	1,635
10	10	1.0250	9	58	232	522	927	1,449	2,086	2,840	3,709
10	10	1.0152	6	36	143	321	571	892	1,285	1,749	2,284
10	10	1.0076	3	18	74	166	294	460	663	902	1,178

Table 8.--Critical pumping rates, in gallons per minute, for wells screened in the upper 65 percent of the freshwater part of the aquifer

Hydraulic conductivity, in feet per day	Horizontal to vertical anisotropy ratio	Saline-water density, in grams per cubic centimeter	Freshwater thickness, in feet								
			100	250	500	750	1,000	1,250	1,500	1,750	2,000
35	1,000	1.0250	28	174	697	1,569	2,789	4,358	6,276	8,542	11,157
35	1,000	1.0152	20	122	488	1,097	1,950	3,047	4,388	5,973	7,801
35	1,000	1.0076	12	77	306	689	1,225	1,915	2,757	3,753	4,902
35	200	1.0250	21	130	519	1,169	2,077	3,246	4,674	6,362	8,310
35	200	1.0152	13	84	337	759	1,349	2,108	3,035	4,131	5,395
35	200	1.0076	8	48	192	432	767	1,199	1,726	2,350	3,069
35	100	1.0250	20	122	489	1,100	1,955	3,055	4,399	5,987	7,820
35	100	1.0152	12	77	309	696	1,238	1,934	2,784	3,790	4,950
35	100	1.0076	7	42	169	379	674	1,054	1,517	2,065	2,698
35	10	1.0250	18	114	458	1,030	1,831	2,861	4,119	5,607	7,323
35	10	1.0152	11	70	280	629	1,119	1,748	2,518	3,427	4,476
35	10	1.0076	6	35	142	319	567	885	1,275	1,735	2,267
20	1,000	1.0250	19	117	467	1,051	1,868	2,919	4,203	5,721	7,472
20	1,000	1.0152	13	84	334	752	1,337	2,088	3,007	4,093	5,346
20	1,000	1.0076	9	54	216	485	862	1,347	1,940	2,641	3,449
20	200	1.0250	13	80	320	720	1,280	2,000	2,880	3,920	5,120
20	200	1.0152	9	53	213	479	852	1,332	1,918	2,610	3,409
20	200	1.0076	5	31	126	283	503	786	1,132	1,540	2,012
20	100	1.0250	12	73	293	658	1,170	1,829	2,633	3,584	4,681
20	100	1.0152	8	47	189	425	756	1,181	1,700	2,314	3,023

Table 8.--Critical pumping rates, in gallons per minute, for wells screened in the upper 65 percent of the freshwater part of the aquifer--Concluded

Hydraulic conductivity, in feet per day	Horizontal to vertical anisotropy ratio	Saline-water density, in grams per cubic centimeter	Freshwater thickness, in feet								
			100	250	500	750	1,000	1,250	1,500	1,750	2,000
20	100	1.0076	4	27	107	240	426	666	959	1,305	1,705
20	10	1.0250	11	66	263	592	1,052	1,644	2,368	3,223	4,210
20	10	1.0152	6	40	161	363	646	1,009	1,452	1,977	2,582
20	10	1.0076	3	21	82	185	330	515	742	1,010	1,319
10	1,000	1.0250	12	74	294	662	1,178	1,840	2,649	3,606	4,710
10	1,000	1.0152	9	54	216	485	862	1,347	1,940	2,641	3,449
10	1,000	1.0076	6	36	143	321	571	892	1,284	1,748	2,283
10	200	1.0250	7	46	183	411	731	1,142	1,645	2,239	2,924
10	200	1.0152	5	31	126	283	503	786	1,132	1,540	2,012
10	200	1.0076	3	19	77	174	310	484	697	949	1,240
10	100	1.0250	6	40	160	360	640	1,000	1,440	1,960	2,560
10	100	1.0152	4	27	107	240	426	666	959	1,305	1,705
10	100	1.0076	3	16	63	141	251	393	566	770	1,006
10	10	1.0250	5	33	133	300	533	833	1,200	1,634	2,134
10	10	1.0152	3	21	82	185	330	515	742	1,010	1,319
10	10	1.0076	2	11	43	96	171	268	386	525	686

A set of parameters that most closely represents hydraulic characteristics of the Hueco Bolson was chosen on the basis of aquifer characteristics used in the flow model. These characteristics include a horizontal hydraulic conductivity of 35 feet per day and a ratio of horizontal to vertical hydraulic conductivity of 200 (table 7). Critical pumping values were calculated for saline water with a density within the range of 10,000 to 30,000 milligrams per liter (about 1.0076 to 1.025 grams per cubic centimeter) beneath freshwater in the New Mexico part of the Hueco Bolson (fig. 34). Calculations assumed that the well was screened in the upper 45 percent of the freshwater zone. Upconing probably will not pose much of a problem for wells pumping in areas where the freshwater thickness is greater than 1,000 feet (fig. 34). However, the proposed pumping in the Chaparral, New Mexico, area is located where freshwater thickness is much less than 1,000 feet (fig. 27). Pumping rates proposed for wells in areas where freshwater thickness is less than about 1,000 feet need to be carefully evaluated using tables 6-8 as a guideline.

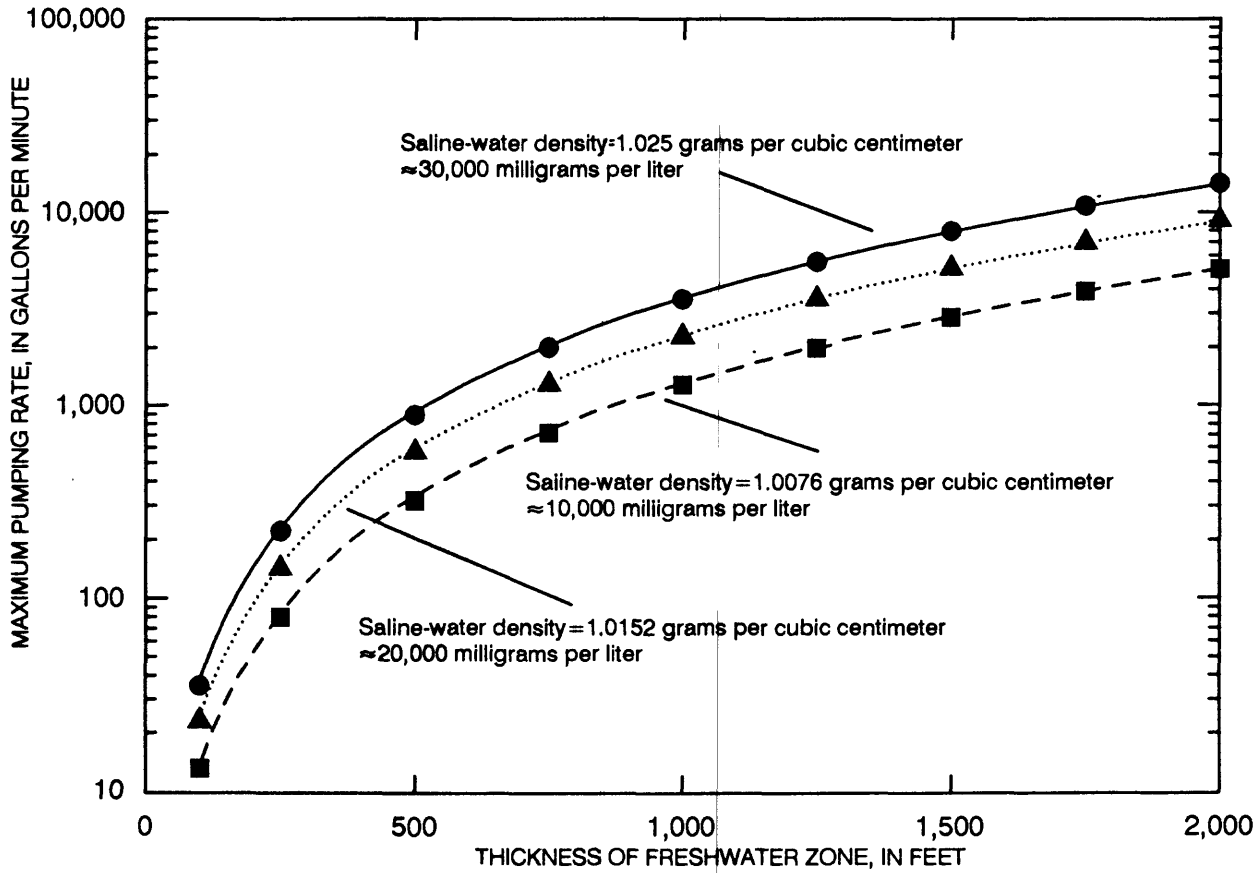

Figure 34.--Critical pumping values for a well screened in the upper 45 percent of the freshwater zone in the Hueco Bolson, New Mexico (analysis assumes a horizontal hydraulic conductivity of 10 feet per day and an anisotropy ratio of 200).

Upconing Analysis Including Hydrodynamic Dispersion

The critical pumping rates determined from the sharp-interface analysis should provide a guide to long-term pumping that can be sustained without inducing saline-water upconing. However, because the interface between freshwater and saline water is not a sharp one, some saline water will be drawn to the pumped well by hydrodynamic dispersion even if pumping is limited to the estimated critical amount. Therefore, a two-dimensional solute-transport model was used radially to estimate the magnitude of possible changes in dissolved-solids concentration caused by hydrodynamic dispersion.

A solute-transport model, Saturated-Unsaturated TRAnsport (SUTRA) that includes density-related flow (Voss, 1984) was used for this analysis (fig. 35). The finite-element grid in radial coordinates consisted of 41 nodes variably spaced in the radial direction and 51 nodes equally spaced in the vertical direction. In the radial direction, distance between nodes began at 1 foot and increased by a factor of 1.5 to a maximum separation of 1,000 feet. The vertical distance between nodes was either 5 or 10 feet, depending upon the thickness of freshwater being simulated. Hydraulic properties from line 4 in table 6 were assigned to the model, and horizontal and vertical dispersivities were assumed to be 30 and 6 feet, respectively, on the basis of values used in a study of a similar unconsolidated aquifer (Reilly and others, 1987).

Boundary conditions for the model were assigned to correspond as nearly as possible to conditions used in the sharp-interface model and represent a worst-case analysis. Recharge was added along the top boundary at a rate of 0.2 inch per year of freshwater. The bottom boundary was set to a constant pressure that represented the saline-water interface. Saline water having a density of 1.025 grams per cubic centimeter (about 30,000 milligrams per liter) was assumed to occur below this boundary. The node at the water table along the outermost radial boundary also was set to a constant pressure to allow recharged water to flow out of the system. A partly penetrating pumped well was located at the axis of the model. The well was simulated by specified flux distributed uniformly down the length of the well screen from the upper 45 percent of the freshwater thickness. Pumping rates between about 100 and 800 gallons per minute were simulated.

The model was used to investigate possible changes in the salinity of water pumped from areas where freshwater is less than 1,000 feet thick. Pumping rates as great as the critical amounts from line 4 in table 6 were tested using the model to determine if these amounts provide reasonable guidelines to maximum pumping rates. Results for aquifer thicknesses of 500 and 250 feet are shown in figure 36. Although pumping was simulated at the critical rate or less, the model indicates that hydrodynamic dispersion will cause some saline water to be pumped. Although these estimates are sensitive to the value of dispersivity used in the model, they demonstrate that some mixing can be expected even if wells are pumped at less than the critical rate.

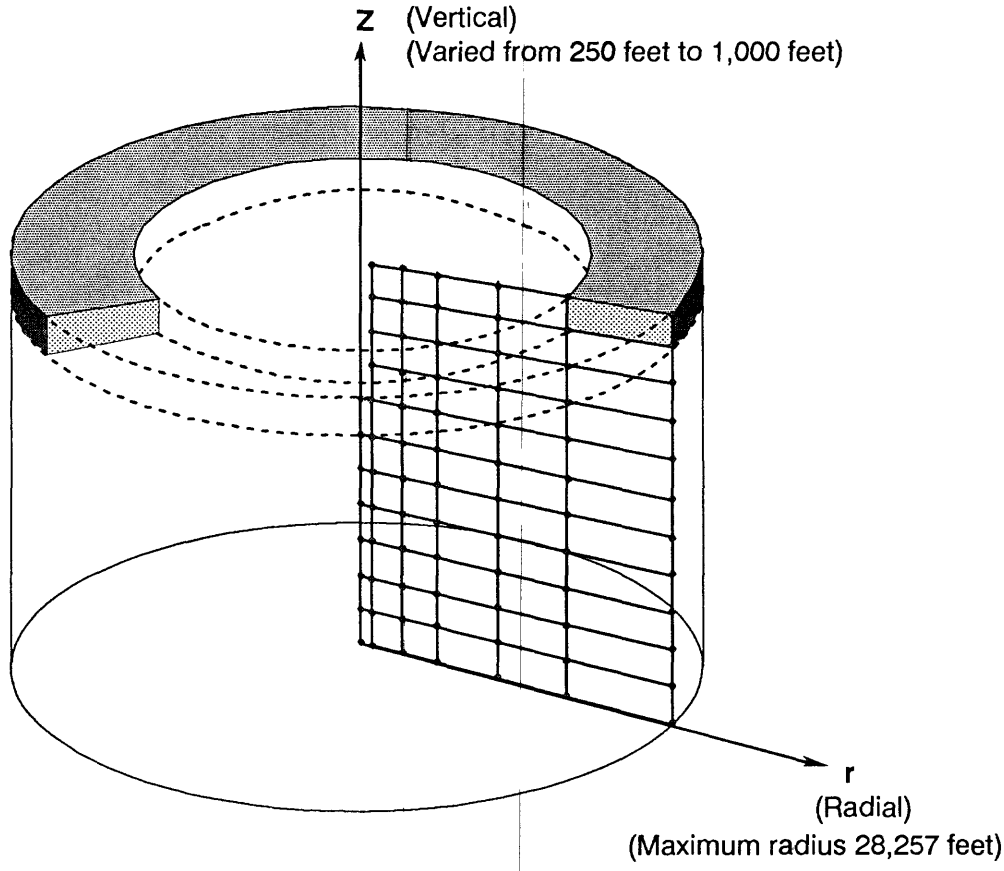

Figure 35.--Finite-element grid in radial coordinates for the Saturated-Unsaturated TRAnsport (SUTRA) model (from Voss, 1984, p. 138).

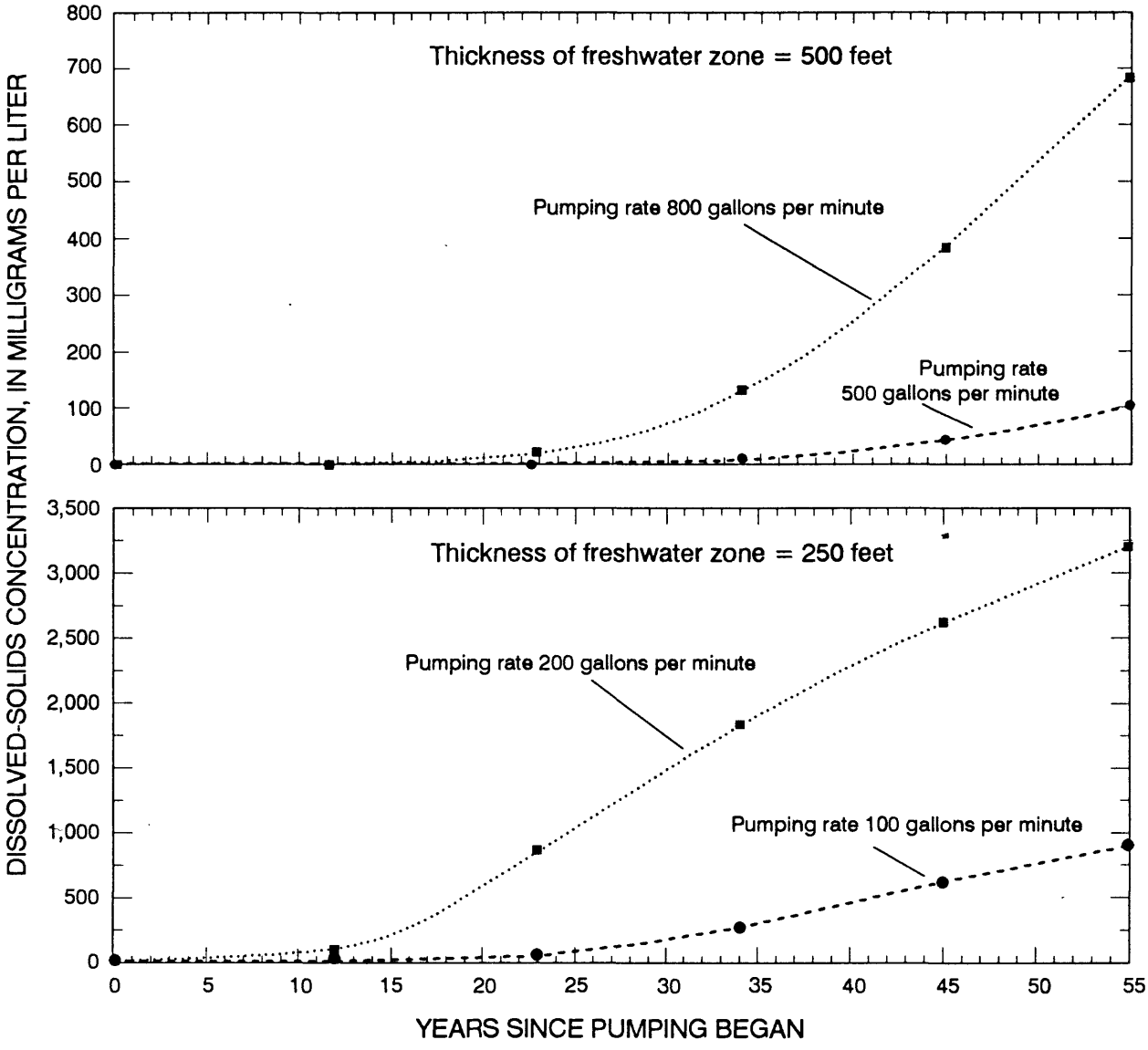

These simulations assume the following hydrologic conditions and properties:

Hydraulic conductivity = 35 feet per day
Ratio of horizontal to vertical hydraulic conductivity = 200
Density of saline water = 1.025 grams per cubic centimeter
Areal recharge = 0.2 inch per year
Horizontal dispersivity = 30 feet
Vertical dispersivity = 6 feet

Figure 36.--Estimated change in dissolved-solids concentration of well discharge caused by upward movement of saline water, assuming specific hydrologic conditions and properties.

SUMMARY

The New Mexico part of the Hueco Bolson contains freshwater-saturated sediments that are being considered for potential ground-water development. Extensive withdrawal of water in the New Mexico part of the bolson may result in declining water levels and deterioration of water quality.

The Hueco Bolson is a structural basin that contains basin-fill deposits that range in thickness from zero on the east to possibly 8,000 feet along the deepest part of the trough. Fluvial deposits of the Camp Rice Formation as much as 1,000 feet thick in the northern part of the Hueco Bolson are underlain by lacustrine clay and evaporites and are bordered by alluvial-fan sand, gravel, and clay.

The hydraulic conductivity of basin-fill deposits ranges from less than 1 foot to more than 200 feet per day. A small ratio of vertical to horizontal hydraulic conductivity is attributed to discontinuous, thinly bedded clay layers. In the long term, the storage coefficient approaches the specific yield of the aquifer.

Basin-fill deposits overlying a horst in Fillmore Pass between the Organ and Franklin Mountains may provide hydraulic connection with the Mesilla Basin to the west. Saturated sediments may be less than 400 feet thick and ground-water flow through the pass probably is minimal.

Mountain-front recharge to the ground-water system takes place on coarse-grained alluvial-fan deposits in response to surface runoff. Discharge from the northern part of the Hueco Bolson occurs as ground-water flow to the south and as pumpage; because of deep ground-water levels, evapotranspiration is not a major source of discharge except along the Rio Grande south of El Paso, Texas.

A three-dimensional numerical model with three layers was used to simulate ground-water flow in the northern part of the Hueco Bolson. Hydraulic conductivity for layer 1 of the model ranged from 1 to 40 feet per day. A hydraulic conductivity of 2 feet per day was assigned to layers 2 and 3. Simulations used an annual recharge rate of 4,500 acre-feet, which is 3.1 percent of the total estimated precipitation over mountain drainages. The simulated steady-state hydraulic gradient was southward and ranged from 2.5 to 4 feet per mile.

The historical simulation spanned the period 1905-83. Simulated pumpage stresses increased from approximately 3,600 acre-feet per year in stress period one (1905-14) to approximately 144,000 acre-feet per year in stress period eleven (1980-83). The adjusted distribution of specific yield for layer 1 ranged from 0.05 to 0.20.

By 1983, most ground-water flow was toward El Paso, Texas, and Ciudad Juarez, Mexico. Water-level declines of approximately 25 feet were simulated at the New Mexico-Texas State line. Declines less than 25 feet were simulated over most of the northern part of the Hueco Bolson in New Mexico. By 1983, pumping accounted for most of the water moving out of the study area; 122,000 acre-feet per year was being removed from storage. Net leakage from the river increased from 800 to 18,800 acre-feet per year from 1905 to 1983 in response to drawdown from pumpage. Approximately 3.2 million acre-feet of water had been removed from storage by 1983.

The aquifer response in the Hueco Bolson was simulated to 2030 using two pumping scenarios. Scenario 1 assumed that pumpage stresses after 1990 remained constant. Scenario 2 assumed that pumpage stresses continued at the same rate as pre-1983 trends. Both scenarios assumed that 10,000 acre-feet per year of pumpage was shifted to New Mexico.

In scenario 1, by 2030, the simulated cone of depression had deepened considerably around El Paso and Ciudad Juarez. Ground-water flow from the north in layer 1 was completely diverted toward the pumping center. A deepening trough had formed in the potentiometric surface to the north, partially in response to shifting of pumpage into New Mexico. The hydraulic gradient at the New Mexico-Texas State line ranged from about 6 to 12 feet per mile, and flow was to the south and southwest. Water-level declines in New Mexico near the State line were as much as 100 feet. The rate of removal of water from storage by 2030 exceeded 127,000 acre-feet per year, and a total of 9.8 million acre-feet was removed from storage from 1905 to 2030.

The cone of depression around the El Paso-Ciudad Juarez area for scenario 2 was significantly deeper than that for scenario 1. Ground-water flow from the north again was completely diverted toward the pumping center. The hydraulic gradient at the New Mexico-Texas State line was to the south and southwest and ranged from 6 to 18 feet per mile. Water-level declines in New Mexico near the State line ranged from 25 to 125 feet. The rate of removal of water from storage increased to more than 255,000 acre-feet per year by 2030, and more than 12.8 million acre-feet of water was removed from storage from 1905 to 2030.

The sensitivity of the transient model to doubling and halving hydraulic conductivity uniformly in all three layers generally was slight. Water-level differences generally differed by less than 10 feet from those of the standard simulation.

Slight water-level changes generally occurred in the transient model in response to doubling and halving mountain-front recharge. Water-level differences from the standard simulation generally were 5 feet or less.

The transient simulation was moderately sensitive to a 20-percent increase and 20-percent decrease in specific yield for layer 1. Differences in water levels between simulations using the standard and modified specific yield ranged from 1 to 24 feet.

Freshwater-saturated deposits may be as thick as 2,000 feet in the Soledad Canyon reentrant. Elsewhere, thicknesses range from about 1,000 feet on the west to a feather edge on the east. The thickest sections of freshwater-saturated deposits are present in coarse-grained fluvial and alluvial-fan deposits east of the Organ and Franklin Mountains. More saline water occurs in fine-grained deposits.

Large-scale ground-water withdrawals could cause saline-water encroachment toward wells completed in the freshwater part of the aquifer. Encroachment depends upon thickness of freshwater-saturated deposits, well location, pumping rate, depth of well completion, hydrologic properties of the basin-fill deposits, and density of the surrounding saline water. The two principal avenues of encroachment are lateral movement and vertical movement (upconing) of saline water to wells.

On the basis of simulations of steady-state conditions, freshwater in the western part of the basin was estimated to move parallel to the approximate boundary between freshwater and saline water at rates between 0.10 and 0.20 foot per day. Movement of saline water in the eastern part of the basin was estimated to be about 0.02 to 0.05 foot per day. By 1983, simulated freshwater velocity had increased across the Texas State line to about 0.6 foot per day in response to pumpage stresses, but most of the simulated freshwater flow continued to move along the mountain front. A major change in flow direction occurred along a 3-mile section of the eastern freshwater boundary near Newman, New Mexico, probably causing lateral movement of saline water in that area. At the freshwater boundary near Newman, simulated ground-water velocity increased from 0.10 foot per day in 1905 to about 0.20 foot per day in 1983, possibly resulting in a maximum simulated saline-water encroachment of 1 mile.

In scenario 1, by 2030, the simulated flow velocity at the boundary between freshwater and saline water near Newman increased to nearly 0.4 foot per day, resulting in movement of the saline-water front of about 1.5 miles from 1983 through 2030. If larger ground-water withdrawals occur, as described in scenario 2, the flow velocity could be as large as 0.5 foot per day toward the pumped wells, possibly resulting in saline-water encroachment of about 2 miles from 1983 through 2030.

Upconing of saline water could cause degradation in the quality of water pumped from wells. The critical pumping rate, the rate at which saline water moves into the well screen under vertically uniform flow to the well, is sensitive to the aquifer characteristics, position of the well screen, and saline-water density. Upconing probably will not pose much of a problem for wells in areas where the thickness of the freshwater zone is greater than 1,000 feet. However, proposed ground-water withdrawals are in the Chaparral, New Mexico, area where the thickness of the freshwater zone is much less than 1,000 feet.

Even at less than critical pumping rates, worst-case radial solute-transport simulations indicate that dispersive processes will cause some saline water to be pumped. Although these worst-case estimates are sensitive to the value of dispersivity used in the model, they demonstrate that some saline mixing can be expected.

SELECTED REFERENCES

Alvarez, H.J., and Buckner, A.W., 1980, Ground-water development in the El Paso region, Texas, with emphasis on the resources of the lower El Paso Valley: Texas Department of Water Resources Report 246, 346 p.

Audsley, G.L., 1959, Records of wells and results of exploratory drilling in the El Paso Valley and Hueco Bolson southeast of El Paso, Texas: U.S. Geological Survey Open-File Report, 147 p.

Ballance, W.C., and Basler, J.A., 1966, Runoff from a paved small watershed at White Sands Missile Range, New Mexico: U.S. Geological Survey Open-File Report, 21 p.

Bennett, G.D., Mundorff, M.J., and Hussain, S.A., 1968, Electric-analog studies of brine coning beneath fresh-water wells in the Punjab region, West Pakistan: U.S. Geological Survey Water-Supply Paper 1608-J, 31 p.

Bisdorf, R.J., 1985, Schlumberger sounding results in the Hueco Bolson, New Mexico: U.S. Geological Survey Open-File Report 85-607, 120 p.

Cliett, Thomas, 1969, Groundwater occurrence of the El Paso area and its related geology, in Guidebook of the border region: New Mexico Geological Society, 20th Field Conference, p. 209-214.

Davis, M.E., 1965, Development of ground water in the El Paso district, Texas, 1960-63, progress report no. 9: Texas Water Commission Bulletin 6514, 34 p.

Davis, M.E., and Leggat, E.R., 1967, Preliminary results of the investigation of the saline-water resources in the Hueco Bolson near El Paso, Texas: U.S. Geological Survey Open-File Report 67-79, 27 p.

Follett, C.R., 1954, Records of water-level measurements in El Paso County, Texas: Texas Board of Water Engineers Bulletin 5417, 50 p.

Frenzel, P.F., and Kaehler, C.A., 1990, Geohydrology and simulation of ground-water flow in the Mesilla Basin, Doña Ana County, New Mexico, and El Paso County, Texas, with a section on Water quality and geochemistry by S.K. Anderholm: U.S. Geological Survey Open-File Report 88-305, 179 p., 5 pls.

Garza, Sergio, Weeks, E.P., and White, D.E., 1980, Appraisal of potential for injection-well recharge of the Hueco Bolson with treated sewage effluent--Preliminary study of the northeast El Paso area, Texas: U.S. Geological Survey Open-File Report 80-1106, 37 p.

Gates, J.S., and Stanley, W.D., 1976, Hydrogeologic interpretation of geophysical data from the southeastern Hueco Bolson, El Paso and Hudspeth Counties, Texas: U.S. Geological Survey Open-File Report 76-650, 37 p.

SELECTED REFERENCES--Continued

Gates, J.S., White, D.E., Stanley, W.D., and Ackermann, H.D., 1980, Availability of fresh and slightly saline ground water in basins of westernmost Texas: Texas Department of Water Resources Report 256, 108 p.

Herrick, E.H., 1960, Ground-water resources of the headquarters (cantonment) area, White Sands Proving Ground, Doña Ana County, New Mexico: U.S. Geological Survey Open-File Report, 203 p.

Herrick, E.H., and Davis, L.V., 1965, Availability of ground water in the Tularosa Basin and adjoining areas, New Mexico and Texas: U.S. Geological Survey Hydrologic Investigations Atlas HA-191, scale 1:500,000, 1 sheet.

Hickerson, J.T., 1971, Water requirements and available resources of El Paso, Texas: El Paso Water Utilities Report, 12 p.

_____1979, Benefits of the Hueco Bolson as a water supply for the city of El Paso: El Paso Water Utilities Report, 8 p.

Hood, J.W., 1963, Tularosa and Hueco Bolsons, New Mexico and Texas, in Thomas, H.E., ed., Effects of drought in basins of interior drainage: U.S. Geological Survey Professional Paper 372-E, p. E3-E6.

International Boundary and Water Commission, United States and Mexico, 1984, Flow of the Rio Grande and related data: International Boundary and Water Commission Water Bulletin 54, 147 p.

Johnson, A.I., 1967, Specific yield--Compilation of specific yields for various materials: U.S. Geological Survey Water-Supply Paper 1662-D, 74 p.

Johnson Division, Universal Oil Products Company, 1972, Ground water and wells: A reference book for the water-well industry, 2d printing, 440 p.

Kelly, T.E., 1973, Summary of ground-water data, Post Headquarters and adjacent areas, White Sands Missile Range: U.S. Geological Survey Open-File Report, 66 p.

Kelly, T.E., and Hearne, G.A., 1976, The effects of ground-water development on the water supply in the Post Headquarters area, White Sands Missile Range, New Mexico: U.S. Geological Survey Open-File Report 76-277, 97 p.

King, W.E., Hawley, J.W., Taylor, A.M., and Wilson, R.P., 1971, Geology and ground-water resources of central and western Doña Ana County, New Mexico: Socorro, New Mexico State Bureau of Mines and Mineral Resources Hydrologic Report 1, 64 p.

Knowles, T.R., and Alvarez, H.J., 1979, Simulated effects of ground-water pumping in portions of the Hueco Bolson in Texas and Mexico during the period 1973 through 2029: Texas Department of Water Resources Report LP-104, 26 p.

Knowles, D.B., and Kennedy, R.A., 1958a, Ground-water resources of the Hueco Bolson, northeast of El Paso, Texas: U.S. Geological Survey Water-Supply Paper 1426, 186 p. (also published as Texas Water Commission Bulletin 6203).

_____1958b, Ground-water resources of the Hueco Bolson, northeast of El Paso, Texas, Franklin and Hueco Mountains, Texas, in G.B. McBride, compiler: West Texas Geological Society, 1958 Field Trip Guidebook, p. 55-66.

Kottlowski, F.E., and LeMone, D.V., eds., 1969, Border stratigraphy symposium: Socorro, New Mexico Bureau of Mines and Mineral Resources Circular 104, 123 p.

Land, L.F., and Armstrong, C.A., 1985, A preliminary assessment of land-surface subsidence in the El Paso area, Texas: U.S. Geological Survey Water-Resources Investigations Report 85-4155, 96 p.

Lansford, R.R., and others, 1981, Sources of irrigation water and irrigated and dry cropland acreages in New Mexico, by county, 1975-1980: Las Cruces, New Mexico State University Agricultural Experiment Station Research Report 454, 41 p.

Lee Wilson and Associates, Inc., 1981, Water supply alternatives for El Paso: Unpublished consultant's report prepared for the El Paso Water Utilities Public Service Board, 75 p.

_____1986, Exhibit 1 of the City of El Paso in support of its applications to appropriate ground water in New Mexico: Unpublished consultant's report prepared for the El Paso Water Utilities Public Service Board.

Leggat, E.R., 1957a, Memorandum on the water-supply wells at Biggs Air Force Base, El Paso, Texas: U.S. Geological Survey Open-File Report, 8 p.

_____1957b, Memorandum on ground-water conditions and suggestions for test drilling in the Logan Heights area, El Paso, Texas: U.S. Geological Survey Open-File Report, 12 p.

_____1962, Development of ground water in the El Paso district, Texas, 1955-60, progress report no. 8: Texas Water Commission Bulletin 6204, 65 p.

Leggat, E.R., and Davis, M.E., 1966, Analog model study of the Hueco Bolson near El Paso, Texas: Texas Water Development Board Report 28, 26 p.

Livingston, Penn, and Birdsall, J.M., 1944, Progress report on the ground-water supply of the El Paso area, Texas: U.S. Geological Survey Open-File Report, 16 p.

Lohman, S.W., 1972, Ground-water hydraulics: U.S. Geological Survey Professional Paper 708, 70 p.

Maker, H.J., Neher, R.E., Derr, P.H., and Anderson, J.U., 1971, Soil associations and land classification for irrigation, Doña Ana County: Las Cruces, New Mexico State University Agricultural Experiment Station Research Report 183, 41 p.

Mattick, R.E., 1967, A seismic and gravity profile across the Hueco Bolson, Texas, in Geological Survey Research 1967: U.S. Geological Survey Professional Paper 575-D, p. D85-D91.

McDonald, M.G., and Harbaugh, A.W., 1988, A modular three-dimensional finite-difference ground-water flow model: U.S. Geological Survey Techniques of Water-Resources Investigations, book 6, chap. A1, various pagination.

McLean, J.S., 1970, Saline ground water in the Tularosa Basin, New Mexico, in Guidebook of the Las Cruces Country: New Mexico Geological Society, 26th Field Conference, p. 237-238.

Meinzer, O.E., and Hare, R.F., 1915, Geology and water resources of Tularosa Basin, New Mexico: U.S. Geological Survey Water-Supply Paper 343, 317 p.

Meyer, W.R., 1976, Digital model for simulated effects of ground-water pumping in the Hueco Bolson, El Paso area, Texas, New Mexico, and Mexico: U.S. Geological Survey Water-Resources Investigations Report 58-75, 31 p.

Meyer, W.R., and Gordon, J.D., 1972a, Development of ground water in the El Paso district, Texas, 1963-70: Texas Water Development Board Report 153, 50 p.

_____1972b, Water-budget studies of lower Mesilla Valley and El Paso Valley, El Paso County, Texas: U.S. Geological Survey Open-File Report, 43 p.

Orr, B.R., and Myers, R.G., 1986, Water resources in basin-fill deposits in the Tularosa Basin, New Mexico: U.S. Geological Survey Water-Resources Investigations Report 85-4219, 94 p.

Orr, B.R., and White, R.R., 1985, Selected hydrologic data from the northern part of the Hueco Bolson, New Mexico and Texas: U.S. Geological Survey Open-File Report 85-696, 88 p.

Peterson, D.M., Khaleel, Raz, and Hawley, J.W., 1984, Quasi three-dimensional modeling of ground-water flow in the Mesilla Bolson, New Mexico and Texas: Las Cruces, New Mexico Water Resources Research Institute Technical Completion Report 178, 185 p.

Reilly, T.E., Frimpter, M.H., LeBlanc, D.R., and Goodman, A.S., 1987, Analysis of steady-state salt-water upconing with application at Truro well field, Cape Cod, Massachusetts: Ground Water, v. 25, no. 2, p. 194-206.

Richardson, G.B., 1909, Description of the El Paso district: U.S. Geological Survey Geologic Atlas of the United States, Folio 166.

Sayre, A.N., 1938, Estimating safe yield as illustrated by El Paso, Texas, ground-water investigation: Economic Geology, v. 33, p. 697-708.

_____1940, Ground-water supplies of the El Paso area, Texas: U.S. Geological Survey Open-File Report, 4 p.

Sayre, A.N., and Livingston, Penn, 1945, Ground-water resources of the El Paso area, Texas: U.S. Geological Survey Water-Supply Paper 919, 190 p.

Scalapino, R.A., and Irelan, Burdge, 1949, Ground-water resources of the El Paso area, Texas, progress report no. 6: Texas Board of Water Engineers Miscellaneous Publication M079, 25 p.

Scott, A.G., 1970, Estimated mean-annual runoff at Post Headquarters area, White Sands Missile Range, New Mexico: U.S. Geological Survey Open-File Report, 13 p.

Seager, W.R., 1980, Quaternary fault system in the Tularosa and Hueco Basins, southern New Mexico and west Texas, in Trans-Pecos region: New Mexico Geological Society, 31st Field Conference, p. 131-135.

Seager, W.R., Hawley, J.W., Kottlowski, F.E., and Kelley, S.A., 1987, Geology of east half of Las Cruces and northeast El Paso 1° x 2° sheets, New Mexico: Socorro, New Mexico Bureau of Mines and Mineral Resources Geologic Map 57, scale 1:25,000, 5 sheets.

Slichter, C.S., 1905, Observations on the ground waters of Rio Grande valley: U.S. Geological Survey Water-Supply Paper 141, 83 p.

Smith, R.E., 1956, Ground-water resources of the El Paso district, Texas, progress report no. 7: Texas Board of Water Engineers Bulletin 5603, 36 p.

Sorensen, E.F., 1977, Water use by categories in New Mexico counties and river basins, and irrigated and dry cropland acreage in 1975: New Mexico State Engineer Technical Report 41, 34 p.

_____1982, Water use by categories in New Mexico counties and river basins, and irrigated acreage in 1980: New Mexico State Engineer Technical Report 44, 51 p.

Strain, W.S., 1966, Blancan mammalian fauna and Pleistocene formations, Hudspeth County, Texas: Texas Memorial Museum Bulletin 10, 55 p.

_____1969, Cenozoic rocks in the Mesilla and Hueco Bolsons, in Delaware Basin exploration (Guadalupe Mountains, Hueco Mountains, Franklin Mountains, geology of the Carlsbad Caverns): West Texas Geological Society Publication 68-55a, p. 83-84.

SELECTED REFERENCES--Concluded

Sundstrom, R.W., 1945, Memorandum on ground-water resources of the El Paso, Texas, area, progress report: U.S. Geological Survey Open-File Report, 12 p.

Sundstrom, R.W., and Hood, J.W., 1952, Results of artificial recharge of the ground-water reservoir at El Paso, Texas: Texas Board of Water Engineers Bulletin 5206, 19 p.

U.S. Bureau of Reclamation, 1977, Ground water manual: Bureau of Reclamation Water Resources Technical Publication, 480 p.

Voss, C.I., 1984, A finite-element simulation model for saturated-unsaturated, fluid-density-dependent ground-water flow with energy transport or chemically reactive single-species solute transport: U.S. Geological Survey Water-Resources Investigations Report 84-4369, 409 p.

Walton, W.C., 1970, Groundwater resource evaluation: New York, McGraw-Hill Book Company, 664 p.

White, D.E., 1983, Summary of hydrologic information in the El Paso, Texas, area, with emphasis on ground-water studies, 1903-80: U.S. Geological Survey Open-File Report 83-775, 77 p.

Wilson, C.A., and Myers, R.G., 1981, Ground-water resources of the Soledad Canyon re-entrant and adjacent areas, White Sands Missile Range and Fort Bliss Military Reservation, Doña Ana County, New Mexico: U.S. Geological Survey Water-Resources Investigations 81-645, 22 p.

Wilson, C.A., and White, R.R., 1984, Geohydrology of the central Mesilla Valley, Doña Ana County, New Mexico: U.S. Geological Survey Water-Resources Investigations 82-555, 144 p.

Wilson, C.A., White, R.R., Orr, B.R., and Roybal, R.G., 1981, Water resources of the Rincon and Mesilla Valleys and adjacent areas, New Mexico: New Mexico State Engineer Technical Report 43, 514 p.

Zohdy, A.A.R., Jackson, D.B., Mattick, R.E., and Peterson, D.L., 1969, Geophysical surveys for ground water at White Sands Missile Range, New Mexico: U.S. Geological Survey Open-File Report 69-326, various pagination.

*U.S. GOVERNMENT PRINTING OFFICE 1992-0-675-716/65102